University College London (UCL)

Molecular Tuning Of Telomerase Activity In Senescent Human T cells

Alessio Lanna, B.Sc., M.Res., M.Phil.

A thesis submitted to the

University College London (UCL)

for the degree of

DOCTOR OF PHILOSOPHY

The Rayne Building

Division of Infection and Immunity

UCL Medical School

March 2016

I, Alessio Lanna, confirm that the work presented in this thesis is my own. Where information has been derived from other sources, I confirm that this has been indicated in the thesis.

Abstract

Telomerase, a RNA-dependent DNA polymerase that adds telomeric DNA at the ends of eukaryotic chromosomes, is essential for the lifelong preservation of the proliferative potential of antigen specific T lymphocytes. However, senescent T cells that have low telomerase activity, short telomeres and lack of replicative capacity accumulate in old humans, patients with chronic viral infections and cancer. The mechanisms inhibiting telomerase in these cells are poorly understood. Here I investigated the molecular pathways causing telomerase dysfunction and defined an unrecognized mode of p38 MAPK activation in T cells. To identify mechanisms involved in telomerase down-regulation, I activated T cells in the presence of IFN-α, an inflammatory cytokine that inhibits telomerase. Telomerase down-regulation was mediated in part by p38 activation. I further investigated the upstream regulatory network of p38 MAPK in senescent T cells. Unexpectedly, spontaneous p38 activation in these cells was not regulated by either the 'canonical' MAPK cascade or the 'alternative' pathway downstream of the T cell receptor, in contrast to the current paradigm of how this pathway is activated in T cells. Instead, the senescence-related DNA damage response pathway activates the low nutrient sensor AMPK, which in turn induces p38 auto-phosphorylation through the scaffold molecule TAB1. These findings establish a third, 'intra-sensory' pathway for p38 activation in T cells in which low nutrient and genotoxic signalling converge to inhibit proliferative responses. This can be reversed by blocking AMPK/TAB1 mediated activation of p38, which may represent a selective way for boosting T cell activity during ageing.

Acknowledgements

Over the past four years, I had the life-changing privilege of being awarded a Medical Research Council (MRC) Fellowship to carry out my doctoral studies at University College London, in the Division of Infection & Immunity. Most and foremost, I would like to express my greatest gratitude to my Primary Supervisor, Professor Arne Akbar, who supported me in ways that would have been hard to either imagine or predict. His constant guidance, advice and support have been essential for both my scientific and personal growth. I will be constantly inspired by him. I would also like to thank my Second Supervisor, Dr. David Escors, for introducing me to the lentivector technology and for his continuous help during my PhD studies. I am grateful to Dr. Ornella Franzese for triggering my very first interest towards T cell signaling. This work would have not been possible without my friend, Sara. I will always remember and be grateful for our nighttime- often divergent- scientific discussions. I would like to especially thank my family, Antonella, Lucio & Ludovica, for their uncoditional help and support.

Dedicated to love, the real driving force of life.

In memory of my grandmother, Esi, lifelong example and inspiration;

and of Giancarlo, the best life (and tennis) coach I could have ever had.

Contents

Chapter I: Introduction

Chapter II: Materials and Methods

Chapter IV: p38 activation in T cells: Challenging the paradigm

Chapter V: p38 is activated by AMPK/TAB1 in senescent human $CD4^+$ T cells

Abbreviations

AMPK: AMP-responsive protein kinase

APC: Antigen presenting cell

ATM: apical kinases ataxia telangiectasia mutated

ATR: ATM and RAD-3 related

ATP: Adenosine triphosphate

ATF2: activating transcription factor 2

BCR: B cell receptor

CAMKK2: Ca^{2+}/calmodulin-dependent protein kinase II

CDK: cyclin dependent kinase

CMV: citomegolarovirus

DLG1: Discs-large homologue 1

DDR: DNA damage response

E2F1: elongation 2 factor 1

ERK: extracellular-related kinase

HDAC: histone deacetylase

HIV: Human Immunodeficiency Virus

H2AX: H2A histone family, member X

hTERT: human telomerase reverse transcriptase

IFN: interferon

JAK1: Janus kinase 1

JNK: c-JUN N-terminal kinase

LAT: linker for T cell activation

LCK: lymphocyte specific signalling kinase

LKB1: liver kinase beta 1

MAPK: Mitogen-activated protein kinase

MAPKAPK2: MAP kinase-activated protein kinase 2

MHC: Major histocompatibility complex

mTORC: mammalian target of rapamycin complex

MKK: Mitogen activated kinase kinase

NFAT: nuclear factor of activated T cells

NFkB: Nuclear-factor-kappa B

PDK1: phosphoinositide-dependent kinase 1

PI3K: phosphatidylinositol 3-kinase

PLC-γ 1: phospholipase-γ 1

PKC: protein kinase C

PP2A: protein phosphatase 2 A

pRb: retinoblastoma protein

RAPTOR: regulatory-associated protein of mTOR RAPTOR

RICTOR: RAPTOR-independent companion of TOR

SASP: Senescence-associated secretory phenotype

STAT: signal transducer and activator of transcription

TAB1: TGF beta activated kinase binding protein 1

TAK1: TGF beta activated kinase

TCR: T Cell Receptor

TYK2: tyrosin kinase 2

TRAF6: TNF receptor associated factor 6

XLP: X-linked lymphoproliferative syndrome

ZAP70: Zeta-chain associated protein 70

List of publications

Lanna A, Henson SM, Escors D & Akbar AN. The kinase p38 activated by the metabolic regulator AMPK and scaffold TAB1 drives the senescence of human T cells. *Nature Immunology*, **15**, 965-972 (2014).

Lanna A, Coutavas E, Levati L, Seidel J, Rustin M, Henson SM, Akbar AN & Franzese O. IFN-α Inhibits Telomerase in Human $CD8^+$ T Cells by Both hTERT Downregulation and Induction of p38 MAPK Signalling. *The Journal Of Immunology*, **191,** 3744-3752 (2013).

Awards and Merits

Bright Sparks in Immunology, ECI 2015.

UCL Dean's Prize 2014, nominated candidate.

Best Research. UCL Division Of Infection & Immunity. PhD Colloquium, 2014.

Conferences and Abstracts

Invited Speaker, Bright Sparks, **4th European Congress Of Immunology (ECI)**. Vienna. Austria Sept. 6-9 2015. **Lanna A*** & Akbar AN. 'The Discovery Of Intra-Sensory Signaling In Human T Lymphocytes'. ***Corresponding Authorship***

Invited Speaker, **15th International Congress of Immunology (ICI).** Milan. ITALY. Aug 22-27 2013. **Lanna A*,** Henson SM, Escors D & Akbar AN. *Frontiers in Immunology.* Conference Abstract: 15th International Congress of Immunology (ICI). **'**Molecular Tuning Of Telomerase Activity In Highly Differentiated Human Primary CD28–CD27– T cells'. ***Corresponding Authorship***

List of figures

List of Tables

Chapter I: Introduction

1.1 The immune response: general premises

An immune system is essential for the lifelong preservation of human health. Immunity is characterized by both innate and adaptive components, which have evolved to either preserve endogenous (self) or disrupt exogenous (non-self) structures. While innate immunity comprises non-specific mechanisms of immune-protection, adaptive responses are antigen-specific and rely on T and B-lymphocyte activation. The process is generally triggered by an immunogen, a non-self substance capable of eliciting an inflammatory response, which culminates in lymphocyte activation by antigen presenting cells (APCs) at the level of the secondary lymphoid organs.

The ability of the immune system to elicit an immune response progressively declines during ageing (Akbar and Henson, 2011), a process known as immune-senescence, and changes in both inflammatory and antigen related signals are involved in this decline (Boraschi et al., 2013). Recent studies froum our group highlighted that some key aspects of immune senescence may be reversible (Henson et al., 2014, 2015; Di Mitri et al., 2011). This is the case for T cells, an essential componenent of adaptive immunity, whose function is severely impaired during ageing (Boraschi et al., 2013; Weng et al., 2009). Understanding how senescent T cells function may reveal unrecognized strategies to restore immune protection in old humans, or in patients with chronic viral infections and cancer, who often exhibit features of premature immune-senescence (Chou et al., 2013; Crespo et al., 2013). The aim of the present study was to delineate strategies to

restore human senescent T cell function. Below, I introduce T cells, and dissuss properties of their development, function and end-stage differentiation.

1.2 T cells: development and function

T lymphocytes can either orchestrate an immune response, which defines T helper (Th) cells, or target non-self cells to destruction, which identifies cytotoxic T cells. Most T cells (above 95% in healthy individuals) possess an antigenic surface receptor, the T cell receptor, which is a heterodimer of α and β-chains that recognises antigens presented by major histocompatibility complex (MHC) molecules (Brownlie and Zamoyska, 2013). In addition, mature T cells possess either a CD8 or CD4 co-receptor that is important, together with α/β TCR molecules, for recognition of MHC class I and class II bound antigens, respectively (Germain, 2002).

Conversely, about 5% of unconventional T cells express a TCR of γ and δ–chains that recognises antigens, especially lipids, independently of MHC molecules. These cells are mostly located in peripheral tissues where they have been proposed to control local responses, providing a bridge between innate and adaptive immunity (Hayday and Tigelaar, 2003). In both rodents and humans, T helper cells are generally $CD4^+$ while cytotoxic cells are $CD8^+$; however cytotoxic $CD4^+$ T cells (especially when becoming senescent) have also been reported (Appay, 2004; Libri et al., 2011; Quezada et al., 2010).

T cells develop in the thymus, a lobulated lymphoid and retro-sternal organ, in a multi-step process. First, hematopoietic stem cells (HSC) enter the thymus, giving rise to a heterogeneous population of $CD4^-$ $CD8^-$ (double negative, DN1) $CD25^-$

$CD44^+$ thymocytes. Next, T cell precursors expressing either α/β or γ/δ TCR molecule diverge during the T cell lineage commitment. Thirdly, $CD4^+$ $CD8^+$ double positives (DP) thymocytes stem from late T cell precursors, namely DN4 thymocytes, following an intra-thymic beta-selection reaction. Finally, allo-reactive single positive $CD4^+$ or $CD8^+$ mature T cells, that only express α/β TCR molecules, are selected (in a 2:1 ratio) and allowed to exit the thymus (Germain, 2002). Importantly, because mechanisms of central tolerance exist to avoid auto-immunity, self-reactive mature T cells undergo intra-thymic apoptosis (Germain, 2002).

1.3 Human T cell differentiation

An important feature of human T lymphocytes is that the expression of various cell surface markers can be used to distinguish cells at different relative stages of differentiation (Akbar and Henson, 2011). Changes in phenotipic marker expression and T cell function are thus directly linked. Naïve (NA) T cells which express both the co-stimulatory receptors CD27 and CD28 along with the membrane-bound intracellular phosphatase CD45RA and high levels of CC-chemokine receptor 7 (CCR7) possess the longest telomeres and exhibit the highest proliferative and telomerase activity upon activation (Akbar and Fletcher, 2005). In contrast, human memory T lymphocytes represent a heterogenous cell compartment. This comprises central memory (CM) T cells that have lost either CD27 (in $CD4^+$ T cells) or CD28 (in $CD8^+$ T cells) expression and that have switched to a shorter variant of the phosphatase receptor CD45, namely CD45RO, exhibit elevated proliferative potential (Akbar and Fletcher, 2005; Weng et al., 2009). Effector memory (EM) T cells are $CD27^-$ $CD28^-$ $CCR7^-$ CD45RO

lymphocytes in both the human $CD4^+$ and $CD8^+$ pools. These cells exhibit features of end-stage differentiation including very short telomeres, low proliferative potential, decreased telomerase activity (Weng et al., 2009), as well senescence-associated DNA damage foci (Henson et al., 2014; Di Mitri et al., 2011). Thus, EM T cells are approaching replicative senescence (Weng et al., 2009). Finally, effector memory $CD27^-$ $CD28^-$ T lymphocytes that re-express CD45RA (EMRA) have the lowest telomerase and proliferative potential and highest expression of senescence associated markers yet not the shortest telomeres (Henson et al., 2014; Di Mitri et al., 2011). These cells accumulate in old humans especially within the $CD8^+$ T cell pool (Akbar et al., 2004). Although the reason why these cells re-express CD45RA is not clear, it has been proposed that EMRAs may exhibit features of telomere-independent senescence (Akbar and Henson, 2011; Di Mitri et al., 2011). However, despite the loss of proliferative potential *in vivo*, both EM and EMRA cells retain high functionality. These cells (especially EMRAs) can release high levels of pro-inflammatory cytokines (e.g. TNF-a, IL-6), metallo-proteins, granzymes and perforins indicating that they may be senescent yet not functionally exhausted cells (Akbar and Henson, 2011). Whether this inflammatory signature resembles *in toto* the senescence-associated secretory phenotype (SASP) displayed by senescent fibroblasts (Campisi and d'Adda di Fagagna, 2007) is currently under investigation in our laboratory. Interestingly, human end-stage T cell sub-populations also acquire expression of surface inhibitory/cytotoxic natural killer receptors such as CD57 and KLRG1 (Akbar and Henson, 2011; Henson et al., 2009). Signalling via these receptors (e.g. KLRG1) has been recently proved to actively inhibit proliferation in primary human highly differentiated $CD27^-$ $CD28^-$ $CD8^+$ T lymphocytes (Henson et al., 2009), indicating

that the phenotypic switches characterizing human T cell differentiation are strictly linked with the regulation of T cell functions. The relative expression of CD27 and CD28 receptors identifies 3 discrete populations within the primary human T cell compartment at different stages of progressive differentiation. As discussed, undifferentiated populations of these cells express both CD27 and CD28, cells at an intermediate stage of differentiation express CD28 but not CD27 while senescent populations express neither molecule (Weng et al., 2009). Profound changes in T cell signalling are therefore likely due to the loss of key co-stimulatory receptors, during human T cell differentiation. However at present little is known about the regulation of signalling pathways in primary human highly differentiated T cells. So far defective AKT and mTOR activity (unlike other senescent cells such as fibroblasts), reduced telomerase activity and a spontaneous but unexplained increase of p38 MAPK phosphorylation inhibiting their mitogen capacity have been reported (Henson et al., 2009, 2014; Di Mitri et al., 2011; Plunkett et al., 2007). In **table 1**, the main phenotypic and functional features of T cells at the different stage of differentiation are summarized. Below, an overview on T cell signalling is provided.

Markers	Differentiation →		
CD27	+++	+/-	-
CD28	+++	+/-	-
CD45RA	+++	+/-	+/-
CCR7	+++	++	-
CD57	+	++	+++
Functions			
p-p38	+	++	+++
Cytotox.	+	++	+++
IFN-γ	+	++	+++
IL-2	+++	+	-
TNF	+	++	+++
Senescence			
Telomerase	+++	++	-
Telomeres	+++	++	+
Proliferation	+++	++	-

Table 1. Characteristics of functional changes of human T cell differentiation. The main known characteristics of human T cell differentiation are shown. The role of p38 signalling will be extensively discussed in the text. Adapted from (Akbar & Henson, 2011).

1.4 T cell activation: biochemical and functional considerations

Optimal T cell activation requires both TCR and co-stimulatory receptor engagement. The α and β chains of the TCR possess both variable (extracellular) and constant (trans-membrane) domains that are non-covalently bound to an invariant CD3 chain complex, coupling antigenic recognition to intracellular biochemical events (T cell signalling) (Chakraborty and Weiss, 2014). There are two important factors that modulate early TCR signalling: antigen specificity of the receptor and binding-avidity of the TCR (Alarcon et al., 2003; Schamel and Alarcón, 2013). While the former is regulated through the interaction between MHC-peptides on APC and complementary determining regions within the variable domains of both TCR α and β chains (Dustin, 2014), the latter is thought to distinguish between productive (agonist) and non-productive (or antagonist) MHC-TCR interactions (Stone et al., 2009). However, the exact determinants which regulate binding avidity of the TCR are presently unknown. Individual TCR molecules can oligomerize within cholesterol-enriched portions of the T cell membrane (Molnár et al., 2012), a process known as TCR nanoclustering, thereby enchancing TCR sensitivity (Alarcón et al., 2011; Schamel and Alarcón, 2013). Importantly, despite elevated antigen specificity, naïve T cells have generally low binding avidity/sensitivity for antigens, which increase upon activation and differentiation. Therefore, memory T cells are more prone to trigger an immune response than their naïve counterparts (Corse et al., 2011). Down-stream of TCR activation, important biochemical events are regulated in concert to co-ordinate T cell responses. Excellent comprehensive reviews on T cell signalling are available (Acuto et al., 2008; Chakraborty and Weiss, 2014; Navarro and Cantrell, 2014). Because the TCR does not possess intrinsic enzymatic activity, signal

transduction downstream of the receptor relies on a series of trans-phosphorylation cascades. Precisely, the cytoplasmic domains of the CD4 and CD8 co-receptors are bound by the lymphocyte specific signalling kinase LCK which in turn phosphorylates immune-receptor tyrosine-based activation motives (ITAMs) within the CD3 cytoplasmic tails of the receptor. Upon activation, the phosphorylated ITAMs in turn recruit the signalling kinase ZAP70 through SH2 domains. Next, ITAM-bound ZAP70 is further phosphorylated by LCK and this leads to conformational changes within ZAP70 that are important for downstream signal propagation. The most characterized (but not sole) biological target of activated ZAP70 is the linker for T cell activation (LAT), which serves to recruit a multimeric platform that orchestrates a variety of biochemical and functional processes important for T cell transcription, growth, activation and ultimately differentiation into effector populations. Crucial components of this complex (also known as 'LAT-signalosome') includes the distal T cell-signalling adaptors SLP76 and VAV1, the phospholipase PLCγ1, the growth factor receptor-bound protein GRB2, its adaptor protein GADS, and the kinase ITK. Three main biochemical cascades are activated in turn by this 'LAT signalosome': calcium, mitogen-activated protein kinase (MAPK) and nuclear factor-κB (NF-κB) signalling pathways. In order, rapid calcium influx is regulated by the ITK-dependent activation of PLC-γ 1 that is essential to trigger activation of the inositol cascade. This generates second lipid-derived messengers (diacyl-glycerol and inositol-triphosphates) to activate protein kinase C (PKC) isoforms and the calcineurin-nuclear factor of activated T cells (NFAT) signalling pathways, respectively. Thus, ITK is essential for T cell activation. The MAPK cascade is also triggered by diacyl-glycerol generation through the PKC-dependent activation of the guanine

nucleotide-binding protein Ras. Upon activation, Ras interacts with Raf1, a MAPK kinase kinase, which in turn activates a signaling cascade where the MAPK kinases 1/2 (MEK1/2) downstream activate the extracellular-regulated protein kinases 1/2 (ERK1/2), prototype member of the MAPK pathway. Activated ERKs orchestrate a variety of downstream biological substrates (i.e. ELK1, stathmin) that regulate cell-cycle progression, cytokine production, T cell metabolism, protein expression and cytoskeleton remodelling. Other two prototype MAPK pathways, involved in diverse aspects of T cell biology, are the JNK and p38 signaling cascades. Both pathways share with ERK the same structure of the activation module, but they are regulated through separate upstream cascades. JNK, which is important for T cell differentiation but seems to be dispensable fo T cell activation (Dong et al., 2000), is directly activated by the kinases MEKK4 and MEKK7 which are in turn activated by a plethora of upstream MKKKs. While expression of JNK proteins can be induced by TCR triggering alone, co-stimulatory signals (i.e. CD28 engagement) seem to be important to induce JNK activation in T cells (Su, 1994). This is different from the activation of ERK (and p38) that can occur even in the absence of costimulation (Ashwell, 2006). As per ERK, JNK function is mediated by various biological substrates, mostly transcription factors (for instance, c-JUN), that are activated by direct JNK phosphorylation. The role and activation of the p38 MAPK pathway is discussed in detail in a dedicated session. The NF-κB pathway is another pivotal regulator of T cell function and is linked to the 'LAT signalosome' through PKC theta activation . PKC theta collects upstream activation signals from both the TCR and co-stimulatroy receptors to orchestrate in turn formation of a signaling complex with the proteins CARMA1, BCL10 and MALT1 ('CBM complex'). Formation of this CBM complex is essential

for NF-κB activation in response to TCR triggering, however how the CMB complex is itself regulated is not fully understood. Conversely, the downstream activation of NF-κB is more established. In unstimulated T cells, NF-κB is kept in the cytosol by its inhibitor, IκBα. Upon TCR activation, IκBα is degraded through poly-ubiquitination by its upstream regulatory complex, the IKK. Therefore, the IKK complex links NF-κB activation to the CBM complex and (further upstream) to the LAT signalosome. NF-κB signaling plays a crucial role in the inflammatory response, as well T cell development and can promote either Th1 or Th2 differentiation directing distinct transcriptional programs (Oh and Ghosh, 2013).

A well-defined property of T cell signaling networks, important to ensure functional plasticity, is downstream signaling divergence. Thus, a multitude of transcription factors have to be activated to dictate immune-related gene expression, in a T cell-subset specific way. For instance, $CD4^+$ T helper 1 and 2 cells express, respectively, either T–bet or GATA-3, transcription factors essential for their functions (Ho et al., 2009; Kanhere et al., 2012; Lazarevic et al., 2013); conversely the transcription factor Eomes is required for $CD8^+$ T cell function (Pearce et al., 2003). In addition to TCR signalling, co-stimulatory receptor (e.g. CD28 engagement) and environmental signals (e.g. cytokines) are also important to drive the activation, differentiation and function of T lymphocytes. Indeed, CD28 co-stimulation is required to avoid T cell anergy (that is, the inability of T cell clones to respond to antigens in the absence of appropriate co-stimulation) (Abbas et al., 2004; Parijs et al., 1997). Upon activation, the cytoplasmic domain of CD28 binds to the phosphatidylinositol 3-kinase (PI3K) to generate inositol-triphosphates, which recruit the signalling kinases phosphoinositide-dependent

kinase 1 (PDK1) and AKT at the cell membrane. Activated PDK1 also contributes to NF-κB activation and convege at the point of PKC theta. This in turn leads to AKT phosphorylation (on Thr308) by PDK1. To become fully activated, AKT has to be further phosphorylated (on Ser473) by another kinase, namely mTOR complex 2 (that consists of mTOR, mLST8, SIN1 and Rictor) (Rudd and Schneider, 2003). In turn, activated AKT is thought to control the activation of pleiotropic anabolic pathways via activation of the anabolic signaling kinase mTOR (further details on mTOR are discussed in the next session). This concept has recently been challenged, however, when AKT was shown to be nonessential for T cell metabolism but required for cytotoxic T cell fate (Finlay et al., 2012; Macintyre et al., 2011). Cytokine signalling is also involved in tuning signal transduction in T cells. In general, cytokines signalling acts via the STAT transcription factor family that is well recognised to polarize T cell function. For instance, if IFN-γ and/or IL12 are present in the activation milieu of the immunological synapse, STAT1 and STAT4 activation promotes T-bet expression (Moriggl et al., 1998), required for T helper 1 induction which in turn boosts the activity of phagocytes to eradicate pathogens (mostly bacteria and protozoa); conversely IL-4 and IL-6 trigger STAT6 activity to induce GATA3 expression and related shift toward T helper 2 functions that is essential to induce B cell mediated humoral (antibody-mediated) immune-responses (Wurster et al., 2000). Thus, cytokine signalling regulates $CD4^+$ T cell activity in a non-reduntant manner. Of note, because positive feedback mechanisms exist, the same pool of cytokines that induce specific T cell polarization are also produced by the specific T cell subsets, upon induction. **Figure 1** illustrates the main biochemical pathways that regulate T cell activation, proliferation and functional activities.

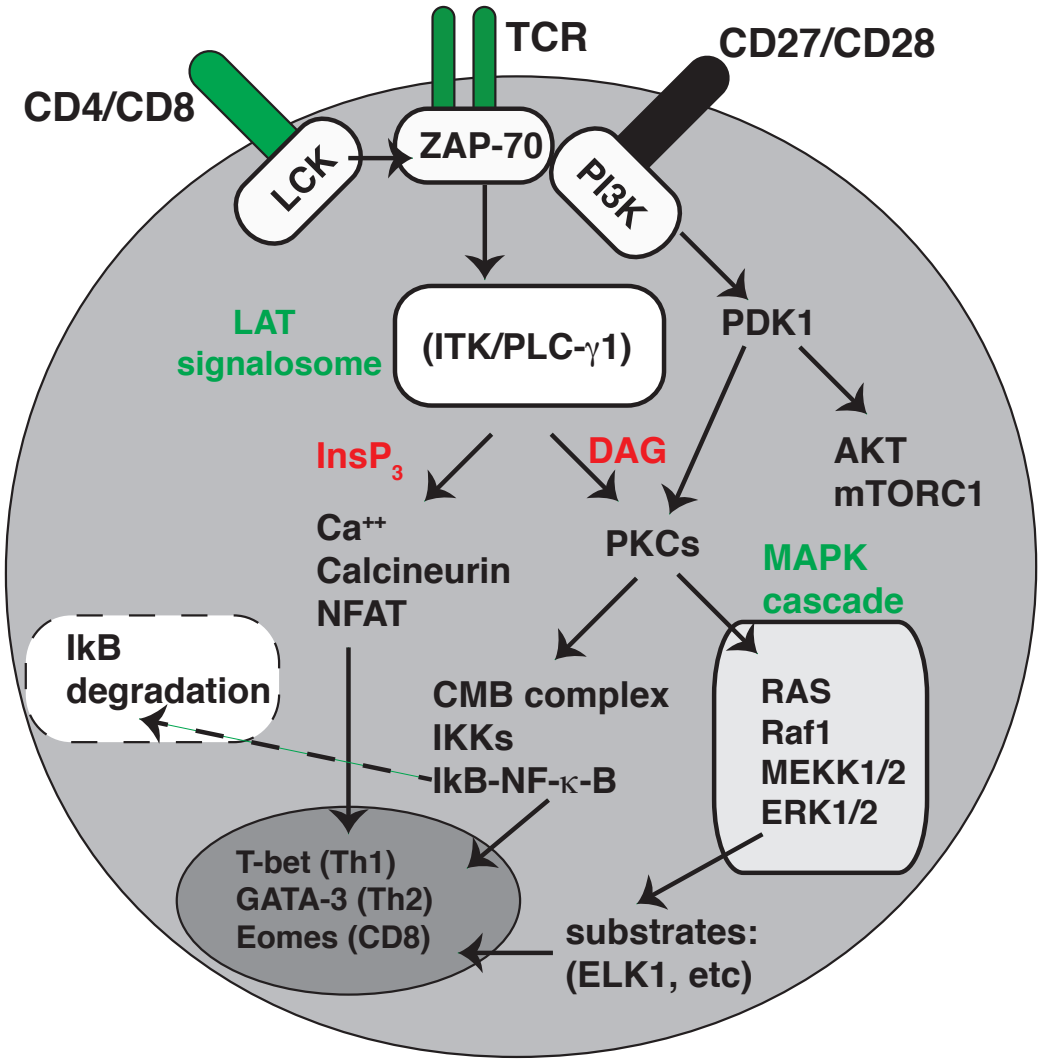

Figure 1: T cell signalling.
An overview of T cell signalling is provided. Activation cascades are discussed in details in the text, and are important to drive T cell differentiation, proliferation and effector functions. Briefly, antigen presentation triggers TCR signalosome activation by phosphorylation of Src kinases (e.g. LCK) and Syk kinases (e.g. ZAP70) that in turn phosphorylate various tyrosine sites within the CD3-ζ chain (ITAMs, not shown). LAT and SLP76 are downstream components of the TCR signalosome which in turn activate PLC-γ1 to trigger inositol triphosphate leading to the calcium dependent activation of NFAT. PLC activation also leads to release of diacylglycerol (DAG) important for the PKC-dependent activation of the NF-κ-B (via the CMB and IKK complexes) and the MAPK cascade via RAS. NF-κ-B activation relies on IkB degradation and is linked to LAT signalosome via the IKK and CMB complexes. The MAPK cascade is a three-tier module where an upstream kinase phosphorylates another. Activated MAPK substrates, NF-κ-B and NFAT undergo nucleus shuttling and activate various transcription factors (T-BET, GATA-3, Eomes) to establish different functional programs within the T cells. Protein translation is supported by mTORC1 activation downstream of PI3K/AKT, in response to CD28 engagement. Co-stimulatory signaling can converge on NF-κ-B via PKC and also on the MAPK JNK (not shown). mTOR activation also triggers mTORC2 dependent signalling that reinforces AKT activation (not shown). The upstream regulatory network of mTORC2 is presently unknown.

1.5 T cell metabolism: signal integration by mTOR and AMPK.

The intertwining of T cell activation and metabolic pathways has received recently renewed interest as an attractive way to modulate T cell responses (Wellen and Thompson, 2012). There are two important metabolic-checkpoint kinases that orchestrate either T cell anabolic or catabolic pathways: the mTOR and AMP-responsive protein kinase, respectively. The former is a member of the PI3K family that integrates both TCR and co-stimulatory signals to orchestrate T cell activation, clonal expansion and functional differentiation in response to upstream activation by the AKT pathway (Laplante and Sabatini, 2012; Pollizzi and Powell, 2014), or (at least in cytotoxic CD8 T cells), by PDK1 independently of AKT (Finlay et al., 2012). mTOR is a serine-threonine kinase whose activity is regulated through the assembling of two distinct super-molecular complexes: mTORC1 and mTORC2 (Delgoffe et al., 2011). Characteristic of either mTORC1 or mTORC2 are the regulatory-associated protein of mTOR (RAPTOR) and the scaffolding protein RAPTOR-independent companion of TOR (RICTOR), respectively. This dictates that mTORC1 yet not mTORC2 activity can be pharmacological inhibited by rapamycin, an immunosuppressive drug that prevents RAPTOR recruitment to the mTOR (Sabatini et al., 1994). However, it has been reported that T cell mTORC2 can be inhibited by modest rapamycin concentration as well, perhaps through unrecognized off-target effects (Pollizzi and Powell, 2014). Both mTOR complexes are important for inducing T cell activation, proliferation and polarization although the mechanisms by which mTORC2 act are much less characterized. The control of T cell metabolism by mTOR is essential for the regulation of T cell function. Importantly, the so-called Warburg effect dictates that proliferating cells- including T cells- rely on aerobic glycolysis (that is, the cytoplasmic oxidation of glucose into

pyruvate) rather than the more efficient oxidative phosphorylation (that is, the mitochondrial break up of nutrients) to generate their energy, possibly through the generation of important glycolytic by-products. Indeed, mTOR activity promotes the Warburg effect in T cells by up-regulating the glycolytic-machinery and activating various biosynthetic pathways that are important for the incorporation of molecules into daughter cells (Finlay and Cantrell, 2011; Finlay et al., 2012; Sinclair et al., 2013). This is essential during an immune response when naïve T lymphocytes that are metabolically quiescent and rely on basal oxidative metabolism, become effector T cells and switch to aerobic glycolysis (Pearce et al., 2013). Furthermore, aerobic glycolysis is required for effector functions in T cells (Chang et al., 2013b). **Figure 2** resumes the metabolic switches that characterize T cell function.

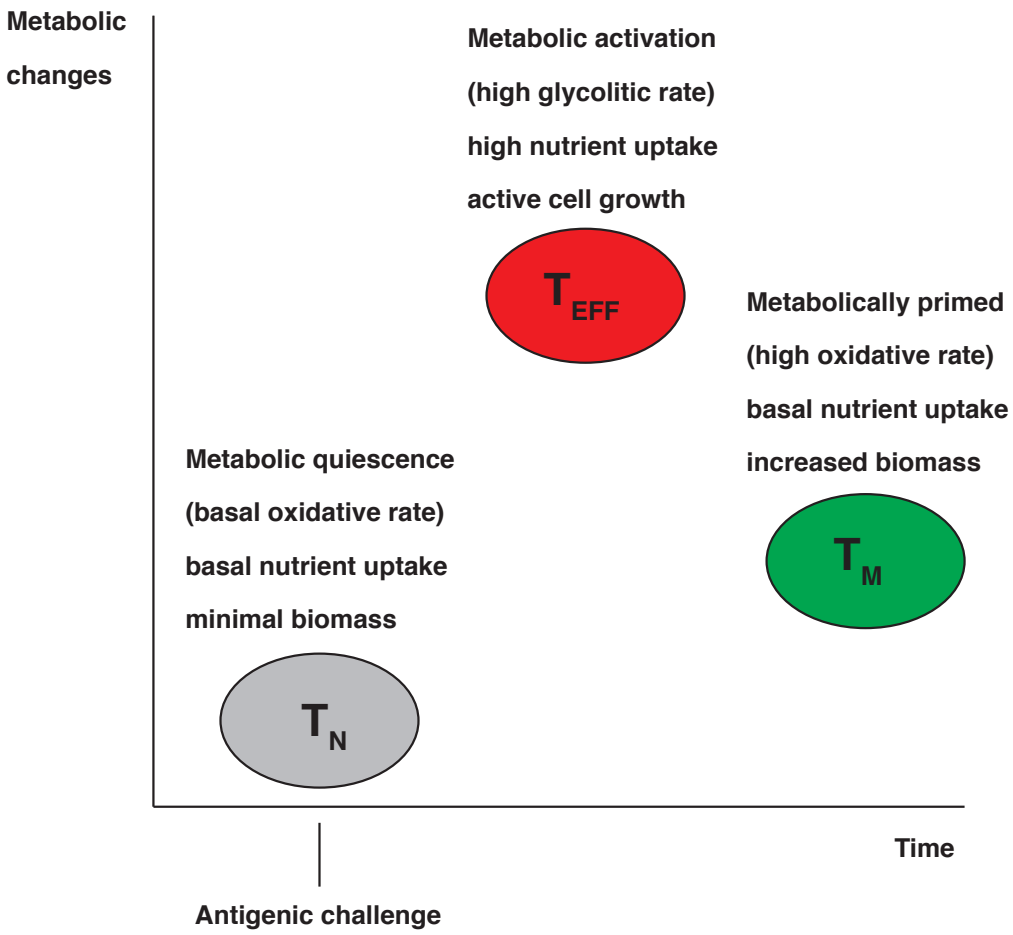

Figure 2: The metabolic changes that dictate T cell function.
The different metabolic switches characterizing naïve T cells (T_N), effector T cells (T_{EFF}) and memory T cells (T_M) are shown. Naïve T cells are metabolically quiescent, have minimal biosynthetic requirements and maintain a basal oxidative profile; upon activation effector T cells undergo clonal expansion that is sustained by elevated glycolytic rates and increased biomass (cell growth) resulting in cell proliferation and robust effector functions; memory T cells switch back to oxidative metabolism for long-term survival but show significantly larger spare-respiratory capacity (SRC) and increased mitochondrial mass than naïve T cells indicating that these cells have been metabolically primed. Adapted from (Pearce EP et al, 2013).

Conversely, the AMP-responsive protein kinase (AMPK) is a heterotrimer of α-β-γ subunits that is a low-energy sensor that is activated by the up-regulation of intracellular AMP: ATP ratios (Hardie et al., 2012). There are two catalytic AMPKα sub-units (α1 ubiquitously expressed and α2 restricted to muscles cells) that are activated by phosphorylation on Thr172 by either the upstream kinases LKB1 or CAMKK2 in response to either glucose-starvation or cytoplasmic calcium-influx, respectively (Shaw et al., 2004; Woods et al., 2005). The latter may be important in activated T cells in which AMPK activation is thought to cope with the increased energetic demand of TCR mediated cell proliferation (Tamás et al., 2006). In addition, the MAPKKK TAK1 activates AMPK but the biological relevance is not well defined (Herrero-Martín et al., 2009). In order to become activated, AMPK has to undergo conformational changes that are dependent on its γ and β regulatory subunits (**Figure 3**). There are 3 different AMPK γ-subunits (γ1, γ2 and γ3) that are differentially expressed in tissues, with AMPK-γ1 ubiquitously distributed, AMPK-γ2 mostly expressed in muscle cells while AMPK-γ3 expression is restricted to neurons. Each γ−subunit contains four nucleotide-binding sites, one of which constantly occupied by AMP, another of unknown function and the remaining two that can bind either AMP or ATP and possibly also ADP (Cardaci et al., 2012; Hardie et al., 2012). Upon AMP binding, a myristoyl modification of the AMPK-β regulatory subunit allows AMPK to become activated and promote the switch toward catabolic, ATP-producing pathways, especially through the activation of oxidative metabolism. At the same time, AMPK activity inhibits biosynthetic pathways that are ATP-consuming. In T cells, AMPK in part executes this task by mTOR inhibition (Navarro and Cantrell, 2014), which regulates the 'primed' oxidative metabolism characteristic of memory T cells (O'Sullivan and

Pearce, 2015), upon clearance of an antigenic challenge. Indeed both pharmacological AMPK activation or mTOR inhibition promote T cell memory generation in mice (Araki et al., 2009; Pearce et al., 2009). However, mTOR inhibition is not the only way by which AMPK regulates T cell function. In this thesis, I will show that AMPK activation negatively regulates both T cell proliferation and telomerase activity through activation of p38 MAP kinase. Below, I discuss the current, by-phasic model for p38 activation in T cells.

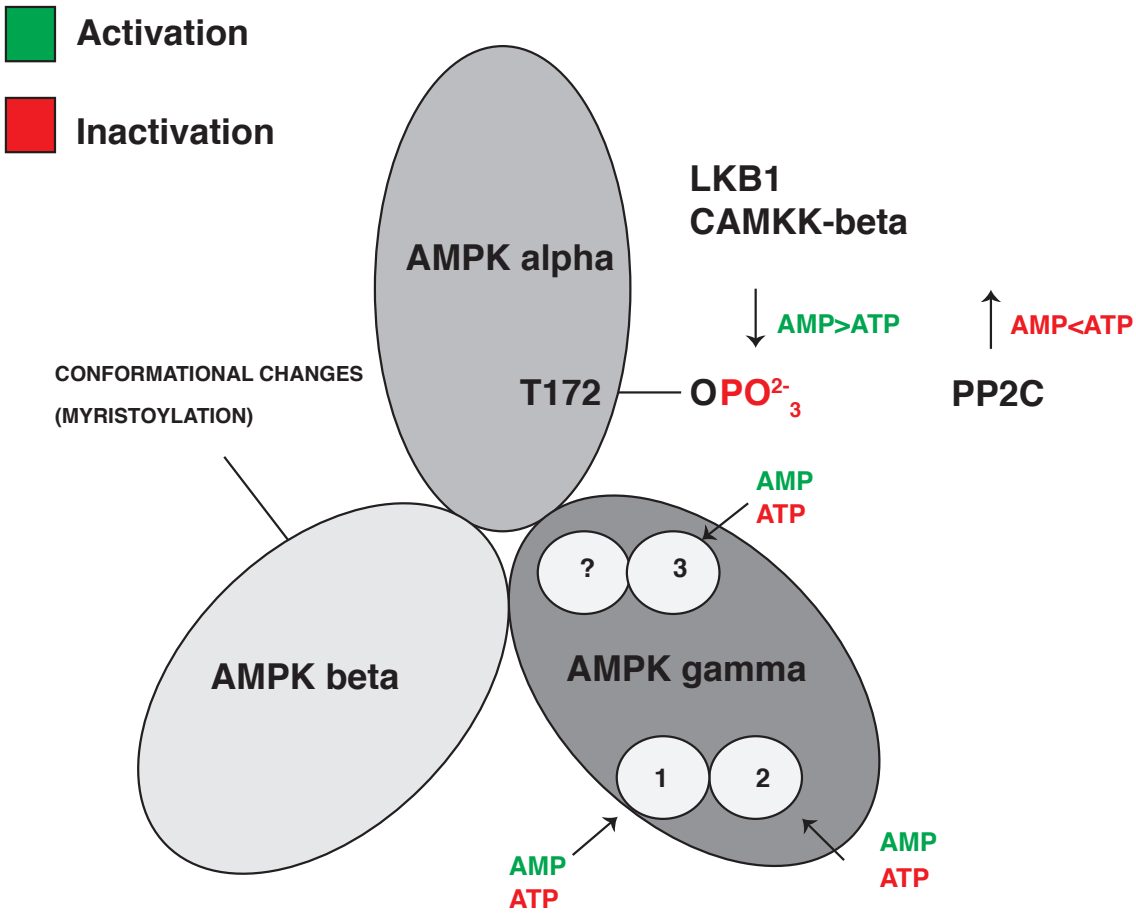

Figure 3: Tuning of a tuner: the metabolic master regulator AMPK.
The structure and biochemical consequences of AMPK activation are shown. AMPK is a heterotrimer of α, β and γ chains activated in response to nutrient deprivation, when energy imbalance elevates AMP over ATP. AMPK is allosterically activated by AMP binding to 3 specific sites within its regulatory γ-subunit; upon AMP binding AMPK undergoes conformational changes that result in AMPK-β myristoylation and robust AMPK-α (Thr-172) phosphorylation by AMPK upstream kinases, LKB1 and CaMKKβ. ATP is an allosteric inhibitor of AMPK and competes with AMP for regulatory binding to AMPK-γ subunit. Activated AMPK re-directs metabolism towards catabolic pathways and activates oxidative phosphorylation. When energy is restored, ATP displaces AMP (or ADP) from AMPK-γ, which renders the molecule targetable by inactivating PP2C dependent de-phosphorylation.

1.6 P38 MAPK signalling in T cells: current understanding

There are three main groups of MAPKs: p38, ERK and JNK (Chang and Karin, 2001). There are four distinct p38 MAPK isoforms: α, β, γ, δ (Ashwell, 2006). T cells mainly express the α and to a lesser extent the β and δ isoforms of p38 (Ashwell, 2006). Like all other MAPKs, p38 is phosphorylated within its activation Thr-x-Tyr loop in response to activatory signals by the canonical MAPK cascade, in which various upstream enzymes (such as MTK1, ASK1 and TAK1), that act as MAPKKK, downstream activates MKK3 or MKK6 that in turn activate p38 (Rincón and Davis, 2007).

MKK4, which normally phosphorylates JNK, can also activate p38 in some cases (Brancho et al., 2003). Many different signals can converge on the canonical MAPK cascade, including environmental stress, DNA damage, inflammatory cytokines and also co-stimulatory receptor engagement, possibly through the activation of the small GTPase Rac1 (**Figure 4, *left side***) (Ashwell, 2006). In turn, p38 can activate a tremendous number of transcription factors and other effector molecules, such as ATF2, p53 and MAPKAPK2 therefore regulating complex biochemical and functional responses (Zarubin and Han, 2005). Importantly, it is also possible that different MAPKs (especially JNK) converge with p38 on the activation of the same subset of biochemical targets (Wagner and Nebreda, 2009), perhaps to strengthen the functional outcome. Given the involvement of active p38 signalling in both stress and inflammatory responses, p38 structure has been determined to allow the development of various p38 inhibitors. Among these compounds, the ATP competitor SB-203580 and lorapemid (BIRB796) that act by both ATP competition (that is, direct inhibition of kinase activity) and targeting of upstream components within the MAPK cascade (Lee et al., 2000). However the

consideration of p38 as a pharmacological target was reduced following disappointing clinical trials in which p38 inhibitors failed (for instance, for the treatment of rheumatoid arthritis and other auto-immune inflammatory conditions) because of toxicity issues. This was possibly due to the ubiquitous expression of p38, which also significantly lowered the therapeutic index (that is, the ratio between therapeutic and adverse effects of a drug). At present there is no p38 inhibitor approved for treating human disease, and it has been proposed that targeting the (complex) upstream regulatory network of p38 may provide a more selective pharmacological intervention (Hammaker and Firestein, 2010).

The role of p38 in immune cells and more specifically in T cells has been extensively studied. For instance in non-senescent T cells, p38 inhibition by SB-203580 dampens T cell proliferation, T helper 1 polarization and related cytokine production in response to TCR activation (Rincón et al., 1998; Zhang et al., 1999). Although it was generally assumed that the MAPK cascade would be the sole regulatory mechanism for p38 activation, Salvador *et al* identified an alternative pathway, in which activated T cells but not B cells, phosphorylate p38 on a previously unrecognized site of Tyr 323 through the upstream activation of the TCR signalling molecules LCK and Zap70, therefore bypassing the canonical MAPK cascade (**Figure 4, *right side***) (Salvador et al., 2005). Subsequently, this leads to p38 auto-phosphorylation on Thr180-Tyr182 within its own activation loop (Salvador et al., 2005). However, recent studies suggested that also B cells can alternatively activate p38 in response to BCR engagement (Liu et al., 2012). The reason for the existence of different modes for the activation of p38 remains elusive, however it has been recently shown that alternative and canonical activated p38 counter-regulate each other in the induction of T cell proliferation

and effector functions by differentially tuning NFAT activity and nuclear import (Alam et al., 2014).

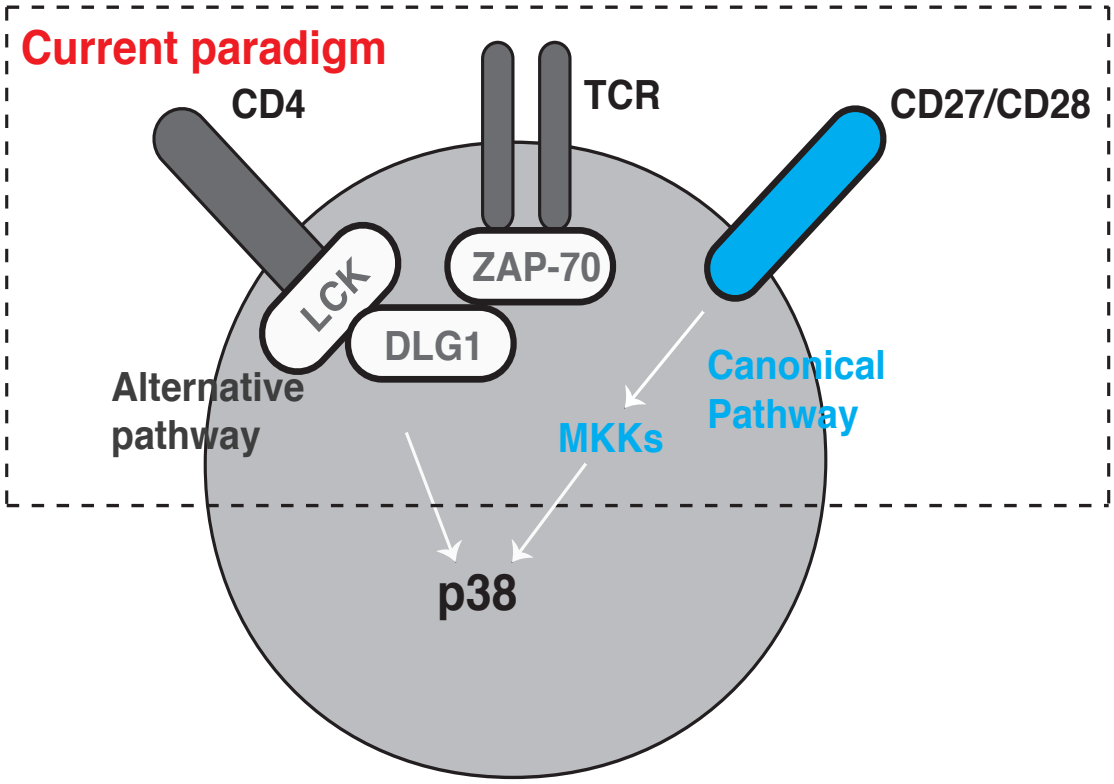

Figure 4: The bi-phasic model for p38 activation in T cells.
The current understanding for p38 activation in T cells is shown. As the JNKs and ERKs do, p38 is also activated through a canonical MAPK cascade in response to CD28 engagement, pro-inflammatory cytokines and stress signals. The canonical MAPK cascade activates p38 by phosphorylation on Thr180/Tyr182 within its activation loop through a series of phosphorylation events in which the most upstream enzyme, a MAPKKK (not shown), downstream activates a MAPKK (either MKK3 or MKK6) that in turn directly phosphorylates p38. Salvador *et al.* identified an alternative pathway in which TCR activation in the absence of co-stimulation triggers p38 activity downstream of TCR signalling machinery. In the alternative pathway, activated LCK in turn activates ZAP70 that then phosphorylates p38 on a previously unrecognized site of Y323 followed by p38 auto-phosphorylation on T180/Y182. Unlike canonical activated p38, alternative activation of p38 downstream of TCR signalosome has been shown to be important for T cell proliferation and Th1 differentiation.

Another MKK-independent mechanism for p38 activation was described in HEK293 cell line in which the scaffold molecule TAB1 can bind to p38α inducing its auto-phosphorylation (Ge et al., 2002). This pathway requires upstream activation by the ubiquitin ligase TRAF6, and operates in response to inflammatory and stress signals (Ge et al., 2002). Because these signals also activate p38 by the canonical MAPK cascade, the need for TRAF6-TAB1 dependent activation of p38 is unexplained. Importantly, TAB1 was also reported to induce p38 auto-phosphorylation in response to AMPK activation in mouse ischemic cardiomyocytes (Li et al., 2005), but two subsequent studies in the same experimental system challenged the former report (Jacquet et al., 2007; Jaswal et al., 2007). Whether TRAF6, which was shown to be important for optimal AMPK activation in mouse T cells (Pearce et al., 2009), may also be involved in this latter mechanism is not known. In this regard, I will describe in this thesis a third pathway for the activation of p38 in T cells that relies on AMPK/TAB1 and spontaneously maintains human T cell senescence.

1.7 Human T Cell Senescence

Because thymic involution occurs in early adulthood, when the thymus is progressively replaced by non-functional adipose tissue, the extra-thymic output of naïve (that is, before antigen-presentation) allo-reactive mature T cells severely constraines during ageing (Boraschi et al., 2013a; Goronzy and Weyand, 2013). However, the human naïve T cell repertoire is maintained throughout life, possibly through mechanisms of homeostatic proliferation and/or long-term survival (Goronzy et al., 2015). Importantly, the cytokine IL-15 and IL-7 have been identified as important factors which regulate the maintance of the overall $CD8^+$ and $CD4^+$ T cell pool *in vivo* (Ku, 2000; Seddon et al., 2003). IL-15 can also induce re-expression of CD45-RA within the human memory $CD8^+$ T cell comportament and has been proposed to act as a quiescence inducing signal (Libri et al., 2011). However, the concept that homestatic proliferation and long-term survival are mediated by the same signaling pathways has been challenged (Seddon et al., 2000). Mice with genetic disruption of the key proximal TCR signaling kinase LCK retain long-term survival but show defective homeostatic proliferation *in vivo* (Seddon et al., 2000).

In humans, the function of elderly naïve T cells, for example their capacity for TCR activation and IL-2 release, is dampened because of a variety of mechanisms including reduced TCR responsiveness and calcium influx due to a decrease in both ERK and JNK signalling (Li et al., 2012; Linton et al., 1996). Importantly, thymic involution also dictates that effector (that is, after antigen-presentation) human T cell populations have to be maintained by repeated episodes of expansion of antigen specific T cells followed by their clearance when the immune

challenge subsides (Akbar et al., 2004). Unlike most adult somatic cells, human T lymphocytes are able to re-activate telomerase (a RNA-dependent DNA polymerase which extends the telomeres; described in section 1.9) upon antigenic challenges and this is essential for the life-long preservation of their proliferative potential *in vivo* (Hodes et al., 2002). However after repeated episodes of activation, T cells progressively differentiate and lose the capacity to up-regulate the enzyme telomerase, which leads to telomere erosion, loss of proliferative capacity and ultimately telomere-dependent senescence (**Figure 5**) (Akbar and Vukmanovic-Stejic, 2007). The proof of principle of the importance of telomerase in T cell differentiation comes from studies in which enforced telomerase expression in human $CD8^+$ T cells significantly delayed the onset of replicative senescence without introducing genetic abnormalities or loss of functional activity (Plunkett et al., 2005).

Highly differentiated, senescent T lymphocytes that have lost expression of both CD27 and CD28 co-stimulatory receptors accumulate in old humans, in patients with chronic viral infections, autoimmune disorders and in those with malignancy (Crespo et al., 2013; Weng et al., 2009). The loss of CD28 expression characterizes about 10% of memory $CD4^+$ T cells and up to 50% $CD8^+$ T cells in humans and other primates, but not in rodents in which T cells stably maintain CD28 expression (Weng et al., 2009). Because CD28 is important for T cell interaction with antigen presenting cells (through CD80-CD86 binding), it is anticipated that loss of CD28 signalling during ageing impairs the formation of an active, functional immunological synapsis (Miller et al 2001; Henson, personal communications). The importance of both chronic T cell activation and CD28 loss in driving the senescence of human T lymphocytes, was highlighted by recent

studies from Plunkett *et al* investigating a group of young individuals (median age of 15 years) affected by an X-linked lymphoproliferative syndrome (XLP), due to a defect in the *SH2D1A* gene encoding for the SLAM-associated protein. These young patients showed accumulation of $CD28^-$ lymphocytes and very short telomeres, similarly to those of healthy old individuals, indicating that abnormal T cell proliferation may accelerate human T cell differentiation, leading to premature immune-senescence independently of the ageing process *per se* (Plunkett et al., 2007).

Besides prolonged antigen presentation, T cell differentiation *in vivo* is also accelerated by an inflammatory microenvironment, which in part contributes to the accumulation of highly differentiated senescent T cells in chronic viral infections and autoimmune disorders (Fujii et al., 2009). Also, it has been recently reported that chronic stimulation by the anti-proliferative cytokine Interferon-β can trigger p53-dependent DNA Damage Response (DDR) signalling and related senescence in human fibroblasts (Moiseeva et al., 2006), offering an interesting parallel with human T lymphocytes in which another Interferon, namely IFN-α, promotes terminal differentiation (Reed et al., 2004), inhibits telomerase activity (Akbar and Fletcher, 2005) and possibly activates senescence via an unknown mechanism.

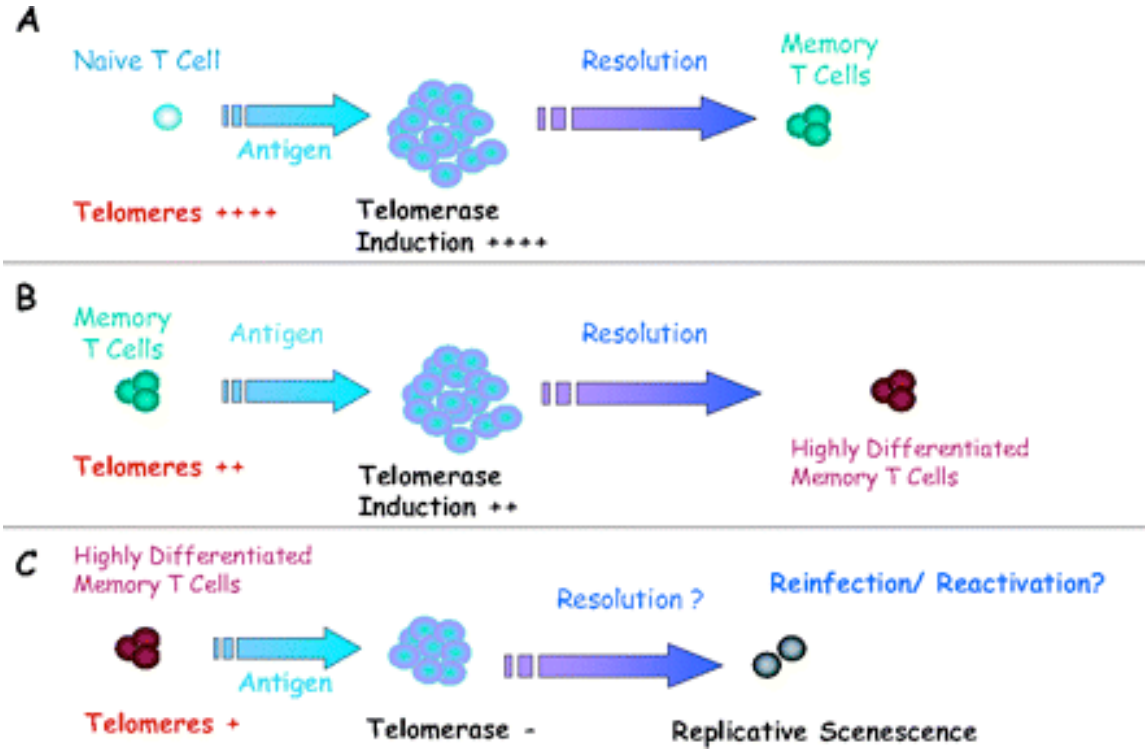

Figure 5: A model for the induction of human T cell senescence.

Naïve T cells potently induce telomerase upon activation that is important for their antigen specific expansion. When the immune challenge is resolved, effector populations contract becoming memory T cells. Memory T cells are long-term surviving cells and undergo repeated episodes of activation upon re-encountering a specific antigen. However following repeated episodes of activation, memory T cells progressively differentiate losing the ability to re-induce telomerase, until a maximum extent at which they become highly differentiated (senescent) T cells that cannot reactivate telomerase even if challenged. As a result, highly differentiated T cells have very short telomeres, activate DNA damage responses and approach replicative senescence *in vivo*. These cells accumulate in the elderly however their role in immunity is not clear. Permission to reproduce this image has been granted by (Akbar et Vukmanovic-Stejic, 2007).

1.8 IFNα: a bridge between immune modulation and senescence?

In response to viral infections, eukaryotic cells release anti-inflammatory and immune-modulatory cytokines known as interferons (IFNs). There are two main groups of IFNs: type I and type II IFNs (Platanias, 2005). There are six different type I IFN genes: IFN-α, IFN-β, IFN-γ, IFN-δ, IFN-ε and IFN-ω (Platanias, 2005). There is only one type II IFN gene that is IFN-γ (Platanias, 2005). In immune cells, IFN synthesis is mainly orchestrated through the Toll-like receptors (TLR) that are part of innate immunity and react toward highly conserved and redundant components of pathogens by activating different transcription factors and effector molecules, such as NF-κ-B and MyD88 (Borden et al., 2007).

The IFN receptor transduces signals from all IFN gene products and consists of two sub-units (IFNAR1 and IFNAR2) that are coupled to the cytosolic tyrosine kinases TYK2 and JAK1 (Borden et al., 2007). As anticipated from other immune-modulatory cytokines, IFNα also acts via the STAT transcription factor family, in particular STAT1 and STAT2 (Meyer, 2009). However, STAT-independent mechanisms are also involved in mediating IFN-α activity, especially through the activation of p38 MAPK. Indeed, blocking p38 signalling by either enforced negative-dominant expression or chemical inhibitors prevent the induction of IFN-α responsive genes (that are, gene-clusters controlled by interferon responsive elements or IRE sequences) (Platanias, 2005). Importantly, p38 blockade does not interfere with IFN-α driven modulation of STAT1/2 activity and related functional outcome, indicating that MAPK and STAT activation cascades by IFN-α are independent.

In humans, IFN-α is produced by plasmacytoid dendritic cells and modulates both innate and adaptive antiviral immunity (Ferrantini et al., 2007; Meyer, 2009). In

both human $CD4^+$ and CD8+ T cells, IFN-α drives important immune-modulatory effects. Firstly, it induces the down-modulation of CD27 and CD28 co-stimulatory receptor expression (Fletcher et al., 2005). Secondly, it accelerates telomere shortening and inhibits telomerase activity (Fletcher et al., 2005; Xu et al., 2000). Thirdly, it potentiates cytotoxic $CD8^+$ T cell killing activity (Brassard et al., 2002). Reed *et al* recently showed that IFN-α down-regulates telomerase activity of skin antigen-specific $CD4^+$ T cells, which may constrain memory T cell expansion that is important for life-long immune protection (Reed et al., 2004).

Among various chronic viral infections, that caused by cytomegalovirus (CMV) is particularly efficient at inducing IFN-α production, which accelerates human T cell differentiation, inhibits telomerase activity and leads to the accumulation of antigen-specific yet hypo-responsive T lymphocytes (Fletcher et al., 2005). Understanding the molecular bases of IFN-α mediated telomerase down-modulation may thus uncover novel interventional targets to boost immune responses during ageing and mitigate immune-senescence. Below, I introduce the enzyme telomerase and discuss its importance, mechanism of action and regulation.

1.9 Telomeres and telomerase

The ends of the eukaryotic chromosomes are characterized by repeated hexameric sequences of GT-rich nucleotides known as telomeres that provide genomic protection and stability (Blackburn, 2000). Functional telomeres require minimal telomere length (above 4-kilo bases (kb)), an intact G-rich 3' DNA overhang and the interaction with specific telomere-binding proteins, the shelterin

(Blasco, 2005). This complex consists of six different proteins (TRF1, TRF2, hRAP1, TIN2, TPP1 and POT1) that negatively regulate the access of the enzyme telomerase at the telomere by both T and D loop formations, structures that impede telomerase-telomere interaction (de Lange, 2009). Although telomeres also interact with the DNA-damage repair machinery of the cell, it has been recently shown that any DNA damage that occurs at the site of the telomere is irreversible and triggers DNA damage responses leading to proliferative arrest, characteristic of replicative senescence (Fumagalli et al., 2012). Importantly, when telomeres become critically short after repeated cell divisions, senescent cells spontaneously activate DNA damage response (DDR) cascades and the replicative capacity ceases (Campisi and d'Adda di Fagagna, 2007). This can be delayed by the up-regulation of the enzyme telomerase, a RNA-dependent DNA polymerase firstly identified in 1985 in the protozoa *Tetrahymena Thermophila* (Greider and Blackburn, 1985). The holo-enzyme, which consists of a catalytic core (hTERT) and a RNA template (hTR or hTERC), acts by physically binding to and extending the G-rich 3' DNA overhang of the telomere, to replenish the loss of genetic material that is due to the semiconservative mechanism of DNA replication (Verdun and Karlseder, 2007). **Figure 6** illustrates a schematic representation of telomerase function.

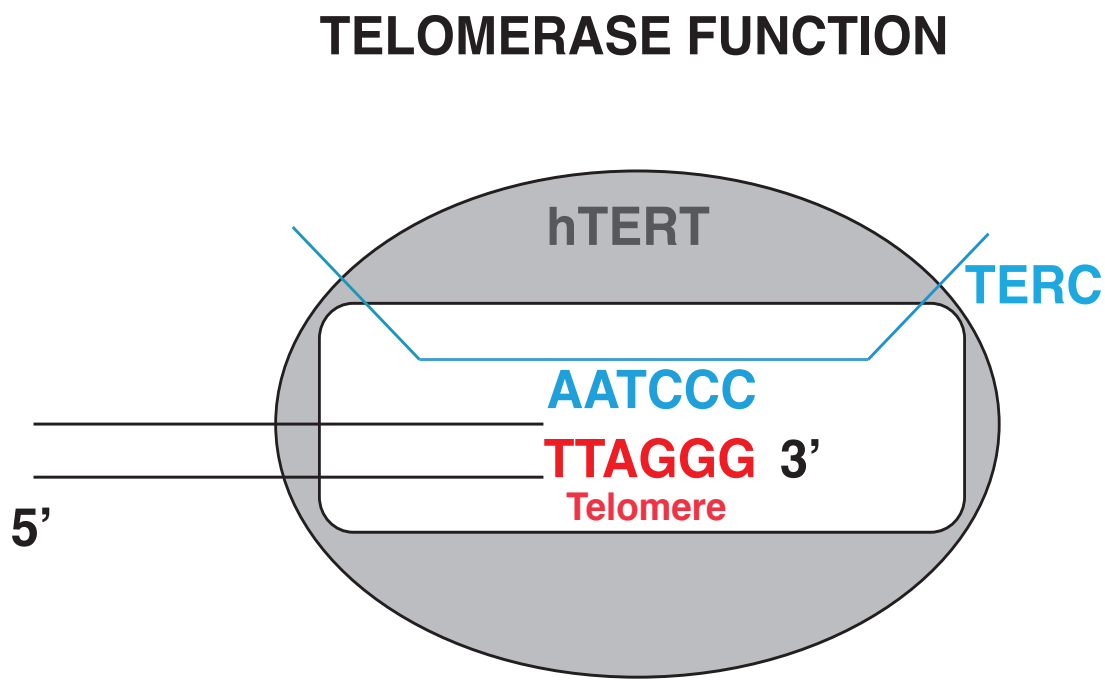

Figure 6: Telomerase function.
The telomere-telomerase complex is shown. Telomerase is a RNA dependent DNA polymerase that extends telomeric DNA at each cell division, preventing telomere shortening. Telomerase function requires both a catalytic subunit (hTERT) and a RNA component (TERC) that directly binds to the single strand 3’ overhangs at the end of eukaryotic chromosomes. Details of telomerase function are provided in the text.

Briefly, because DNA synthesis is unidirectional (5’-3’) (Watson, 1971), each DNA duplex is characterized by one strand that is processed *in toto* (leading strand) while the synthesis of the complementary strand is delayed (lagging strand), giving rise to the Okazaki fragments (which are DNA sequences of 50-100 nucleotides bound to a RNA primer; **Figure 7**). Telomere shortening can be therefore defined as the biochemical reaction occurring at each lagging strand, due to the degradation of the terminal Okazaki fragment, and accounts for the loss of about 50-100 bp of DNA at each cell division. Hayflick was the first to identify the existence of a limit, imposed by mechanisms of telomere erosion, to the extent at

which mammalian cells can proliferate (Hayflick limit) (HAYFLICK and MOORHEAD, 1961). This dictates that adult somatic cells in which telomerase activity is generally very low or undetectable, reach replicative senescence after about 50 cell passages *in vitro* (HAYFLICK and MOORHEAD, 1961). Conversely, elevated telomerase activity in cancer cells confers virtually unlimited proliferative potential (Cong et al., 2002). Fine-molecular tuning of telomerase is therefore needed to control mammalian cell proliferation and ensure a balance between the delaying of cellular senescence and the risk of developing malignancy. Below, I briefly discuss the current understanding of the main mechanisms controlling telomerase expression, nuclear import and activation.

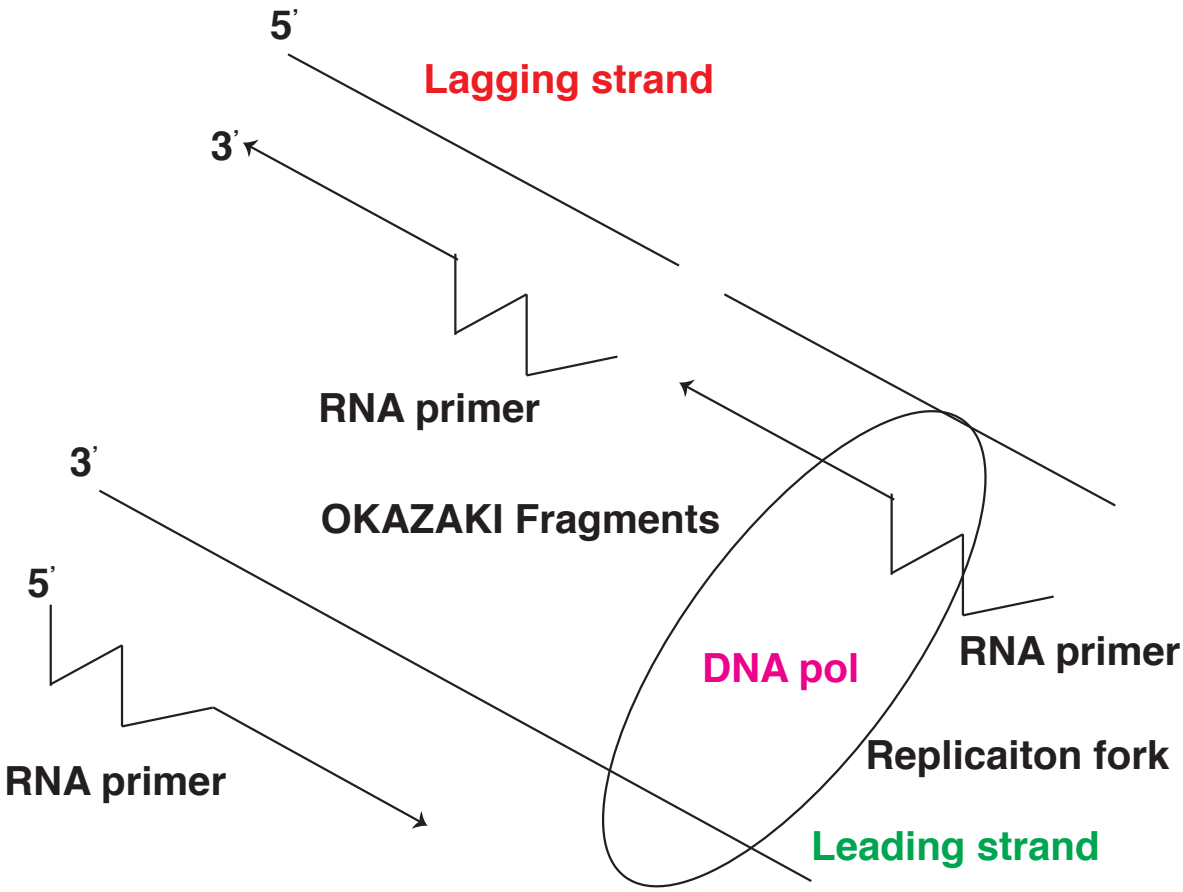

Figure 7: The semi-conservative mechanism of eukaryotic DNA replication.
The mechanism of DNA replication is shown. Helicase activity (not shown) renders parental DNA available to binding by the DNA polymerase within the replication fork to extend 3'-OH of RNA primers on both leading and lagging strands; topoisomerase activity assists this process removing eventual positive or negative super-loops that would impede DNA replication (not shown). Note that while the DNA lagging strand is synthesized from a single RNA primer (bottom), multiple RNA primers are required on the complementary DNA leading strand instead (top), since the activity of the DNA replication fork possesses opposite polarity to the synthesis of this strand. Thus, multiple RNA-DNA hybrid Okazaki fragments originate during lagging strand synthesis. The degradation of the terminal Okazaki fragment is responsible for telomere shortening at each cell division (discussed in the text).

1.10 Complexity of telomerase regulation: transcriptional and post-translational mechanisms.

The biological importance of telomerase is highlighted by the complexity of both transcriptional and post-translational mechanisms tuning the expression of its catalytic sub-unit, hTERT (Tesmer et al., 1999). The hTERT promoter is well characterized and comprises binding sites for both inhibitory and activatory transcription factors (**Figure 8**) (Kyo et al., 2008). For instance, the transcription factor c-MYC binds to the hTERT promoter at regulatory sites known as 'E-boxes', hence inducing hTERT transcription (DePinho et al., 1991). This has been well documented in studies where elevated hTERT expression was directly induced by increased c-MYC activity, in cancer cells (Kyo et al., 2008). Between the E-boxes, the hTERT promoter possesses at least five distinct GC-rich DNA sequences (CpG islands) that are important for Sp1-mediated hTERT up-regulation. Similarly, the p65 sub-unit of the transcription factor NF-KB has been reported to up-regulate hTERT expression (Akiyama et al., 2003), however the precise binding regulatory site has not been identified. Conversely, E2F1 is an inhibitor of hTERT transcription, and four related binding sites have been identified, in which its action is coordinated by the histone deacetylase HDAC (Crowe, 2001). It is also well recognized that the tumour suppressor p53 inhibits hTERT expression, possibly preventing the binding of Sp1 to the hTERT promoter (Xu et al., 2000).

Although the transcriptional regulation of hTERT has been initially considered the sole regulatory mechanism, it has recently arisen that post-translational mechanisms are also involved in telomerase regulation (see also **Figure 8**). In accordance with this, Liu and colleagues firstly reported the existence of notable differences between the levels of hTERT transcripts and telomerase activity in

human lymphocytes (Liu et al., 2001). In an extension of this work, the kinase AKT has been shown to phosphorylate hTERT (at 220-GARRRGGSAS-229 and 817-AVRIRGKSYV-826 sites), a process required for its nuclear import and activity (Kang et al., 1999). Indeed, defective AKT signalling is a molecular feature of human highly differentiated T cells that have low telomerase activity (Henson et al., 2009; Plunkett et al., 2007). In addition to AKT, hTERT also binds to mTOR; this interaction can be disrupted by PP2A activity, a tumour suppressor phosphatase that dephosphorylates AKT and possibly also hTERT (Li et al., 1997). More recently, reports on the existence of AKT-independent mechanisms in controlling telomerase activity in human highly differentiated T cells that in part involve spontaneous activation of p38 MAP kinase through an unknown mechanism (Di Mitri et al., 2011). Intervention at the point of telomerase regulating pathways may be important to restore immune cell function during ageing. Below, I describe the senescence response and highlight the many knowns and unknowns that characterize it.

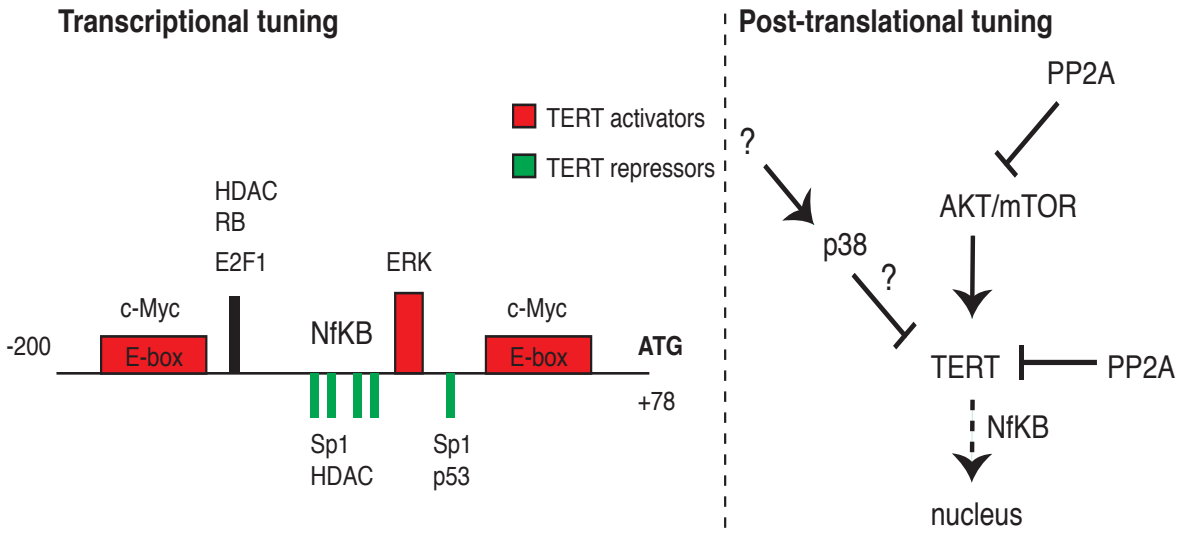

Figure 8: Molecular tuning of telomerase.

An overview of both transcriptional (*left*) and post-translational mechanisms (*right*) regulating the catalytic subunit of telomerase hTERT is shown. An extract (sites comprised between -200 and +78) of the telomerase catalytic sub-unit hTERT gene is reproduced, depicting the main transcriptional activators (c-MYC, Sp1, NFkB, and ERK) and repressors of hTERT expression (p53, E2F1, phosphorylated Rb and HDAC). Various regulatory elements have been identified within the hTERT promoter that directly or indirectly interacts with transcriptional regulators; the role of both E-box sites binding to c-MYC and Sp1-binding sites between the E-boxes is described in the text. NFkB promotes hTERT transcription but the precise binding on the hTERT promoter has not been identified. ATG in bold indicates gene hTERT start. The post-translational tuning of telomerase is less well characterized; AKT can directly phosphorylate hTERT promoting its nuclear import; mTOR binds to hTERT and promotes its activity through an unknown mechanism; NfKB promotes hTERT nuclear import; PP2A inhibits telomerase activity by de-phosphorylating both AKT and hTERT; and p38 has been proposed to inhibit telomerase but bot upstream and downstream signals regulating this process have not been identified.

1.11 Ageing and Cellular Senescence

The reasons for ageing, the progressive detrimental decay of cellular and tissue homeostasis, are presently unknown. However various types of non-dividing, senescent cells significantly accumulate during ageing (van Deursen, 2014). Ageing and senescence are evolutionary regarded as an important example of antagonistic pleiotropy, which characterizes a mechanism (senescence) that protects young organisms from cancer at the expenses of their own ageing (Campisi and d'Adda di Fagagna, 2007). Three progressive phases characterize the senescence response (**Figure 9**). In order, senescence is caused by the accumulation of persistent DNA damage (phase 1), related activation of the DDR pathway in cell (phase 2), eventually leading to growth arrest (phase 3) (Akbar and Henson, 2011). DNA damage can originate at the telomere (e.g. due to the progress towards the Hayflick limit), and this is defined as telomere-dependent senescence (d'Adda di Fagagna et al., 2003). Conversely, when the source of DNA damage is not due to telomere shortening, the process is known as telomere-independent senescence. In such cases, DDR signalling can be induced by ionizing radiations, oxidative stress, growth factor deprivation and aberrant oncogene activation. Of note, there are also important differences in the senescence manifestations in both humans and rodents, in that rodents maintain significantly longer telomeres than humans, suggesting that telomere-independent mechanisms of senescence may be an important regulator of the short mouse life span (Kipling, 2001). Whether telomere-dependent and independent senescence rely on the same signalling pathways remains elusive, although it appears that p53 activation may be an essential downstream component of an effective DDR. Mechanistically, DDR signalling occurs at active DDR foci which comprise a

complex of DDR-sensors (such as: RPA, RPC, the 911 and MRN complexes), activation of the apical kinases ataxia telangiectasia mutated (ATM) and ATM and RAD-3 related (ATR) and downstream phosphorylation of chromatin re-modellers (e.g. H2AX) and other kinases (CHK1/2) (Fumagalli and d'Adda di Fagagna, 2009). Although there is now ample evidence that senescence is an anti-cancer mechanism, elevated secretory activity in senescent cells can in turn alter the tissue microenvironment through paracrine signalling (e.g. stimulating angiogenesis), which may paradoxically lead to neoplastic transformation of the surrounding cells (Campisi and d'Adda di Fagagna, 2007). The set of inflammatory factors that are secreted by senescent cells (e.g. IL-6, IL-8, TNF, metallo-proteins) is known as 'senescence-associated secretory phenotype' (SASP), and at least in fibroblasts, is controlled by active p38 MAPK signaling (Freund et al., 2011). Notably, SASP does not only contribute to tissue remodelling yet also reinforces senescence itself, in an autocrinous manner (Acosta et al., 2008). Importantly, the current understanding on the biochemical processes regulating senescence is mainly based on studies of senescent fibroblasts; it is presently unknown whether the DDR and/or the SASP may be regulated by identical mechanisms in different cell types. If so, this may lead to setting up a common strategy for reversal of senescence in different tissues.

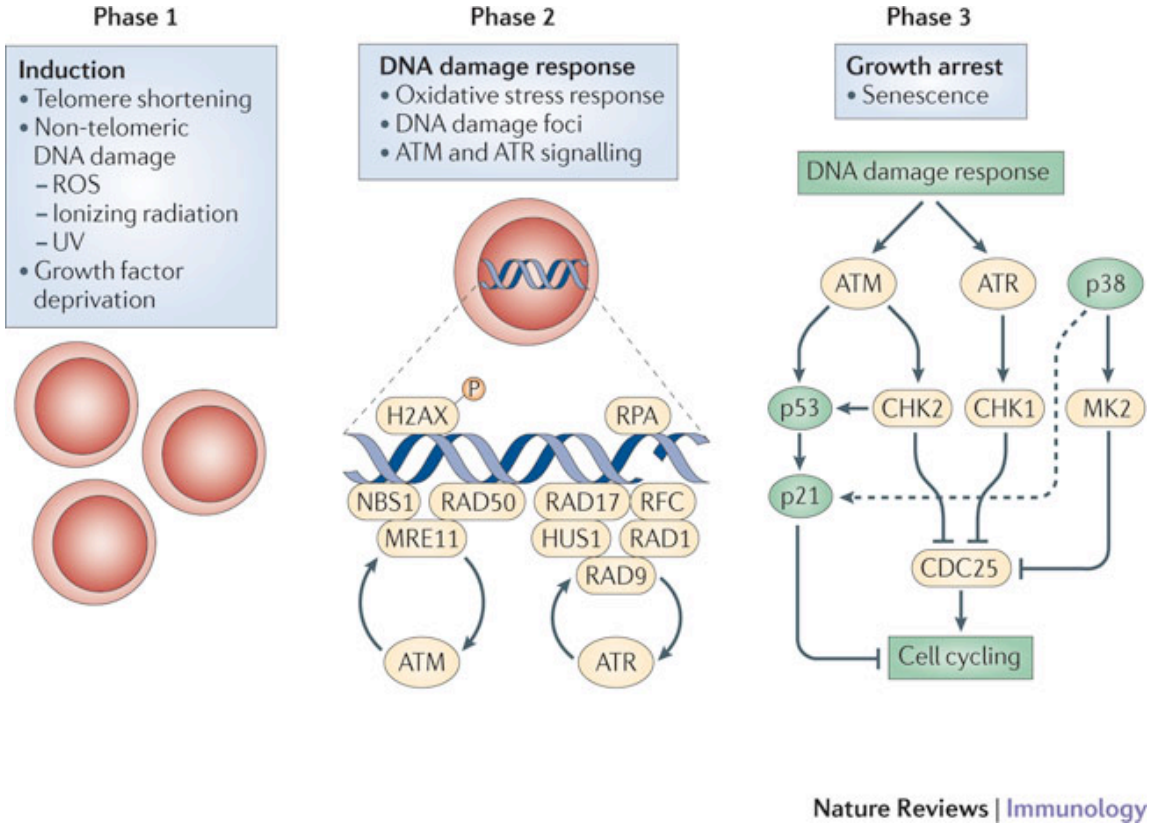

Figure 9: The three-phase model for the induction of cell senescence.

Induction of cellular senescence. In phase 1, persistent (telomeric or non telomeric) DNA damage occurs and triggers the activity of the apical kinases ATM and ATR that in turn activate and recruit a plethora of DNA damage sensors at the level of DDR foci (phase 2). Various biochemical effectors downstream of ATM/ATR mediate the DNA damage response; and on the basis of the extent, nature, and localization of the damage, DDR signalling triggers different physiological outcomes, leading to apoptosis, transient cell cycle arrest or senescence (irreversible growth arrest, phase 3). The exact mechanism determining the specific activation of any of these programs remains elusive. The most important components of the figure are discussed in more detail in the text. p38 MAPK activation may be involved in the senescence response, possibly upstream of p53-p21, but its role is not firmly established. Activation of the transcription factor p53 seems to be a foundamental biochemical requirement for generation of the robust, persistent DNA Damage response characterizing senescence. Permission for reproducing this picture has been granted by (Akbar & Henson, 2011)

1.12 Cell cycle regulation: implications for cellular senescence.

The study of cellular senescence is directly linked with the modulation of the cell cycle machinery. Proliferating cells distribute within four distinct, highly regulated phases: the G1 (for anabolic growth), S (for DNA synthesis), G2 (in preparation to mitosis) and M phase (during which mitosis (or cell division) occurs) (Chandler and Peters, 2013). The transitions from each of these phases, especially the G1/S and G2/M transitions, are tightly regulated in cell. However because senescent cells accumulate DNA damage, they are mostly retained within the G1 part of the interphase (that is, the time spent by proliferating cells between two consecutive M phases) to avoid synthesis of irreversibly damaged DNA (d'Adda di Fagagna et al., 2003). Because G1 cycling-cells engage anabolic reactions, it is well recognized that senescent cells retain high metabolic activity and significantly enlarge (Campisi and d'Adda di Fagagna, 2007). In fribroblasts, senescence appears to be regulated by active mTOR signalling (Laberge et al., 2015). Downstream of the DDR and in addition to p53 activation, there are important events to induce (or maintain) senescence. This includes changes in the phosphorylation and/or expression of the retinoblastoma protein (pRB), as well as the coordinated down-modulation of cyclins (e.g. D, E) and up-regulation of cell-cycle inhibitors (e.g. p21, p27), that dictate the proliferative arrest of senescent cells at the G1 phase (Giacinti and Giordano, 2006). In particular, the abundance of under-phosphorylated pRb levels is perhaps the most recognized regulator of cell-cycle progression. In dividing cells, pRb is phosphorylated by various cyclin dependent kinases (CDKs), therefore losing the ability to bind and inhibit E2F1, which leads to the G1/S transition (Giacinti and Giordano, 2006). In senescent cells, persistent

p53 activation antagonizes this mechanism through the transcription of p21, an inhibitor of CDKs, resulting in lower pRb phosphorylation and cell cycle termination (Riley et al., 2008). Despite the well-recognized role of p53 in the senescence response, the exact mechanism linking DDR and p53 signalling is not clear. Also, how cells decide to undergo either apoptosis (that is, the programmed cell death on genetic bases) or senescence that are both controlled by p53 activation in response to irreversible DNA damage remains elusive. Inactivating mutations in any cell cycle related mechanism favour neoplastic transformation, indicating that cell cycle regulators act as tumour suppressor genes (Fumagalli and d'Adda di Fagagna, 2009). The relationship itself between senescence and apoptosis appears to be cell type dependent, in that senescent fibroblasts yet not leukocytes are apoptosis-resistant (Akbar and Henson, 2011). However the mechanisms regulating senescence in leukocytes remain poorly defined. In this study, unrecognized mechanisms of senescence in primary human $CD4^+$ T cells have been identified.

1.13 AIM OF THE WORK

The worldwide demographic shift towards an older age is associated with an increase in the incidence and severity of many infectious diseases (Pawelec et al., 2005; Wikby et al., 2002). This is attributed to the decline of immunity during ageing (Akbar et al., 2004; Weng, 2006). A global challenge therefore is to identify mechanisms involved with immune dysfunction and to identify ways to restore immunity during ageing. The loss of telomerase and proliferative potential are well-recognized yet mechanistically poorly defined hallmarks of human senescent T cells. The aim of this PhD was to identify mechanisms involved in human T cell

senescence and whether intervention is possible to restore telomerase and proliferative activity in these cells.

To achieve this goal, three related strategies were conceived:

1) Identifying mechanisms of telomerase down-regulation by an inflammatory signal, IFNα, which is known to accelerate human T cell differentiation both *in vitro* and *in vivo*.

2) Understanding in parallel the upstream regulatory network of a signalling molecule, p38 MAPK, which is shown to be required for telomerase down regulation in both IFN-treated T cells and natural occurring senescent T cells.

3) Restoring telomerase and proliferation in human senescent T cells by both genetic and pharmacological modulation of a novel T cell p38 MAPK activation pathway.

Here I found evidence to challenge the current paradigm for activation of p38 in human T cell populations and I present a previously unrecognized mode of MAPK activation in T cells. This, a prototype mechanism linking immune-modulation, senescence, metabolism and cancer. Thus, the present study contributes to enhance our understading on both human ageing and senescence, with the potential to reverse it.

CHAPTER II: Materials and Methods

2.1 Cellular Biology

2.1.1 Isolation of Peripheral Blood Mononuclear Cells (PBMC)

Heparinized peripheral blood samples were taken from healthy volunteers (aged 25-65, median 52, male 55% and female 45%; n=85). All samples were obtained with the approval of the Ethical Committee of Royal Free and University College Medical School and voluntary informed consent was obtained in accordance with the Declaration of Helsinki. Donors did not have any co-morbidity, were not on any immunosuppressive drugs, and retained physical mobility and lifestyle independence. Peripheral blood mononuclear cells (PBMC) were isolated by gradient separation based on the addition of Lymphoprep™ (Axis-Shield) to fresh blood. Blood was diluted 1:4 using Dulbecco's Phosphate Buffered Saline solution (D-PBS) and carefully layered on 20 mL Lymphoprep gradient in 50-mL Falcon tubes. Samples were then centrifuged at 2000 rpm for 20', brake-off, which resulted in erythrocytes sedimentation and mononuclear cell-ring layering at the interface between (enucleated) erythrocytes on the bottom and plasma on the top of the tubes. Next the mononuclear cell-ring was aspired. PBMC were then washed 3 times in D-PBS for 30', 20' and 15' respectively, to remove Lymphoprep contamination. Cells were then resuspended in 10 mL of either Magnetic Activated Cell Sorting buffer if further isolated (MACS buffer, filtered and ready to use, Miltenyi Biotec) or D-PBS, counted and used for downstream applications.

2.1.2 Cell counting

Cells were diluted using Trypan-blue dye (Life Technologies 15250-061), to which only dead cells are permeable, loaded onto on a Haemocytometer and counted on a light microscope. Cells within 2 large grids were enumerated and total cell number was assessed using the formula:

$N = n * D/ 10^4$

where *N* is cell concentration per mL, *n* is the number of cells counted in the grids and *D* is the cell dilution factor.

2.1.3 Isolation of human $CD8^+$ or $CD4^+$ T cells

Primary human $CD4^+$ and $CD8^+$ T lymphocytes were isolated from PBMC preparations by immunomagnetic separation. Cells were isolated by either 'positive' or 'negative' selection. In the former procedure, PBMC were pelleted by centrifuging at 1600 rpm for 7' and, after supernatants were discarded, resuspended in 80 μl of MACS buffer per 10^7 cells followed by addition of 20 μl of magnetic microbeads bound to monoclonal antibody to either CD4 or CD8 receptor (CD4 or CD8 Microbeads, Miltenyi Biotec). Receptor labelling was then allowed by incubating cells 15' in the fridge (between 4-8° C). Next, cells were washed by adding 1-2 mL of MACS buffer per 10^7 cells and centrifuged at 1200 rpm for 10'; and after supernatants being discarded, resuspended in 500 μl of MACS buffer per 10^8 cells. Meanwhile, LS-magnetic separation columns (130-042-401, Miltenyi Biotec) were allocated in a magnetic MACS Separator (Miltenyi Biotec) and equilibrated by 3 consecutive washes using 3 mL of MACS buffer. At this stage, cell suspensions were loaded through the equilibrated columns, followed by 3 consecutive washes using 3 mL of MACS buffer. The unlabelled

fraction containing $CD4^-$ or $CD8^-$ cells was then discarded and columns were displaced from the magnetic separator and the labelled cell fraction was instead flushed off the column into a falcon tube with 5 mL of MACS buffer. Cell purity (above 95%) of either $CD4^+$ or $CD8^+$ T cell populations was assessed by flow-cytometry.

For $CD4^+$ T cell isolation followed by further purification into the CD27/CD28 relative sub-populations, 'negative selection' was used. PBMC pellets were resuspended in 40 μl of MACS buffer per 10^7 cells and incubated with 10 μl of biotin-conjugated antibody cocktail (130-096-533, Miltenyi Biotec) against CD8, CD14, CD15, CD16, CD19, CD36, CD56, CD123, TCRγ/δ, and CD235a (Glycophorin A) per 10^7 cells (that is, to magnetically label all mononuclear immune cell types, except $CD4^+$ T cells). Receptor labelling was then allowed for 5' in the fridge. Next, 30 μl of MACS buffer per 10^7 cells were added to cell suspensions along with 20 μl/10^7 cells of MicroBead cocktail bound to monoclonal antibody to biotin and CD61 (130-096-533, Miltenyi Biotec). Cells were incubated for additional 10' in the fridge. Subsequently, cells were washed by centrifuging at 1200 rpm for 10', resuspended in 500 μl MACS buffer and loaded on equilibrated LS-magnetic columns as above described. The columns were eluted by 3 consecutive washes using 3 mL of MACS buffer and, at this time, elutes containing 'untouched' $CD4^+$ T cells were collected. Cell purity (above 95%) was verified by flow-cytometry.

2.1.4 Isolation of CD27/CD28 related subsets of human $CD4^+$ T cells

The relative expression of CD27 and CD28 receptors identifies three separate populations of human $CD4^+$ T cells directly *ex vivo*. To begin to isolate relatively undifferentiated $CD27^+$ $CD28^+$ $CD4^+$ T cells, the above-purified 'untouched' $CD4^+$ T cell population was pelleted by centrifugation and resuspended in 80 μl of MACS buffer per 10^7 cells followed by the addition of 20 μl/10^7 cells of MicroBeads conjugated to monoclonal antibody to CD27 receptor. Receptor labelling was then allowed for 15' in the fridge. Cells were washed in 2 mL MACS buffer per 10^7 cells by centrifugation and then resuspended in 500 μl MACS buffer. Cell suspensions were loaded into LS columns, equilibrated as above described, and eluted were downstream collected in a falcon tube by 3 consecutive washes using 3 mL MACS buffer each time. The unlabelled cell fraction contained both intermediate differentiated $CD27^-$ $CD28^+$ and highly differentiated (senescent) $CD27^-$ $CD28^-$ $CD4^+$ T cells (that is, because human $CD4^+$ T cells first lose CD27 followed by CD28 expression during their differentiation). Instead, positively labelled cells retained by the column were flushed off the columns into a falcon tube. These cells were relatively undifferentiated (non-senescent) $CD27^+$ $CD28^+$ $CD4^+$ T cells.

To continue to isolate intermediate differentiated $CD27^-$ $CD28^+$ and highly differentiated (senescent) $CD27^-$ $CD28^-$ $CD4^+$ T cells, elutes were counted, pelleted by centrifugation and resuspended in 100 μl of MACS buffer per 10^7 cells followed by addition of 10 μl/10^7 cells of magnetic, PE-conjugated monoclonal antibody to CD28 receptor. Receptor labelling was then allowed for 15' in the fridge. Next, cells were washed by centrifugation in 2 mL of MACS buffer per 10^7 cells, and again resuspended in 80 μl of MACS along with 20 μl of anti-PE beads,

per 10^7 cells. Cells were incubated in the fridge for additional 15', followed by washing and re-suspension in 500 μl MACS buffer. Cell suspensions were loaded into MS-columns (130-042-201, Miltenyi Biotec) equilibrated by rinsing with 500 μl of MACS buffer. Columns were eluted into a falcon tube by 3 consecutive washes using 500 μl of MACS buffer each time. Elutes were $CD27^-$ $CD28^-$ $CD4^+$ T cells. To flush off the column and collect the CD28 positively labelled population, 1 mL of MACS buffer was used. These cells were $CD27^-$ $CD28^+$ $CD4^+$ T cells. Cell viability was assessed by tripan bue exlusion test. A representative purity profile depicting the dichotomy between non-senescent and senescent T cell populations on which this work is based is shown in **Supplementary Figure 1**. These cells were then analysed for functional or signalling readouts either directly *ex vivo* or upon genetic modifications, as described below.

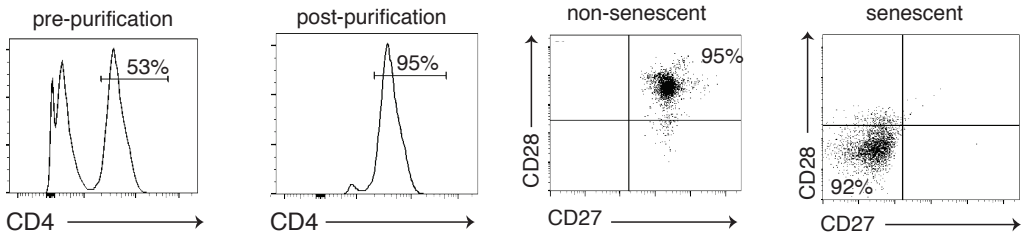

Fig. S1: Purity of non-senescent *versus* senescent $CD4^+$ T cells.

2.1.5 Human T cell activation

Primary human $CD4^+$ and $CD8^+$ T lymphocytes were cultured in RPMI 1640 medium supplemented with 10% heat-inactivated FCS, 100 U/ml penicillin, 100 mg/ml streptomycin, 50 μg/ml gentamicin, and 2 mM L-glutamine (all from

Invitrogen) at 37°C in a humidified 5% CO_2 incubator. Cell culturing was set up in 24, 48 or 96 well-plates (according to cell numbers) that were previously 'coated' for 2 hours at 37° C, using a solution of anti-CD3 antibody (αCD3, purified OKT3 clone; 86022706; Sigma-Aldrich) diluted in D-PBS at the concentration of 0.5 μg/mL, followed by gentle washing in D-PBS to remove the unbound antibody fraction. Human $CD4^+$ and $CD8^+$ T cell populations, counted and resuspended in complete medium at 10^6/mL, were seeded in the so-coated plates with the addition of either rh-IL2 (R&D Systems, 10 νg/mL) or anti-CD28 antibody (αCD28; 37407; MAB342; R&D Systems; 0.5 μg/mL), as indicated.

For activation of human $CD8^+$ T cells in the presence of IFN-α (R&D Systems), the cytokine was added at the beginning of the culture at the concentration of either 500 U/mL or 100 U/mL for either short-term (up to 72 hours) or long-term cultures, respectively. In long-term experiments, human $CD8^+$ T cells were re-activated every 10 days, at which time IFN-α (100 U/mL) was added back in culture.

For lentiviral vector transduction, primary human highly differentiated $CD27^-$ $CD28^-$ $CD4^+$ T cells were activated in the presence of plate-bound αCD3 (0.5 μg/ml) plus recombinant human IL-2 (10 ng/ml) and then, at 48 and 72 h after activation, were transduced with pHIV1-Siren lentiviral particles using a 10 multiplicity of infection (MOI, described below). Fresh medium was replaced every 2-3 days; and transduced cells were maintained in activation medium and analysed for functional readouts four days post-transduction (day 7). For long-term cultures, transduced cells were reactivated every 10 days in a new αCD3-coated plate and analysed up to 4 weeks later. Relatively undifferentiated $CD27^+$ $CD28^+$

$CD4^+$ T cells were cultured and transduced as their $CD27^-CD28^-$ counterparts were, but cells were activated by plate-bound αCD3 plus αCD28, both at 0.5 μg/ml.

2.1.6 Phenotypic Analysis

Isolated human $CD8^+$ and $CD4^+$ T Cells (between 10^5 to 10^6 cells) were resuspended in D-PBS additionated with 2% fetal calf serum (FCS) and then surface stained with anti-CD27 (337169; BD Biosciences) and anti-CD28 (348040; BD Biosciences), dilution 1:100. Cells were incubated 15' at room temperature in the dark. Next, cells were washed twice in D-PBS by centrifuging at 1600 rpm for 4', resuspended in 200 μl FACS buffer and immediately run using an LSR Fortessa (BD Biosciences).

2.1.7 Proliferation Assays

Proliferation of transduced highly differentiated $CD27^-$ $CD28^-$ $CD4^+$ T cells was assessed four days post-transduction (day 7) by either radioactive or non-radioactive based methods.

For radioactive measurement, cells were activated in 96-well plates and transduced as above described followed by over-night probing with the nucleotide analogue ^3H thymidine (Perkin Elmer 201112) diluted 1:400 in culture (= 0.5 μCi). The next day, cells were harvested onto a printed filtermat A (Perkin Elmer 1205-401) using a 96-well plate harvester (TOMTEC). Proliferation was determined as proportional to scintillation emission countering. Short-term proliferative activity is

presented as incorporation of ^{3}H thymidine (as count per minutes, c.p.m.) and results are means +/- standard error of triplicate means.

For non-radioactive measurement, a Cell-Trace Violet dye dilution assay, which binds to protein ammines, was used (C34557, Invitrogen). Dye dilution stock (5 mM) were made by re-suspending an anhydrous aliquot of dye in 18 μl of DMSO and used in culture at the final concentration of 5 μM. The working dye solution was added to freshly isolated cells prior to activation by incubation 20' at 37°C, protected from light. To remove any unbound dye, cells were then washed in 5 times the incubation volume with fresh medium containing 1% of proteins. Cells were washed by centrifugation, resuspended in fresh pre-warmed complete RPMI 1640 medium and incubated for additional 10' before stimulation, to allow intracellular acetate dye hydrolysis. Rate of proliferation of transduced cells was evaluated 96 hours post-transduction by flow-cytometry based analysis of the emission peaks of the diluted dye (between 405-450 nm) using an LSR Fortessa.

Alternatively, non-radioactive measurement of T cell proliferation was assessed by analysis of the cell cycle related Ki67 nuclear antigen, using the nuclear FoxP3 staining buffer (130-093-142, Miltenyi Biotec). Cells were fixed at room temperature for 15' using Fix/Perm Solution 1 diluted 1:4 in Fix/Perm Solution 2 (both provided with the kit). Cells were then washed twice by centrifugation in Stain Buffer (BD Biosciences) at 1800 rpm followed by permeabilization for 30' on ice using the kit-provided Permeabilization Buffer diluted 1:10 in ddH2O. During the permeabilization phase, cells were directly stained with fluorochrome-labeled

anti-Ki67 antibody (1:20, BD Bioscience). Next, cells were washed and immediately analyzed by flow-cytometry using a LSR Fortessa.

For long-term expansion rate, population doublings of transduced $CD27^-$ $CD28^-$ $CD4^+$ T cells were calculated as follows: log10 (number of cells counted after population expansion) – log10 (number of cells seeded) / log10 2.

2.2 Molecular Biology

2.2.1 Phospho Flow Analysis

After surface staining, cells (between 10^5 to 10^6 cells) were resuspended in Stain Buffer (BD Pharmingen) using 96 round well-plates and fixed for 10 min at 37 °C with warm Cytofix Buffer, diluted 1:1 (BD Biosciences). Cells were then washed by centrifuging at 1600 rpm for 4' and permeabilized for 30 min at 4 °C with 100 μl ice-cold Perm Buffer III (BD Biosciences). Next, cells were washed twice in Stain Buffer by centrifugation at 1600 rpm for 4' and then incubated for 30' at room temperature with phycoerythrin-conjugated antibody to p38 phosphorylated at Thr180 and Tyr182 (612565), phycoerythrin-conjugated antibody to γ-H2AX phosphorylated at Ser139 (562377), phycoerythrin-conjugated antibody to under-phosphorylated Rb (550502) and antibody to Rb phosphorylated at Ser807 and Ser811 (558549; all from BD Biosciences); and antibody to AMPKα phosphorylated at Thr172 (40H9), antibody to ATM phosphorylated at Ser1921 (D25E5), antibody to ATF2 phosphorylated at Thr71 (9221), antibody to p53 phosphorylated at Ser46 (2521), anti-cyclin D1 (DCS6) and anti-p27 (D69C12; all from Cell Signalling). Primary unconjugated antibodies were subsequently probed for 30 min at room temperature in the dark with a secondary antibody, either

phycoerythrin-conjugated goat anti–rabbit IgG (P-2771MP; Life Technologies) or fluorescein isothiocyanate-conjugated goat anti–rabbit IgG (65-6111; Life Technologies). Cells were finally washed in Stain Buffer and immediately analysed with a LSR Fortessa (BD Biosciences). In some experiments, cells were pre-incubated for 60 min with the AMPK agonist A-769662 (150 μM; Tocris Bioscience), the ATM inhibitor KU-55933 (10 μM; Calbiochem) or PMA (phorbol 12-myristate 13-acetate; 20 ng/ml; Sigma) before being fixed. Data were analysed with FlowJo software (TreeStar). For signalling studies with transduced cells, events were gated on the GFP^+ compartment.

2.2.2 Western Blot

For Western blot analysis of whole-cell extracts, purified primary human $CD8^+$ T cells were activated as abode described. Primary human $CD4^+$ T cells were sorted ex *vivo* immediately after separation into subsets defined by expression of CD27 and CD28. Alternatively, purified human highly differentiated $CD27^-$ $CD28^-$ $CD4^+$ T cells were harvested 4 days after transduction.

Cells were normalized by equal cell number enumeration and harvested by centrifuging 2 times at 1800 rpm for 15' followed by ultra-centrifugation at 13000 rpm for 2', at 4° C. Pellets from 2 x 10^6 cells were then dried and stored at -80°C. Lysates were obtained by incubating samples in 40 μl of RIPA buffer (Sigma Aldrich) followed by incubation on ice for 20'. Lysates were then cleared by ultra-centrifuging at 13000 rpm for 20' at which time supernatants containing protein extract were collected in fresh eppendorf tubes and either stored at -80° C (for not immediate use) or immediately stained with 10 μl of Protein Loading Buffer (0,25

M Tris-HCl, pH 6.8; 10% (p/v) SDS; 50% (p/v) glycerol; 0,05% (p/v) BBF; 0,5 M DTT), and samples were then boiled for 5' at 95°C to allow protein denaturation. Lysates were separated by protein electrophoresis at 120 V for 2 hours on 10% SDS-PAGE pre-cast gels (Invitrogen) using MOPS-SDS 1X running buffer (0,05 M MOPS; 0,05 M Tris; 0,1% (p/v) SDS; 1,025 mM EDTA); a 'rainbow' pre-stained protein marker (LC5800, Invitrogen) was loaded alongside to gel samples for molecular weight analysis. Next, proteins were transferred to Hybond-P membranes (Amersham Pharmacia Biotech, Piscataway, NJ) activated by rinsing 30'' in Methanol followed by 30'' in ddH2O. Protein transfer was done overnight in the cold room, using transfer protein buffer (25 mM Tris; 200 mM glycine; 20% (v/v) methanol) and assembling the so-displaced following elements (all soaked in transfer buffer) in the Western transfer machine (X-Cell II Blot Module from Invitrogen): 3 Whatman filter papers (Bio-Rad 170-39-32), 2 foams, the gel, the activated membrane and 3 Whatman filter papers plus 2 foams on top of this 'transfer sandwich'. The next day, membranes were pre-blocked using a blocking solution of 5% (p/v) Blocking Agent (Amersham Biosciences) in Tris/Tween-20 buffer (Tween/Tris buffered saline, T/TBS; 25 mM Tris; 0,15 M NaCl; 0,1% (v/v) Tween-20; pH 7.2). Membranes were then incubated over night in the cold room with the indicated western blotting antibodies (please see Table 1 below) diluted in blocking solution, followed by 3 washes of 15' each in T/TBS and incubation with secondary anti-mouse or anti-rabbit antibody (diluted 1:3000) in blocking solution for 1 hour at room temperature. Membranes were then rinsed 3 times 15' in T/TBS, incubated for 5' at room temperature with ECL Plus Western detection reagents (Amersham Pharmacia Biotech) and transferred into an autoradiography cassette. Time course exposures with x-ray films were executed followed by

automatic development. Prior to re-probing with different antibodies, membranes were stripped at 37°C in agitation using Restore™ Western Blot Stripping Buffer (Thermo Scientific), followed by extensive washing in T/TBS buffer for 60'. **Table 2** shows primary antibodies used for Western Blot analysis.

Table 2: Signalling antibodies used in Western Blot applications

Protein Target	Molecular Weight	Origin and Isotype	Dilution	Producer
p-Akt1/2/3 (Ser 473)	p-Akt 1: 60 kDa p-Akt 2: 56 kDa p-Akt 3: 60 kDa	Rabbit Polyclonal Antibody – IgG	1:200	Santa Cruz Biotechnology, inc.
p-Akt1/2/3 (Thr 308)	p-Akt 1: 60 kDa p-Akt 2: 56 kDa p-Akt 3: 60 kDa	Rabbit Polyclonal Antibody – IgG	1:200	Santa Cruz Biotechnology, inc.
Akt 1	62 kDa	Mouse Monoclonal Antibody – IgG_1	1:200	Santa Cruz Biotechnology, inc.
p-AMPK-α (Thr172)	62 kDa	Rabbit Polyclonal Antibody – IgG	1:1000	Cell Signaling Tech.
AMPK-α	62 kDa	Rabbit Polyclonal Antibody – IgG	1:1000	Cell Signaling Tech.
β-actin	42 kDa	Rabbit Polyclonal Antibody – IgG	1:200	Santa Cruz Biotechnology, inc.
DLG1	110 kDa	Rabbit Monoclonal Antibody – IgG	1:200	Santa Cruz Biotechnology, inc.
GAPDH	38 kDa	Rabbit Polyclonal Antibody – IgG	1:200	Cell Signaling Tech.
Histone H1	33 kDa	Mouse Monoclonal Antibody – IgG_{2a}	1:200	Abcam
GAPDH	38 kDa	Rabbit Polyclonal Antibody – IgG	1:200	Cell Signaling Tech.

LAT	38 kDa	Rabbit Polyclonal Antibody – IgG	1:1000	Cell Signaling Tech.
Lck	56 kDa	Rabbit Polyclonal Antibody – IgG	1:1000	Cell Signaling Tech.
MKK3	40 kDa	Rabbit Polyclonal Antibody – IgG	1:1000	Cell Signaling Tech.
MKK6	36 kDa	Rabbit Polyclonal Antibody – IgG	1:1000	Cell Signaling Tech.
p-MKK3/6 (Ser189/ Ser207)	p-MKK3: 40 kDa p-MKK6: 41 kDa	Rabbit Polyclonal Antibody – IgG	1:1000	Cell Signaling Tech.
p-p38 (Thr180/ Tyr182)	38 kDa	Rabbit Polyclonal Antibody – IgG	1:1000	Cell Signaling Tech.
Total p38-α	38 kDa	Rabbit Polyclonal Antibody – IgG	1:1000	Cell Signaling Tech.
p-p38 (Tyr 323)	38 kDa	Rabbit Polyclonal Antibody – IgG	1:1000	ECM-Biosciences
PP2A-α/β	36 kDa	Rabbit Polyclonal Antibody – IgG	1:200	Santa Cruz Biotechnology, inc.
p-PP2A (Thr307)	36 kDa	Rabbit Polyclonal Antibody – IgG	1:200	Santa Cruz Biotechnology, inc.
PLC-γ1	155 kDa	Rabbit Polyclonal Antibody – IgG	1:1000	Cell Signaling Tech.
SLP-76	76 kDa	Rabbit Polyclonal Antibody – IgG	1:1000	Cell Signaling Tech.
TAB1	TAB1-α: 60 kDa TAB1-β: 50 kDa	Mouse Monoclonal Antibody – IgG_1	1:1000	Cell Signaling Tech.
TAK1	78-82 kDa	Rabbit Polyclonal Antibody – IgG	1:1000	Cell Signaling Tech.
TERT	120 kDa	Rabbit Polyclonal Antibody – IgG	1:200	Santa Cruz Biotechnology, inc.

TRAF6	60 kDa	Rabbit Polyclonal Antibody – IgG	1:1000	Cell Signaling Tech.
Zap70	70 kDa	Rabbit Polyclonal Antibody – IgG	1:1000	Cell Signaling Tech.

2.2.3 Immunoprecipitation

For co-immunoprecipitation analysis, cell lysates were prepared by incubating samples 30' on ice with 200 μl of ice-cold HNGT buffer (50 mM HEPES, pH 7.5, 150 mM EDTA, 10 mM sodium pyrophosphate, 100 mM sodium orthovanadate, 100 mM sodium fluoride, 10 mg/mL aprotinin, 10 mg/mL leupeptin and 1 mM phenylmethylsulfonyl fluoride), followed by ultra-centrifugation (13000 rpm, 20') to collect protein content in fresh eppendorf tubes. Lysates from 20×10^6 primary human relatively undifferentiated $CD27^+CD28^+$ $CD4^+$ T cells were then incubated overnight at 4 °C on a rotary shaker with 10 μl of antibody to either TAB1 or p38 (both from Cell Signaling); for the minor $CD28^-CD27^-$ $CD4^+$ T cell subset, cells from two separate donors were pooled to obtain sufficient cells for analysis.

Extracts were incubated for 3 h at 4 °C with 10 μl of protein A–protein G–conjugated agarose beads (Santa Cruz Biotechnology) that were previously washed by ultra-centrifuging at 7000 rpm 5' in 200 μl of HNGT buffer (plus 1x protein and phosphatase inhibitor cocktails) and resuspended 1:1 in HNGT buffer. Next, samples were washed 3 times in HNGT buffer plus 1x protein and phosphatase inhibitor cocktails (both from Millipore) and were then analyzed by immunoblotting as per Western Blot analysis. Co-immunoprecipitated proteins

were detected with mouse anti-rabbit IgG (conformation-specific antibody; L27A9; Cell Signaling) or mouse antibody to rabbit IgG light chain (L57A3; Cell Signaling), followed by a secondary anti-mouse IgG antibody (7076; Cell Signaling) and ECL Prime Western detection kit (GE Healthcare).

2.2.4 *In vitro* kinase Assay

Proteins were immunoprecipitated with anti-TAB1 or anti-p38 as described above. Samples were washed by ultra-centrifugation (8000 rpm, 7'), twice in lysis buffer and twice in kinase buffer (both from Cell Signaling) supplemented with 1x protein and phosphatase inhibitor cocktails (both from Millipore). Kinase reactions were performed in 50 μl final volume and incubated for 30 min at 30 °C in the presence or absence of 200 μM ATP (Cell Signaling). In some experiments, the ATP competitor and allosteric p38 inhibitor SB-203580 (10 μM) was added directly to the *in vitro* kinase reaction. Total p38 and p38 phosphorylated at Thr180 and Tyr182 were detected by enzyme-linked immune-absorbent assay with a Phospho-Tracer ELISA Kit (Abcam), described below. *In vitro* kinase assays are presented as proportional to the absorbance at 450 nm.

2.2.5 Phospho-Tracer ELISA-based analysis of p38 MAPK

An antibody mix was prepared by adding Capture Antibody Reagent to p-p38 (Thr180/Tyr182) and Detection Antibody Reagent (both provided with the Phospho Tracer kit by Abcam), in a 1:1 ratio, and 50 μl of this antibody mix were added to

the in vitro kinase reaction product (50 μl), loaded in the Phospho Tracer micro-plates. Antibody binding was then allowed for 1 hour at room temperature on a micro-plate shaker. Wells were rinsed three times with 200 μl of 1 X washing buffer (provided with the kit). Meanwhile, a substrate mix was prepared, immediately before use by diluting 1:100 the HR-substrate 10-Acetyl-3, 7-dihydroxyphenoxazine (ADHP) with ADHP Dilution Buffer (both provided with the kit), a stabilized H2O2 solution. Next, 100 μl of this substrate mix were added to each well, and incubated 10' at room temperature on a micro-plate shaker for colour development. The reaction of conversion of ADHP into the fluorescent molecule Resorufin was then stopped by adding 10 μl of stop solution to each well. Signal was read using an Elisa reader micro-plate.

2.2.6 Rapid Extraction of DNA-binding proteins

Pellets from 5 x 10^6 T cells were used for separation of cytosolic and nuclear protein contents. The lysis was performed for 10' on ice in 200 μl of buffer A (10 mM Hepes-KOH, pH 7.9; 1,5 mM $MgCl_2$; 10 mM KCl; 0,5 mM (DTT); 0,2 mM Phenilmethanesulphonylfluoruride (PMSF)) plus 1X protease (Amersham Biosciences) and 1X phosphatase inhibitors (Pierce, Rockford, IL). Samples were then ultra-centrifuged for 10'' at 13000 rpm at 4°C, followed by collection of the (cytosolic) supernatant fraction in fresh eppendorf tubes. The pellet was then resuspended in 100 μl of buffer C (20 mM Hepes-KOH, pH 7.9; 420 mM NaCl; 1,5 mM $MgCl_2$; 0,2 mM EDTA; 0,5 mM DTT; 0,2 mM PMSF; 25% (v/v) glycerol) plus inhibitors (as above). Samples were incubated for 20' on ice followed by ultra-centrifuging at 13000 rpm for 2'. Supernatants (purified nuclear extracts) were then collected in fresh eppendorf tubes. The purity of nuclear extracts was assessed by

immunoblotting with anti-H1 histone.

2.2.7 Telomeric Repeat Amplification Protocol (TRAP) Assay

Telomerase activity was measured using either a radioactive-based TRAPeze telomerase detection kit (Chemicon Europe) or the non-radioactive TeloTAGGG telomerase ELISA kit (Roche). Lysates from 2 x 10^3 cells were prepared in 200 μl of CHAPS buffer (10 mM Tris-HCl, pH 7.5; 1 mM EGTA; 150 mM NaCl; 1 mM $MgCl_2$; 0,25 mM Sodium deoxycholate; 10% (v/v) glycerol; 5 mM β-mercapto-ethanol; 1% (v/v) Nonidet P-40 (NP-40); 0,5% (p/v) 3-(3-cloro-amminopropil) dimethylammonio-1-propanesulfonate (CHAPS); 0,1 mM [4-(2-aminoetil)-benzene sulfonyl fluoride hydrochloride] (AEBSF)). Extracts were incubated 30' on ice, followed by ultracentrifugation at 13000 rpm for 20' at 4°C. Cleared supernatants were then either stored at -80°C (for non immediate use) or immediately used as described below. For detection of nucleus/cytosol telomerase activity, nucleus/cytosol extracts prepared as above described were used.

For radioactive measurement of telomerase activity, 4 μl of cell extracts were mixed to 100 ng of TS - primer, 50 μM of dNTPs and TRAP buffer (20 mM Tris-HCl, pH 8.3; 68 mM KCl; 1,5 mM $MgCl_2$; 1 mM EGTA). This first reaction was incubated at 22° C for 30' (extension phase) to allow the telomerase-dependent extension of the telomeric-like TS primer (5' - AAT CCG TCG AGC AGA GTT - 3'). Next, a PCR mix was made by adding 100 ng of CX-primer, 2 μCi of [α-^{32}P] dCTP (DuPont NEN Research Products, Boston, Ma, USA) and 2 units of Taq-polymerases (DyNAzyme II, Finnzymes) to each sample reaction. **Table 3** shows the PCR amplification settings applied to the radioactive mix.

Denaturation	Annealing	Synthesis	
94°C	50°C	72°C	4° C
30''	30''	1'	∞
× 30 cycles			

Table 3: PCR Settings used in TRAP Assay (radioactive)

This PCR product (40 μl) was mixed to 8μl of 6X DNA loading buffer (0,25% (p/v) bromophenol blue; 0,25% (p/v) xylene cyanol FF; 40% (p/v) sacarose in ddH2O) and resolved by electrophoresis on non-denaturing 12% (p/v) poly-acrylamide gels (19:1 (p/p) acrylamide: bis-acrylamide). Samples were run for 2 hours at 290 V in 1X TBE buffer (90 mM Tris-Borate; 2 mM EDTA). Gels were fixed using a solution of 0,5 M NaCl, 50% (v/v) ethanol and 40 mM Sodium acetate (pH 4.2) and then transferred and incubated with X-ray films (Kodak Rochester, NY) into an autoradiography cassette for 72 hours at -80°C.

For non-radioactive measurements of telomerase activity, 4 μl of cell extracts were mixed to 25 μl of ready-to use PCR Reaction mixture (provided with the kit), and sterile water was added up to 50 μl final volume. Tubes were then transferred to a thermal cycler to perform combined primer elongation/amplification PCR reactions by the following protocol (**Table 4**):

	Time	Temperature	Cycles
Primer elongation	10-30’	25°C	1
Telomerase inactivation	5’	94°C	1
Amplification: Denaturation Annealing Polymerization	 30’’ 30’’ 90’’	 94°C 50°C 72°C	30

Table 4: PCR Settings used in TRAP Assay (non-radioactive)

Next 5 μl of the amplification product were added to 20 μl of kit-provided Denaturation reagent and incubated for 10’ at 20°C. This denaturated biotynilated telomere-amplicons were then hybridized to digoxigenin (DIG)-labeled, telomeric repeat-specific detection probes by adding 225 μl of Hybridization Buffer and transferring 100 μl of this reaction mixture to streptavidin coated micro-plates (both provided with the kit). The biotin-streptavidin binding was allowed for 2 hours on a micro-plate shaker at 37°C. Next, micro-plates were extensively washed 3 times using 250 μl of 1X-washing solution per well (provided with the kit). The abundance of DIG-labeled telomere-amplicons bound to micro-plates was detected by adding to micro-plates 100 μl of (ddH2O-reconstituted) anti digoxigenin-antibody conjugated to peroxidase, followed by micro-plate shaking for 30’ at 20°C. Plates were rinsed by washing 5 times with 250 μl of 1X-washing solution and coloured-substrate development was then allowed by adding 100 μl

of TMB substrate per well and incubating for 10-20'. Reactions were terminated by adding 100 μl stop solution (provided with the kit) per well and read on an ELISA reader as absorbance emission at 450 nM.

2.2.8 Electrophoretic Mobility Shift Assay (EMSA)

Nuclear extracts were obtained as above described. Five (5) μl of extracts were incubated with 30,000 cpm [32P]γ-ATP (Amersham Biosciences) end-labeled oligonucleotides. The radioactive labelling reaction was performed in T4 kinase buffer (10 mM $MgCl_2$; 70 mM Tris-HCl, pH 7.6; 5 mM DTT) in the presence of 5 units of T4 kinase, 3,5 pmol of oligonucleotide and 10 μCi of [γ-^{32}P] ATP (DuPont NEN Research Products, Boston, Ma, USA). The reaction was incubated for 1 hour at 37°C and then terminated by adding 50 mM EDTA and the so-labelled oligonucleotide was resuspended in TE buffer (10 mM Tris HCl, pH 8.0; 1 mM EDTA).

Extracts were incubated with 1,75 pmol of radioactive labeled oligonucleotide (either the sequence corresponding to 2184 to 2161 bp of the hTERT promoter containing the putative E2F site (59–CGCCCAG- GACCGCGCTCCCCACGT–39) or with a commercially available oligonucleotide containing a NF-kB consensus sequence (obtained from Promega). Reactions were performed in a 10 mL volume for 20 min at room temperature in a buffer consisting of 5 mg/ml poly (deoxyinosinic-deoxycytidylic) acid, 10 mM Tris–HCl, 50 mM NaCl, 0.5 mM DDT, 0.5 mM EDTA, 1 mM MgCl2, and 4% glycerol (pH 7.5; Promega). Samples were stained using 10X-gel loading buffer (250 mM Tris HCl, pH 7.5; 0,2% (p/v)

bromophenol blue (BBF); 40% (v/v) glycerol), and Protein–DNA complexes were resolved by electrophoresis on non-denaturing 5% (p/v) poly-acrylamide gels. Gels were run at 350 V for 20' in 0,5 X TBE buffer, dried by vacuum-pumping and transferred and incubated with X-ray films (Kodak Rochester, NY) into an autoradiography cassette for 18 hours at -80°C.

2.2.9 Cloning

Dr. David Escors kindly provided the p-SIREN/HIV-1 lentivector for gene knockdown. The following shRNA sequences that were previously described (Ge et al., 2003; Tangeman et al., 2012) were introduced into this vector:

CCTAAGGTTAAGTCGCCCTCG (shCtrl), GGCGGTCCTTCTCAACAACAAG (shTAB1) and ATGATGTCAGATGGTGAATTT (shAMPK-α).

First, 10 μg of p-SIREN/HIV-1 vector were digested with 10 units of both BaMH1 and EcoR1 restriction enzymes (Promega) in 1X-buffer D (Promega), in a final reaction volume of 40 μl. The reaction was incubated at 37° C for 2 hours, then stained with 10 μl of DNA loading buffer and run (20', 90 mV) by electrophoresis for purification (1% agarose gel in 1X Tris/Borate/EDTA (TBE) buffer and 1:1000 ethidium bromide). A Hyper Ladder was also loaded for size analysis (Bioline 33025). The digestion product was then visualized using a UV-trans-illuminator (Amersham Biosciences) and excised from the gel. The DNA in gel was solubilized in 500μl of Buffer QC (Quiagen) at 55°C and purified by chromatography (DNA purification kit, Quiagen). The column was ultra-centrifuged at 13000 rpm for 1' and then rinsed with 500 μl Washing Buffer PE (Quiagen). Next, the column was ultra-centrifuged twice as above. DNA was eluted from the

column using 30 μl pre-warm Elution Buffer EB.

To insert the shRNA sequences in digested p-SIREN/HIV-1 lentivector, 2 parallel reactions were set up. In the ligation reaction, 4 μl of digested vector were mixed to 4 μl of shRNA nucleotide (bearing specific flanking sequences for integration in BaMH1/EcoR1 digested DNA) and 1 μl of T4 kinase. In the control reaction, 4 μl of ddH20 was added instead of any insert. Reactions were left for 60' at room temperature or overnight at 16°C.

2.2.10 Transformation

Tubes containing HB101 competent bacteria (MCLAB) were thawed on ice for 20'. Next, either control or ligation reactions were added to bacteria. Bacteria were transformed by thermic shock, incubating 2' at 37°C followed by 2' on ice. Bacteria were grown over night at 37° C on LP-Ampicillin agar plates (0,1 mg/mL, Sigma Aldrich). The day after, any bacteria grown in the control plate was considered as a background (as the lentivector bearing an ampicillin resistant gene is not functional upon digestion, control transformed bacteria should not grow on ampicillin treatment).

2.2.11 Mini-Prep

For bacterial clone analysis, between 5-10 individual clones (depending on control background) were expanded by mini prep and then sent for sequencing. For mini prep a standard protocol was used, provided with the Quiagen mini-prep kit. Briefly, bacteria were grown overnight at 37°C in agitation in 15 mL falcon tubes

containing 4 mL of LB-medium plus Ampicillin (1:1000). The next day, samples were centrifuged for 30' at 3000 rpm and the bacterial pellets were resuspended in 250 μl of Buffer P1 (additionated with RNaseA). After addition of 250 μl Lysis Buffer P2, tubes were gently mixed by inversion, to avoid genomic DNA contamination, and incubated for 5' at room temperature. Next, DNA was precipitated by adding 350 μl of Buffer N3. Samples were centrifuged at 13000 rpm for 10'. Supernatants containing non-genomic DNA were filtered on Whatman paper through DNA chromatography columns. Columns were rinsed with 750 μl of Buffer PE (with Ethanol), centrifuged twice, and DNA was eluted by adding 50 μl pre-warm Buffer EB. DNA purity was assessed by nano-drop; DNA preparations were considered pure when A_{260}/A_{280} was equal or above 1.8. The purified lentiviral vector preparations were then sent to the UCL sequencing facility to assess presence of the desired shRNA.

2.2.12 Transfection and Lentiviral Titration

HEK 293 cells were seeded in T75 tissue culture flasks using 10 mL Dulbecco's Modified Eagle Medium (DMEM) additionated with 10% FCS, 100 U/ml penicillin and 2mM L-glutamine (all from Invitrogen), and then cultured at 37°C in a humidified 5% CO_2 incubator. When cells were 80% confluent, old medium was replaced with 10 mL fresh medium and cells were transfected by Fugene-6 (Promega).

For transfection, 1.5 μg of 8.91 plasmid DNA (encoding for gag/pol structural HIV-1 proteins), 1.5 μg of pMDG construct (encoding for VSV-g envelope proteins) and

2.3 μg of lentiviral transfer vector (encoding for both GFP fluorescent protein and the above-cloned specific shRNA) were added in an eppendorf tube along with ddH2O water in a final volume of 50 μl. In a separate eppendorf tube, 27 μl of Fugene 6 liposome transfection reagent were slowly added to 200 μl OPTIMEM medium (Lonza). Next, the DNA mix was added to OPTIMEM/Fugene 6, incubated for 15' at room temperature, and then added drop-wise to HEK 293 cells. Cells were left growing at 37° C and lentiviral supernatants were collected and stored at 4° C 24 hours later, when fresh medium was added back on cells. This operation was repeated twice until 72 hours post-transfection, at which time supernatants were filtered, mixed together and ultra-centrifuged (25000 rpm at 4°C) by layering on 5 mL of a 20% sucrose cushion in D-PBS in centrifuge tubes (Beckman Coulter), followed by re-suspension in 100 μl D-PBS lentiviral stocks and storage at -80° C for future use.

To titrate the lentiviral vector preparations**,** HEK 293 cells (5 x 10^5) were resuspended in DMEM medium and seeded in 6 well plates. The next day, cells were transduced with 1, 2 or 4 μl of 100-fold concentrated viral preparations and left growing at 37° C. Three days post-transduction, GFP expression was analyzed by flow cytometry using the following formula:

(%GFP^+ cells) x (transduced cells)/volume of virus (mL)

Assuming that there is a linear correlation between infecting viral units and transduced cells up to 30% transduction (that is, 1 cell infected by only an individual viral particle), it was possible to estimate the multiplicity of infection

(MOI) as the amount of viral units required to infect a cell population (for instance, an MOI of 10 indicates that 10 viral particles are required to infect a single cell in culture). Titres obtained were elevated, comprised between 10^8-10^9 lentiviral units/mL.

2.2.13 RNA isolation

Pellets from 5 x 10^5 cells were resuspended using 750 μl of TRIzol (Invitrogen). Lysates were obtained by gently pipetting up and down several times, followed by ultracentrifugation at 12,000 rpm at 4°C for 10'. Supernatants were transferred to fresh tubes for the following Phase Separation. Briefly, 200 μl of chloroform were added to the samples, shaked for 15'' and then incubated 10' at room temperature. Samples were then centrifuged at 12,000 rpm for 15' at 4°C. This allowed separation of the RNA content within the aqueous phase solution on the top layer, which was then placed in a new tube for the next RNA Isolation Procedure. Next, 500 μl of Isopropanol were added to the aqueous RNA phase and incubated for 10' at room temperature. Samples were centrifuged at 12,000 rpm for 10' at room temperature. The RNA pellet was then washed using 1 mL of 75% Ethanol, then centrifuged at 7,500 rpm for 5' at 4°C. The pellet was air-dried for 10', followed by resuspension in RNAase-free water (100 ng/mL) and incubated in a heat block set at 55°C for 10' to allow full resuspension.

2.2.14 Real Time PCR

RNA extracts (1 μg/sample) were analysed by Real Time PCR using Taqman probe technology. For cDNA synthesis, 1 μl of either random primers (100 μg/mL) or oligo dTs and 1 μl of dNTPs (10 mM) were added to each RNA sample. Total

RNA was then heated at 70°C for 6' (to allow annealing of the random primers to the RNA) then quickly incubated on ice for additional 10'. Next, the reaction mix was prepared using the following reagents for each RNA sample: 4 μl of 5 x reaction buffer, 2 μl of DTT, 1 μl of Recombinant RNAse inhibitor and 1 μl MMLV Reverse Trancriptase. The cDNA synthesis reaction was then allowed for 1h at 42°C. To stop the process, samples were then incubated for 5' at 65°C. Finally, DEPC-treated water was added to a final volume of 100 μl. For gene target analysis, a master mix for each sample was prepared as it follows: 10 μl of Taqman universal PCR mix, 0.2 μl of Forward/Reverse Primers (900 nM), 0.05 μl of Taqman probes (250 nM) and 4.1 μl of H2O. This Master solution was transferred to a 96 well-plate then incubated with 5 μl of cDNA samples to be analysed (in triplicate). The following probes were used: p38 (Hs00176247_m1), AMPKα_(Hs01562315_m1), TAB1 (Hs00196143_m1) and hTERT (Hs00972656_m1) (all from Applied Biosystems). GAPDH was used as a housekeeping control. The reaction was read using an AbiPrism 7700 sequence detector, set as in **Table 5**.

Incubation	2'	25°C	1 x
Ampli Taq Gold activation	10'	95°C	1 x
PCR	15'' 1'	92°C (denature) 60°C (anneal/extend)	40 x

Table 5: Settings used in Real Time PCR applications

After amplification, relative target expression among samples (normalized to that of the housekeeping GAPDH) was quantified using the ΔΔCT method, where CT (threshold cycle) is the cycle at which there is a statistically significant fluorescence emission of the Taqman probe over the background.

2.2.15 Measurement of telomere length

Telomere length of senescent human $CD27^-$ $CD28^-$ $CD4^+$ T cells was measured using a fluorescence *in situ* flow-cytometry method, four weeks after transduction. First a 2 mM BS3 solution was made immediately before use by resuspending a BS3 powder aliquot into 1750 μl of PBS final volume. Cell were resuspended in 100 μl of PBS and 100 μl of BS3 solution, to obtain a final concentration of 1 mM, vortexed and then incubated for 30' in the fridge. This fixation step was then quenched by adding 1 ml of 50 mM PBS Tris (pH7.2) solution directly to the samples, followed by incubation in the dark at RT for 20', and final wash in PBS. For the hybridization reaction, samples were vortexed in the presence of 1 ml hybridization solution, centrifuged at 2000 rpm for 7' and then resuspended in 300 μl of hybridization solution. Samples were then splitted into 3 different tubes, used as replicates. Next, 5 μl of telomere-Cy5 conjugated probe was diluted by adding 45 μl of sterile water and 3 μl of the diluted probe were further diluted with 97 μl hybridisation solution per tube. (Make in bulk and then distribute 100 μl to each tube). Samples were vortexed, incubated for 10' at 82 degrees in the water bath and then refrigerated on ice water. Finally, samples were incubated for 60' in the dark, washed twice in 1 ml post-hybridization solution and twice in PBS, then

immediately analzyed by flow-cytometry. The tables below summarizes recipes for both hybridization (**Table 6**) and post-hybridization (**Table 7**) solutions used:

Table 6: Hybridization solution

Formamide	7ml	10.5ml	14ml
Tris. HCl	0.2ml of 1M stock	0.3ml of 1M stock	0.4ml of 1M stock
BSA	2.5ml of 4% stock	3.75ml of 4% stock	5ml of 4% stock
NaCl	0.3ml of 5M stock	0.45ml of 5M stock	0.6ml of 5M stock
TOTAL VOL	*10ml*	*15ml*	*20ml*

Table 7: Post-Hybridization solution

Formamide	7ml	14ml	28ml
Tris. HCl	0.1ml of 1M pH7.2	0.2ml of 1M pH7.2	0.4ml of 1M pH7.2
BSA	0.25ml of 4% stock	0.5ml of 4% stock	1ml of 4% stock
Tween20	0.1ml of 10% stock	0.2ml of 10% stock	0.4ml of 10% stock
NaCl	0.3ml of 5M stock	0.6ml of 5M stock	1.2ml of 5M stock
H_2O	2.25ml	4.5ml	9ml

2.3 Statistical analysis

Graphpad Prism was used for statistical analysis. For pairwise comparisons, a paired Student's *t*-test was used. For three matched groups, a one-way ANOVA for repeated measures using a Bonferroni post-test correction. Differences with a *P* value of <0.05 were considered significant.

Chapter III: IFN-α inhibits telomerase in human CD8$^+$ T cells by both hTERT down-modulation and induction of p38 MAPK signalling

3.1 Background and rationale

Telomerase activity confers antigen-specific T cells the ability of long-term proliferation. Thus, lack of telomerase activity in human highly differentiated (senescent) T cells is associated with very short telomeres and low proliferative rates (Akbar and Vukmanovic-Stejic, 2007). As discussed, loss of telomerase activity may be due to both transcriptional and post translational mechanisms, including reduced expression of the catalytic sub-unit hTERT, reduced hTERT phosphorylation by the signalling kinase AKT and changes in NFkB activity affecting both telomerase expression and nuclear import (**Figure 8**). IFN-α is a type I interferon that is an anti-viral and immune-modulatory cytokine that inhibits telomerase activity in T cells (Reed et al., 2004) but the mechanisms for this inhibition are not known. IFN-α also induces loss of both CD27 and CD28 co-stimulatory receptors (Fletcher et al., 2005), hallmark of human highly differentiated T cells that exhibit features of replicative senescence. Because type I IFN has been described to activate senescence related signalling pathways in human fibroblasts (Campisi and d'Adda di Fagagna, 2007), the mechanisms of T cell telomerase down-regulation by IFN-α may resemble those spontaneously occurring in human senescent T cells. In support of this idea, p38 MAP kinase, a key molecule downstream of IFN-α receptor signalling, was recently shown to inhibit telomerase activity and proliferation in both senescent human CD4$^+$ and CD8$^+$ T cells (Henson et al., 2014; Di Mitri et al., 2011). However, it is not known if IFN-α inhibits telomerase activity by one or more of these pathways. Thus, I

sought to investigate the mechanisms of T cell telomerase down-regulation by IFN-α. **Figure 10** illustrates potential mechanisms of hTERT down-modulation by IFN-α in T cells that are herein investigated.

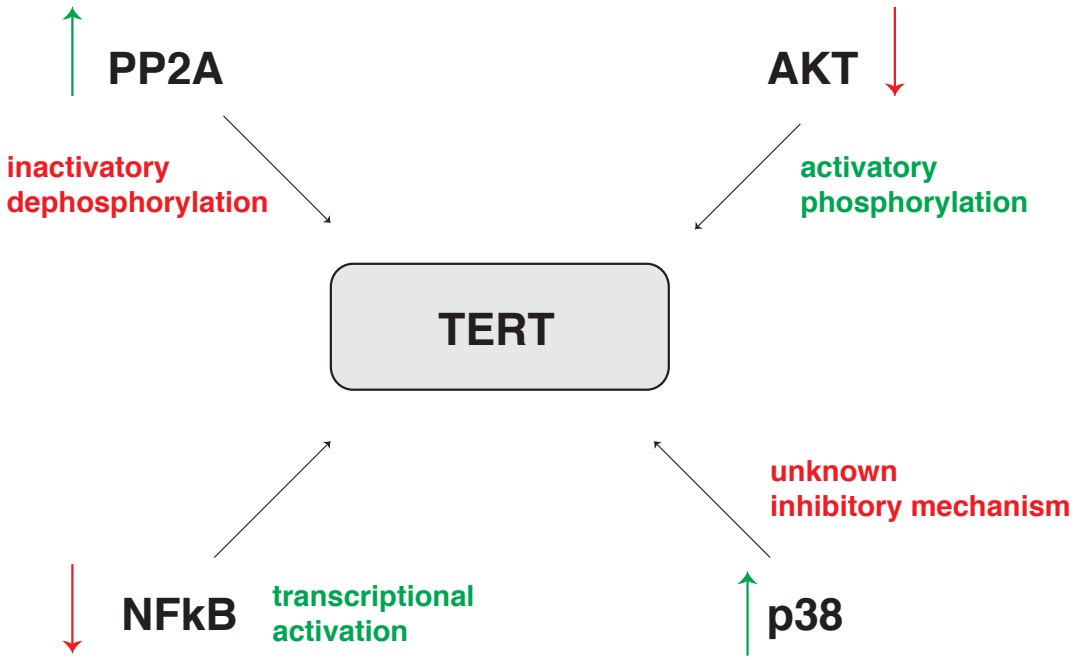

Figure 10: IFN-α mediated telomerase down-regulation. IFN-α may inhibit telomerase activity in T cells by both inactivating activatory pathways (red arrows) or activating inhibitory pathways (green arrows). The role of each individual pathway in telomerase regulation is further discussed in the text. This may offer a prototype model for understanding the mechanistic bases of hTERT modulation in lymphocytes.

3.2 IFN-α down-regulates telomerase activity of human $CD8^+$ T cells

Telomerase activity can be measured using an assay known as TRAP assay (Cong et al., 2002). To confirm that IFN-α inhibited telomerase activity in primary human T lymphocytes, $CD8^+$ T cells were isolated from peripheral blood and then activated by αCD3 and rhIL-2, either in the presence or absence of increasing doses of IFN-α (50 or 500 U/mL). After 72 hours of activation, $CD8^+$ T cells were counted, washed and lysed to extract total protein content. **Figure 11 a** shows that although telomerase activity is increased in activated primary human $CD8^+$ T cells, IFN-α down-regulates this activity in a dose dependent manner in these cells. Results from 3 different donors corroborated these findings (**Figure 11 b**). Importantly, telomerase down-regulation by IFN-α was not due to cytotoxic effects because $CD8^+$ T cell survival was not affected by IFN-α even at the highest concentration tested (**Figure 11 c**). Therefore, 500IU of IFN-α was used for further experiments.

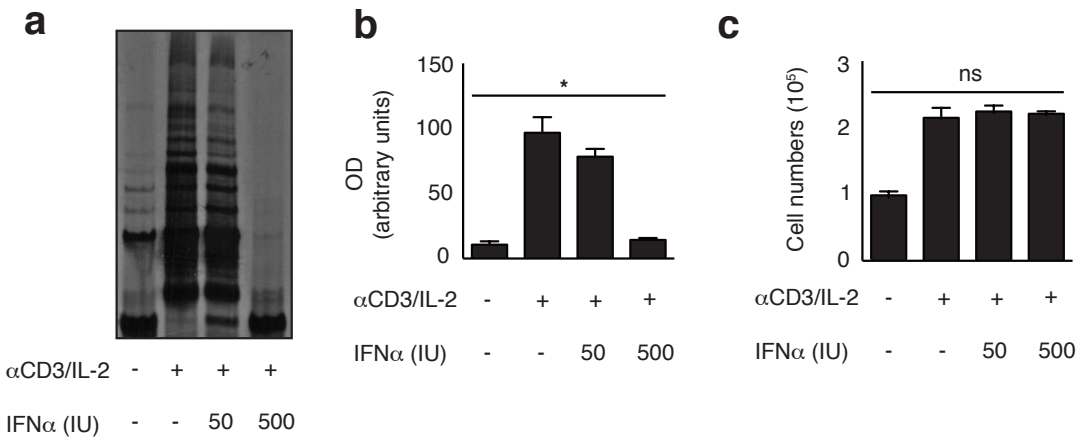

Figure 11: IFN-α inhibits telomerase activity in human CD8$^+$ T cells.

(**a**) Measurement of CD8$^+$ T cell telomerase activity by TRAP assay. Human CD8$^+$ T cells were isolated from peripheral blood by immunomagnetic beads and then activated by αCD3/rh-IL2 for 72 hours either in the absence or in the presence of increasing doses (50 or 500 U/mL) of IFN-α. Extracts from 2 x 10^3 cells were analysed by a radioactive based TRAP assay to assess telomerase activity in samples. The multi-ladder profile shown was resolved on a non-denaturing polyacrylamide gel. (**b**) Pooled results of band intensity from 3 separate experiments performed as in (a) quantified by bi-dimensional densitometry and presented as arbitrary units. (**c**) Survival of human CD8$^+$ T cells cultured as in (a) assessed by trypan blue exclusion test assay, presented relative to that un-stimulated cells, set as 1. Error bars indicate SEM throughout; in (**b**) a one-way analysis of variance (ANOVA) for repeated-measures with a Bonferroni post-test correction. *$p< 0,05$,

3.3 IFN-α down-regulates both hTERT transcription and translation

The control of the expression of the catalytic sub-unit hTERT is the main mechanism for molecular tuning of telomerase (Cong et al., 2002). To investigate if IFN-α inhibits T cell telomerase activity by hTERT down-regulation, both hTERT transcription and translation were assessed in human $CD8^+$ T cells activated by αCD3 and rh-IL2 for 24 hours, either in the presence or absence of IFN-α. To measure hTERT transcripts, activated human $CD8^+$ T cells were analysed by RT-PCR using a specific TaqMan probe to hTERT. The housekeeping beta actin gene was used as an internal control. IFN-α was found to inhibit hTERT transcription, normalized to that of the housekeeping beta-actin gene (**Figure 12 a**).

To study if reduced hTERT transcription by IFN-α resulted in reduced hTERT translation, human $CD8^+$ T cells cultured in identical conditions were analysed by Western Blot. Immunoblotting analysis showed that IFN-α (500 U/mL) inhibited hTERT protein expression in activated human $CD8^+$ T cells (**Figure 12 b**). The densitometric ratio of band intensity of hTERT versus that of the housekeeping control beta-actin from 3 different donors confirmed these findings (**Figure 12 c**). Thus, the inhibition of telomerase activity by IFN-α in activated human $CD8^+$ T cells is associated with down-regulation of both hTERT transcription and translation.

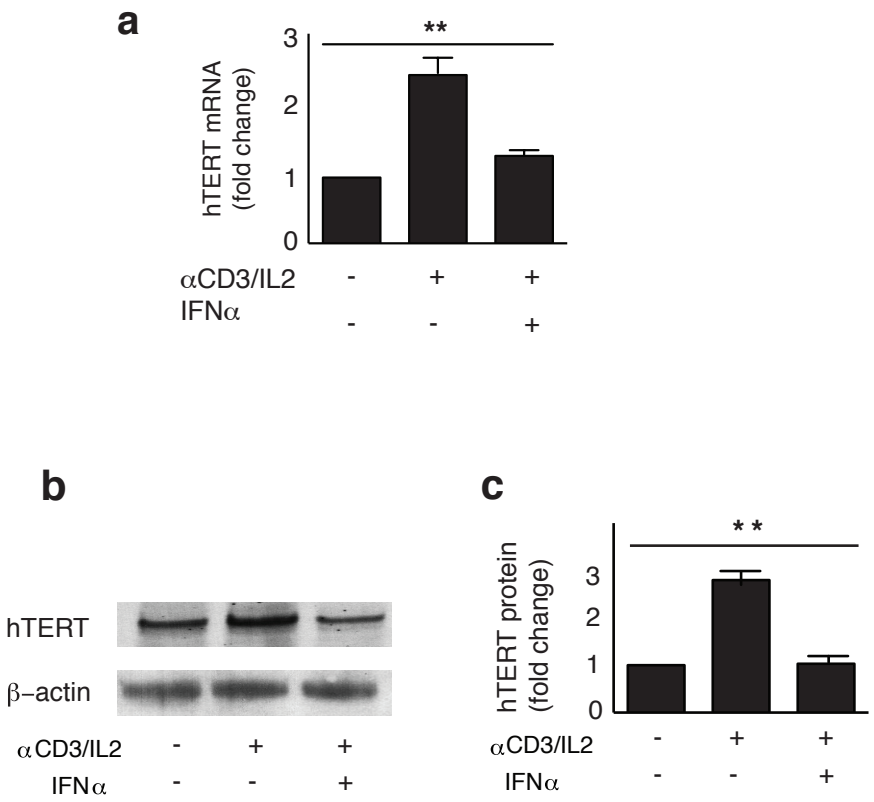

Figure 12: IFN-α down-regulates hTERT expression in human CD8$^+$ T cells.
(a) Measurement of hTERT mRNA expression by Real-time PCR in human CD8$^+$ T cells activated by αCD3 and rh-IL2 for 24 hours, either in the presence or absence of IFN-α (500IU). mRNA from activated T cells were retro-transcribed to cDNA and amplified with TaqMan probes to either hTERT or beta-actin as an housekeeping control; hTERT levels were normalized using the ΔΔ–CT algorithm working out the differential expression between hTERT and the housekeeping beta-actin gene as described in Material and Methods. Samples for quantitative PCR were analyzed from 3 different donors. (**b**) Representative immunoblots of hTERT and beta-actin expression (as a loading control) from CD8$^+$ T cells activated as in (a) for 36 hours. (**c**) The relative protein expression of hTERT normalized to that of housekeeping beta-actin from 3 different experiments performed as in (b). Band intensity calculated by bi-dimensional densitometry and presented relative to that of un-stimulated control, set as 1, is shown. Error bars indicate SEM throughout; in (**a**) a Student's t test for paired measurement was used; in (**c**) a one-way analysis of variance (ANOVA) for repeated-measures with a Bonferroni post-test correction. ***p< 0,01*

3.4 IFN-α inhibits telomerase in both cytosol and nucleus of $CD8^+$ T cells

I next sought to determine in which subcellular compartment IFN-α negatively regulated $CD8^+$ T cell telomerase. $CD8^+$ T cells were activated as described above either in the presence or absence of IFN-α for 72 hours, then lysed and fractionated to separate either cytosolic or nuclear protein content (see Materials and Methods). Cell extracts were then assessed by TRAP assay, which showed that IFN-α down-regulated telomerase activity in both the cytosol and nucleus of activated $CD8^+$ T cells (**Figure 13 a**). Results from 3 independent experiments corroborated these findings (**Figure 13 b**). To determine if reduced cytosolic and nuclear telomerase activity in activated $CD8^+$ T cells was linked to reduced hTERT protein expression in both cell compartments, Western Blot-based experiments were run. Immunoblotting analysis demonstrated reduced hTERT protein expression in both cytosol and nucleus of activated human $CD8^+$ T cells (**Figure 13 c)**. For densitometric analysis, the housekeeping genes beta-actin and histone H1 were used for measurement of either cysolic or nuclear hTERT protein content respectively; this resulted in a strong reduction of hTERT expression in both subcellular compartments (**Figure 14 d**).

Thus, IFN-α inhibits telomerase activity in both the cytosol and nucleus of activated $CD8^+$ T cells and this is associated with reduced hTERT expression in both subcellular compartments.

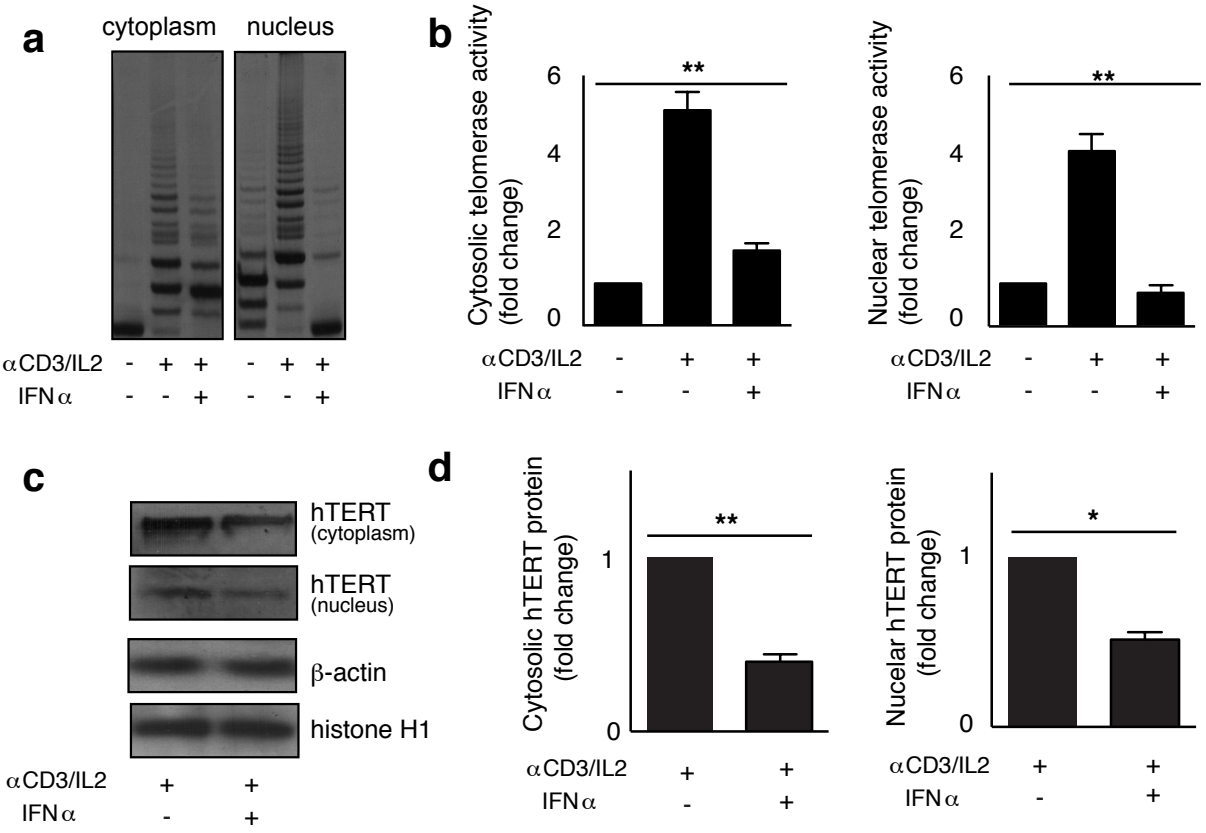

Figure 13: IFN-α inhibits telomerase in cytosol and nuclei of CD8$^+$ T cells. (a) Measurement of CD8$^+$ T cell telomerase activity by TRAP assay. Human CD8$^+$ T cells were activated by αCD3 and rh-IL2 for 72 hours, either in the presence or absence of IFN-α (500IU). Cytosolic and nuclear extracts from 2 x 10^3 cells were purified as described in Materials and Methods and telomerase activity in samples was assessed as in **Figure 11 a**. (**b**) Pooled results of either (left) cytosolic or (right) nuclear telomerase related activity band intensity from 3 separate experiments performed as in (a) quantified by bi-dimensional densitometry and presented as relative to un-stimulated control, set as 1. (**c**) Immunoblots of hTERT expression in cytosolic and nuclear protein extracts from activated human CD8$^+$ T cells cultured as in (a) for 36 hours (top); (bottom) beta-actin and histone h1 expression from the same gel as cytosol or nuclear protein control, respectively. (**d**) The relative protein expression of either cytosolic or nuclear hTERT normalized to that of beta-actin and histone h1 respectively. Band intensity data from 3 different experiments performed as in (c) and presented relative to that of unstimulated control, set as 1, are shown. Error bars indicate SEM throughout; in (**b**) a one-way analysis of variance (ANOVA) for repeated-measures with a Bonferroni post-test correction; in (d) a paired Student's t test. *$p< 0,05$, **$p< 0,01$

3.5 IFN-α inhibits hTERT transcription in part by tuning NF-kB and E2F activity

To explore potential transcriptional mechanisms of hTERT down-regulation by IFN-α, EMSA-based experiments were performed to assess the DNA-binding activity of $CD8^+$ T cell E2F1 and NFkB transcription factors that regulate hTERT transcription (Akiyama et al., 2003; Crowe, 2001). Nuclear protein extracts from human $CD8^+$ T cells, activated in the presence or absence of IFN-α for 24 hours, were incubated with consensus DNA-binding sequences for either the transcriptional hTERT repressor E2F1 or the hTERT activator NFkB, that were previously labelled in the presence of radioactive [32P]γ-ATP. The resulting DNA-protein complexes were run on non-denaturing SDS-page gels, which showed that IFN-α enhanced the binding of proteins from nuclei of activated $CD8^+$ T cells (presumably E2F1) to the specific E2F1-interacting consensus sequence extrapolated from the hTERT promoter (**Figure 14 a, *top line***). At the same time, IFN-α inhibited the binding of proteins from nuclei of activated $CD8^+$ T cells (presumably NFkB) to the specific NFkB consensus sequence (**Figure 14 a, *bottom line***); however although NFkB activity is important to induce hTERT transcription, the exact NFkB binding site on the hTERT promoter has not been identified, suggesting that the interaction may be indirect. These results were confirmed in 3 separate experiments (**Figure 14 b**). Overall these data suggest that the documented inhibition of hTERT transcription by IFN-α may be related to changes in the activity of both the transcriptional hTERT repressor E2F1 and activator NFkB.

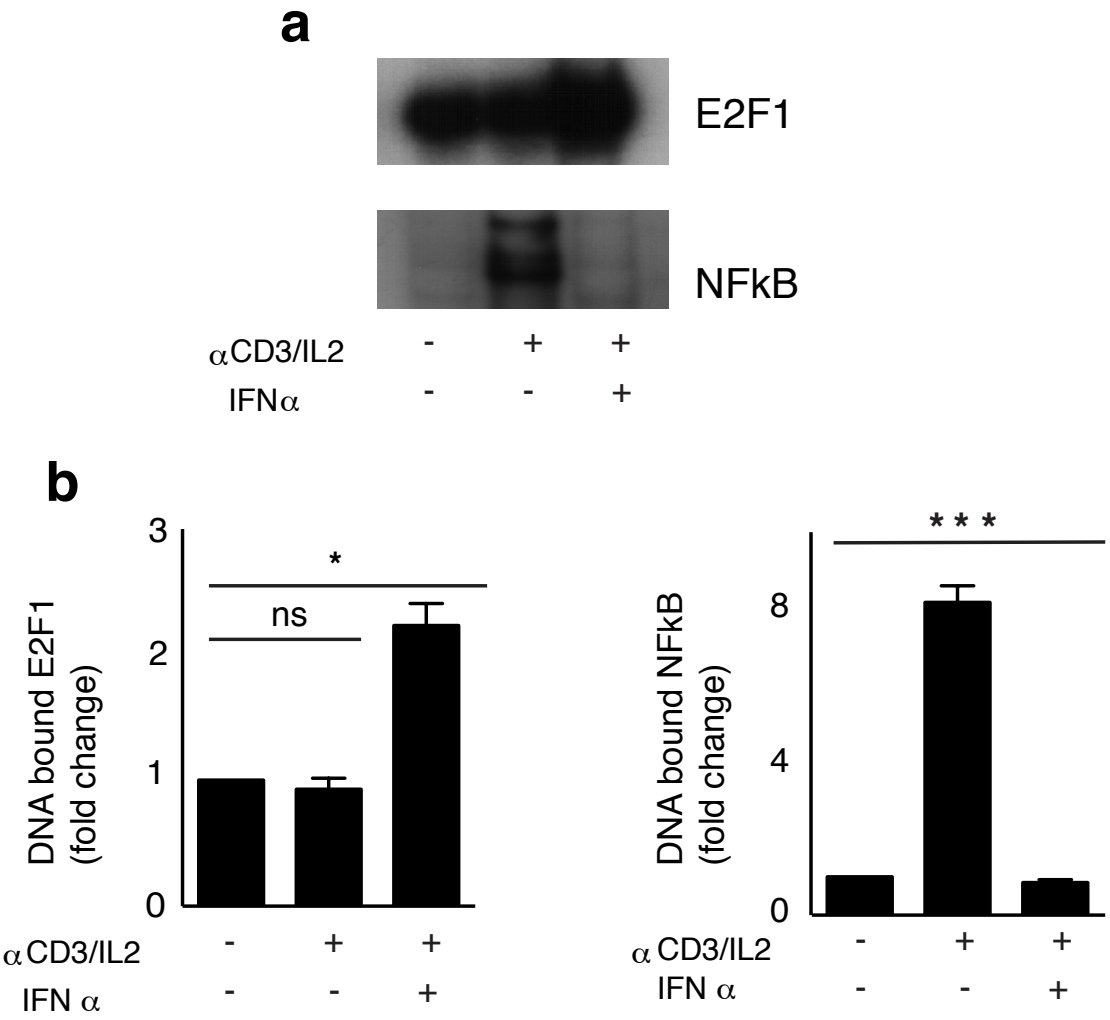

Figure 14: IFN-α modulates E2F1 and NFkB-DNA binding activity. (**a**) Assessment of E2F1 and NFkB DNA binding activity by EMSA assay in nuclei of human $CD8^+$ T cells left either untreated or activated by αCD3 and rh-IL2 for 24 hours, in the presence or absence of IFN-α (500IU). $CD8^+$ T cell nuclear extracts were incubated with a sequence corresponding to –184 to –161 bp of the hTERT promoter containing the putative E2F site (5′-CGCCCAGGACCGCGCTCCCCACGT-3′, *top*) or a commercially available NF-kB consensus oligonucleotide (*bottom*), both radioactively labelled as described in Materials and Methods. DNA-protein complexes were then resolved by gel electrophoresis, followed by autoradiography. (**b**) Pooled results of (*left*) E2F1 and (*right*) NFkB binding activity from 3 separate experiments performed as in (a). Error bars indicate SEM throughout. In (**b**) a one-way analysis of variance (ANOVA) for repeated-measures with a Bonferroni post-test correction. *$p< 0,05$, ***$p< 0,001$

3.6 IFN-α inhibits AKT signalling

The kinase AKT directly phosphorylates hTERT that is essential for enhancing telomerase stability and activity in T cells (Kang et al., 1999). Optimal AKT activation requires phosphorylation at Ser473 and Thr308 however defective AKT phosphorylation at the Ser473 site is a feature of human highly differentiated T cells in which is associated with lack of telomerase activity (Plunkett et al., 2007). To study if telomerase down-regulation by IFN-α was also related to impaired T cell AKT activity, Western Blot-based experiments using specific antibodies to both phosphorylated AKT at Ser473 and Thr308 were performed. Also, an antibody to total AKT was used to measure total AKT expression throughout. To measure changes in AKT activity by IFN-α, human $CD8^+$ T cells were activated in the presence or absence of IFN-α for 24 hours, lysed and analysed by Western Blot and the ratio of band intensity of phosphorylated AKT to total AKT was determined by densitometric analysis. These experiments showed a strong inhibition of AKT phosphorylation at both Ser473 and Thr308 regulatory sites, while total AKT expression was not affected, indicating potent kinase inactivation by IFN-α (**Figure 15 a**). Cumulative data from 3 different donors confirmed these results (**Figure 15 b**).

To explore biochemical mechanisms that may be related to reduced AKT signalling, the activation of the phosphatase PP2A that has been shown to inhibit AKT activity by inducing de-phosphorylation of the regulatory sites (Li et al., 1997) was determined in Western Blot-based experiments. Human $CD8^+$ T cells activated and cultured in the presence or absence of IFN-α were lysed and PP2A activation was measured using antibodies to both phosphorylated PP2A at Thr307

and total PP2A. After 24 hours, IFN-α treatment resulted in both induction of PP2A synthesis and reduced PP2A phosphorylation (**Figure 15 a**). Cumulative data from 3 separate experiments confirmed these observations (**Figure 15 b**). Because phosphorylated PP2A accounts for the inactive form of the enzyme, the densitometric analysis showing reduced ratio of phosphorylated PP2A to total PP2A indicated increased PP2A activation by IFN-α. These data suggest that AKT that is essential for telomerase activity in T cells may be in part inhibited by IFN-α via PP2A activation.

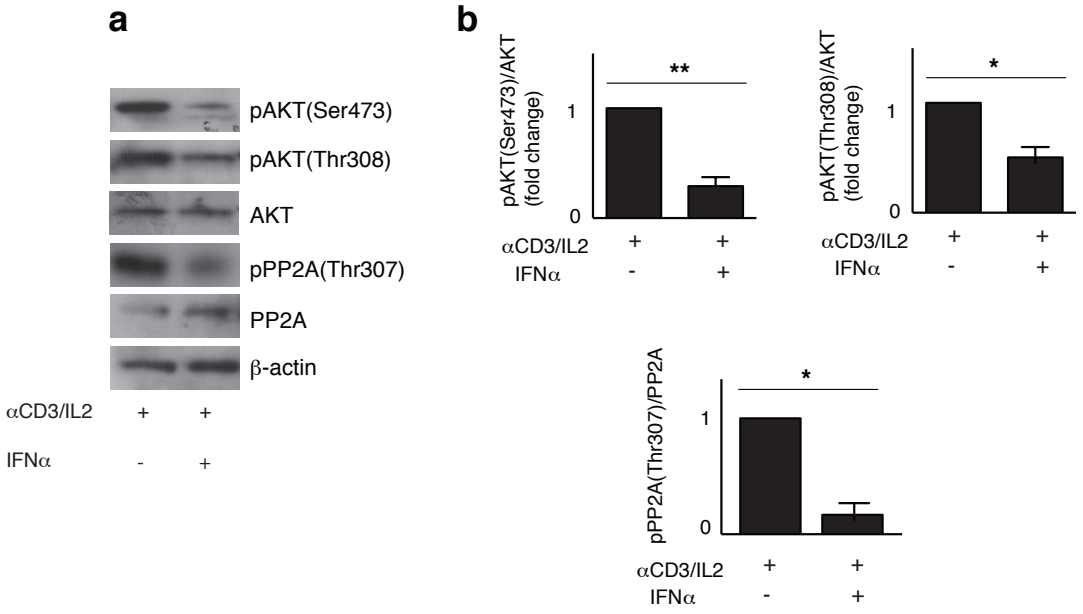

Figure 15: IFN-α inhibits AKT and induce PP2A activity in CD8 T cells. (**a**) Immunoblots of p-AKT (Ser473), p-AKT (Thr308), total AKT, p-PP2A (Thr307), total PP2A and beta actin (as a housekeeping control gene) assessed from whole extracts of human $CD8^+$ T cells activated by αCD3 and rh-IL2 for 24 hours, in the presence or absence of IFN-α (500IU). (**b**) The relative AKT kinase inactivation (*top*) and the relative PP2A phosphatase inactivation (*bottom*) assessed as ratio of AKT phosphorylation at both Ser473 and Thr308 versus total AKT and phosphorylation of PP2A versus total PP2A, respectively. Pooled data of band intensity from 3 separate experiments performed as in (a) and quantified by densitometric analysis are presented as relative to stimulated controls, set as 1. Error bars indicate SEM throughout. In (**b**) a paired Student's T test was used. *$p< 0,05$, **$p< 0,01$.

3.7 IFN-α inhibits telomerase activity in part via p38 MAPK signaling

The data so far suggested that IFN-α inhibited telomerase by multiple mechanisms but direct evidence linking biochemical changes in signalling pathways and inhibition of telomerase activity in T cells required a more direct assessment. Thus, the potential involvement of p38 MAPK that is important for IFN-α signaling was examined. In Western Blot-based experiments, the addition of IFN-α to activated human $CD8^+$ T cells potently induced p38 MAPK phosphorylation at Thr180/Tyr182 sites within the p38 activation loop while total p38 expression was not affected by IFN-α (**Figure 16 a**); re-probing membranes with anti beta actin confirmed equal protein loading throughout (**Figure 16 a**). Densitometric analysis of phosphorylated p38 to total p38 showed indeed strong p38 MAPK activation by IFN-α (**Figure 16 b**). To directly assess the involvement of p38 MAPK signalling in T cell telomerase down-regulation by IFN-α, blocking experiments using the pan-p38 inhibitor BIRB-796 were performed. Purified human $CD8^+$ T cells were incubated with either BIRB 796 at the concentration of 500 nM at which the drug does not inhibit other related kinases e.g. JNK (Di Mitri et al., 2011), or DMSO, as a vehicle control. The cells were then activated in the presence or absence of IFN-α for 72 hours. The cells were normalized by counting total cell numbers, lysed and analysed by TRAP assay to measure changes in T cell telomerase activity, using a non-radioactive variant of the TRAP assay (described in Materials and Methods). Using this method that is equivalent to the radioactive version of the TRAP assay, p38 MAPK blockade was found to restore telomerase activity in IFN-α treated human $CD8^+$ T cell extracts (**Figure 16 c**). Thus, p38 MAPK activation is directly involved in the inhibition of telomerase by IFN-α.

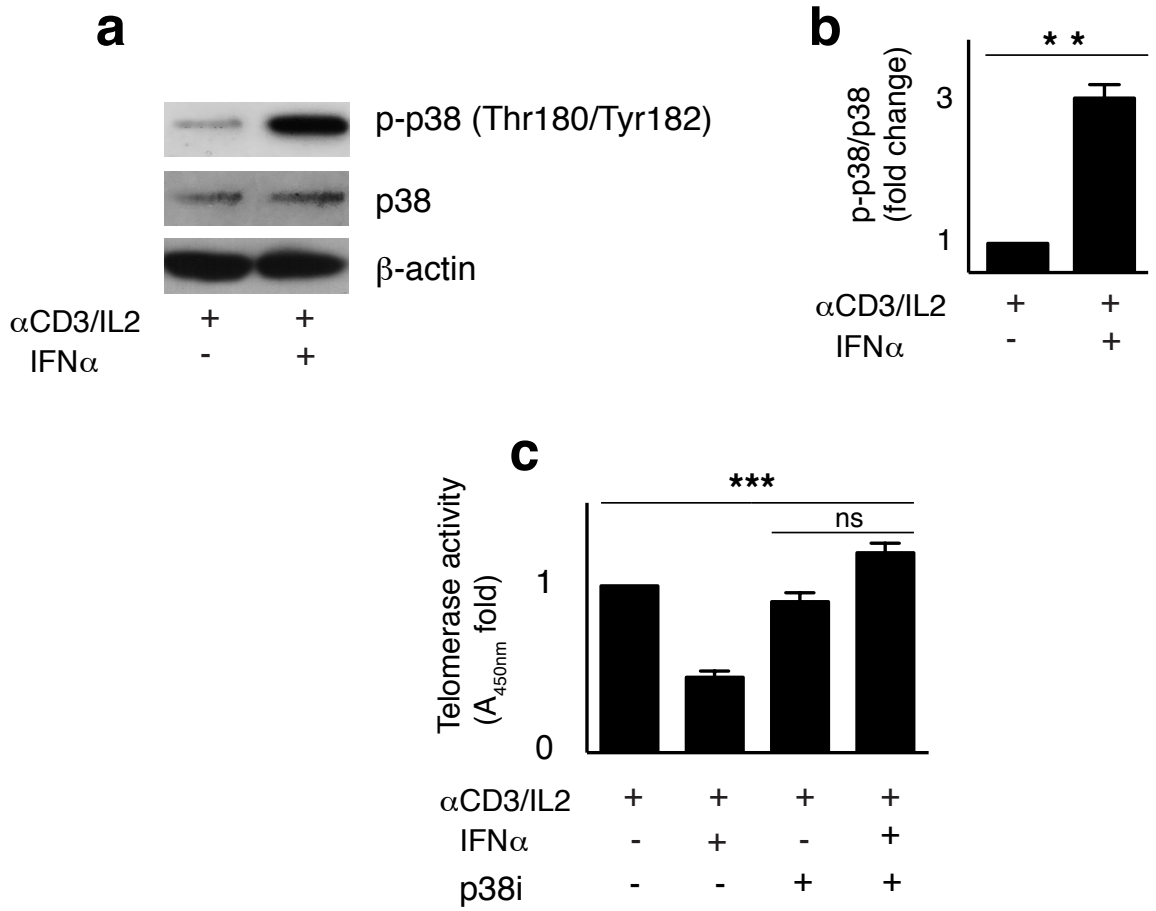

Figure 16: IFN-α inhibits telomerase activity via p38 MAPK in CD8$^+$ T cells
(a) Immunoblots of p-p38 (Thr180/Tyr182), total p38 and beta actin (as a loading control) assessed from whole extracts of human CD8$^+$ T cells activated by αCD3 and rh-IL2 for 24 hours, in the presence or absence of IFN-α (500IU). (**b**) The relative activation of p38 MAPK assessed by ratio of phosphorylated p38 to total p38 in 3 separate experiments performed as in (a), and presented as relative to that of the stimulated control, set as 1. (**c**) Assessment of telomerase activity by an ELISA-based non-radioactive TRAP assay in human CD8$^+$ T cells activated by αCD3 and rh-IL2 for 72 hours, in the presence or absence of IFN-α (500IU); p38 kinase activity was directly blocked by adding in culture the pan-p38 inhibitor BIRB 796 (500nM) as indicated. Extracts from 2 x 10^3 cells were analysed as described in Materials and Methods. Telomerase activity generated a colour metabolite detected at 450 nM by an ELISA reader; pooled data from 3 separate experiments are expressed as fold change over stimulated control, set as 1. Error bars indicate SEM throughout. In (**b**) a paired Student's T test was used; in (**c**) a one-way analysis of variance (ANOVA) for repeated-measures with a Bonferroni post-test correction. **p< 0,05, **p< 0,001, ***p< 0,001.*

3.8 IFN-α accelerates human T cell differentiation

CMV infection is an important driver for the release of IFN-α by plasmacitoid dendritic cells in humans (Fletcher et al., 2005; Libri et al., 2011). To delineate our biochemical findings in a more physiological context, we evaluated the impact of CMV infection on human $CD8^+$ T cell differentiation *in vivo* and whether IFN-α accelerates this process *in vitro*. As shown in **Figure 17 a**, human $CD8^+$ T cells can be divided in three separate subsets on the basis of their relative CD27/CD28 expression profile and old humans have a substantial increase in highly differentiated $CD27^-$ $CD28^-$ $CD8^+$ T cells, as compared to young or middle-age individuals. These cells also showed very little telomerase activity after activation (**Figure 17 b**), which confirmed previous findings from our group (Henson et al, 2009). This suggested that the documented inhibitory effect of IFN-α on human $CD8^+$ T cell telomerase in unfractionated populations (**Figure 11**), is unlikely to reflect a direct modulation on the $CD27^-$ $CD28^-$ cells that already exhibit very little – if any- telomerase activity.

To study the role of chronic CMV infection in human $CD8^+$ T cell differentiation, buffy coats from age-matched either CMV^+ or CMV^- individuals were collected (the sierological state was assessed by the diagnostic laboratory of University College London Hospital) and the frequency of relatively undifferentiated $CD27^+$ $CD28^+$, intermediate differentiated $CD27^+$ $CD28^-$ and highly differentiated $CD27^-$ $CD28^-$ $CD8^+$ T cells was determined by flow-cytometry. There was a linear correlation between ageing and progressive loss of CD27 and CD28 receptor expression in human $CD8^+$ T lymphocytes, in agreement with the notion that repeated episodes of antigen activation throughout life induces CD27 and CD28 down-modulation

(**Figure 17 c *left, right and bottom graphs,* respectively**). The CMV status also affected human T cell differentiation in that highly differentiated $CD27^-$ $CD28^-$ $CD8^+$ T cells accumulated in CMV-chronically infected individuals (**Figure 17 c, *bottom graph***). However, when these results were stratified by age, no correlation was found between CMV status and age, indicating that both ageing and CMV infection can drive human T cell differentiation independently (**Figure 17 c**). Because blood IFN-α levels are higher in chronic viral infected individuals (including those who are CMV^+), one prediction would be that the addition of IFN-α would reproduce the down-modulation of CD28 and CD27 receptors in cultured T cells. To explore this possibility, human $CD8^+$ T cells were activated by αCD3 and rhIL2 and cultured for up to 4 weeks either in the presence or absence of low levels of IFN-α (100 U/mL). Every week cells were washed, reactivated and IFN-α added back in culture; and every 2 weeks the relative expression of CD27 and CD28 receptors was assessed by flow-cytometry. **Figure 17 d** shows a representative CD27/CD28 expression profile depicting an increase proportion of highly differentiated $CD27^-$ $CD28^-$ $CD8^+$ T cells in IFN-α treated cells versus control cells. The cumulative data from 2 independent donors are shown in **Figure 17 e**. Taken together, these data indicate that inflammatory and anti-viral signals may promote the loss of telomerase activity and phenotypic differentiation of human T cells towards replicative senescence, and that p38 MAPK signalling may be directly involved in this process.

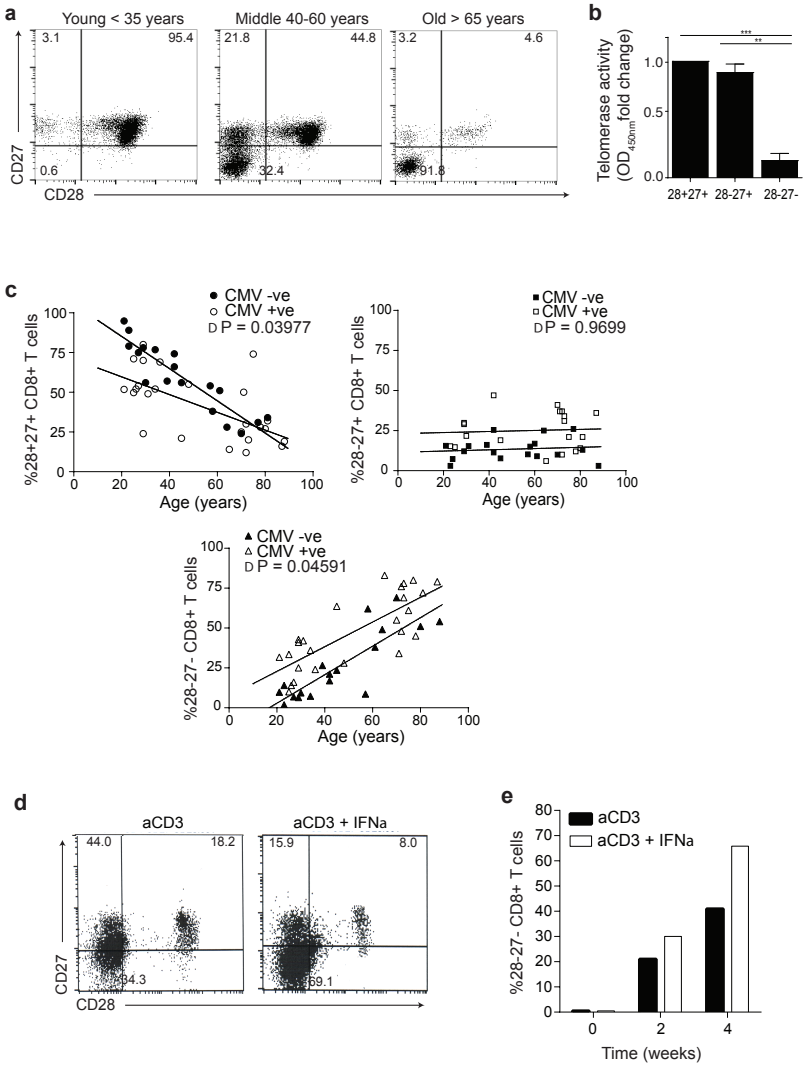

Figure 17: IFN-α accellerates loss of CD27 and CD28 on activated CD8 T cells (a) The relative co-expression of CD27 and CD28 receptors in human $CD8^+$ T cells from young (< 35 years), middle (40-60 years) and old individuals (> 65 years), representative staining. $CD8^+$ T cells were isolated from peripheral blood by positive selection and then stained with antibodies to CD27 and CD28, directly *ex vivo*. Cells were washed and immediately analyzed by flow-cytometry. (**b**) Measurement of telomerase activity by an ELISA-based non radioactive TRAP assay in relatively undifferentiated $CD28^+$ $CD27^+$, intermediate differentiated $CD28^-$ $CD27^+$ or highly differentiated $CD27^-$ $CD28^-$ $CD8^+$ T cells activated by αCD3 and rh-IL2 for 72 hours. Pooled results from 3 different experiments performed as in **Figure 16 c** and presented as relative to that of the relatively undifferentiated $CD28^+$ $CD27^+$ population, set as 1. (**c**) Pooled data of immune-phenotyping of human $CD8^+$ T cells defined by relative CD27/CD28 expression from either CMV positive (+ve) or CMV negative (-ve) individuals, as assessed by the Royal Free Hospital in London, and stratified by age (x axis). (**d**) The relative co-expression of CD27 and CD28 receptors in human $CD8^+$ T cells activated by αCD3 and rh-IL2 either in the presence or absence of low-doses of IFN-α (100 IU). $CD8^+$ T cells were > 98% $CD28^+$ $CD27^+$ before culture, and were maintained in activation medium for 4 weeks; every 10 days cells were re-activated at which time IFN-α was addeded back in culture. At 2 and 4 weeks of culture, cells were immune-phenotyped for CD27 and CD28 expression by flow-cytometry as in (a-b). Error bars indicate SEM throughout. In (**b**) a one-way analysis of variance (ANOVA) for repeated-measures with a Bonferroni post-test correction was used; results in (**d**) and (**e**) are represented of two representative experiments. **p< 0,05, ***p< 0,01.*

3.9 Summary and conclusion

Previous studies highlighted that the inflammatory cytokine IFN-α was involved in T cell telomerase down-regulation both *in vitro* and *in vivo* (Fletcher et al., 2005; Reed et al., 2004). However, the mechanism by which IFN-α inhibited telomerase activity in T cells was not clear. Here I have shown that multiple pathways are engaged by IFN-α to negatively regulate telomerase activity in human $CD8^+$ T cells. Both transcriptional and post-translational mechanisms may be involved in this process. The transcription factors NFkB and E2F1 have been previously shown to either induce or inhibit the expression of the catalytic subunit of telomerase hTERT gene (Akiyama et al., 2003; Crowe, 2001). Correspondigly, I have shown that the reduced hTERT transcription in human $CD8^+$ T cells treated with IFN-α is associated with reduced NFkB and enhanced E2F1 DNA-binding activity at the hTERT promoter. These results suggest that changes in the activity of key hTERT transcriptional regulators may directly inhibit hTERT gene expression in T cells activated in the presence of IFN-α.

The down-regulation of telomerase activity induced by IFN-α in activated $CD8^+$ T cells is also likely to occur at the post-translational level. Previous work highlighted a role for the kinase AKT in direct hTERT protein phosphorylation (Kang et al., 1999), that is important to enhance telomerase stability and nuclear import. I have shown here that IFN-α can potently inhibit AKT phosphorylation at both Ser^{473} and Thr^{308} regulatory sites in activated human $CD8^+$ T cells, indicating potent AKT kinase inactivation. It is possible that the ability of IFN-α to inhibit AKT in T cells is mediated by the phosphatase PP2A, whose activity is strongly induced by IFN-α (**Figure 15 b**). Because PP2A is able to de-phosphorylate (thus inactivating)

both AKT and hTERT proteins (Li et al., 1997), this might explain the exact mechanism linking AKT and hTERT downregulation to IFN-α signalling.

Of note, this study has provided direct evidence showing that the inhibition of telomerase activity by IFN-α is in part due to its ability to strongly activate p38 MAPK signalling. The addition of the specific p38 inhibitor BIRB can significantly rescue telomerase activity in activated human $CD8^+$ T cells treated with IFN-α. However the mechanism by which p38 activation is linked to down-stream telomerase inhibition and whether this occurs at the transcriptional or post-translational level remains to be determined.

Many signalling events described here (reduced AKT phosphorylation, reduced hTERT expression, increased p38 activity) have also been reported to regulate loss of telomerase and proliferative potential in natural occurring human senescent T cells (Henson et al., 2009, 2014; Di Mitri et al., 2011; Plunkett et al., 2007). This raises the intriguing possibility that common mechanisms exist in T cells for telomerase down-regulation that are either endogenously active during senescence or that can be induced by the inflammatory cytokine IFN-α. It would therefore appear that IFN-α is able to reproduce the main biochemical features of human T cell senescence *in vitro*.

Of note, IFN-α can significantly promote human $CD8^+$ T cell differentiation *in vitro* (**Figure 17 d**), a process that was already described for human $CD4^+$ T cells and that might explain the reason why CMV chronic infection, a potent natural trigger of IFN-α *in vivo* (Fletcher et al., 2005), can accelerate CD27/CD28 loss from human $CD8^+$ T cells, independently of age. Our study therefore reinforces the role of IFN-

α in regulating end-stage human T cell differentiation. Other inflammatory cytokines such as TNF-α have also been shown to induce telomerase down-regulation and activate p38 signalling (Akiyama et al., 2003) and it is therefore possible that there is a unique molecular signature that drives the differentiation of human T cells towards senescence. In turn, this suggests a link between inflammation, senescence and the tuning of T cell function.

As discussed, it is likely that the mechanisms described here in unfractionated human $CD8^+$ T cell populations activated in the presence of IFN-α are due to the modulation of signalling pathways in non-senescent T cells, rather than the highly differentiated populations that already exhibit very low telomerase activity. Although some key signalling events appear to be conserved in both senescent and IFN-α primed T cells, the underlying biochemical mechanisms may not be identical in these cells, as different upstream trigger may be involved (senescent and inflammatory signals, respectively).

In conclusion, understanding the molecular tuning of telomerase may identify interventional targets to enhance T cell proliferative responses during ageing and I have shown here a role for IFN-α in T cell telomerase down-regulation through direct inhibition of the expression of the telomerase catalytic sub-unit hTERT and activation of the key signalling molecule p38 MAPK. It is possible that interfering with any of the mechanism reported here may reveal of therapeutic interest to boost T cell proliferative responses in chronic viral infections, by restoring telomerase activity and the related capacity of expansion of antigen-specific T cells (Akbar and Fletcher, 2005). The fact that multiple mechanisms are engaged by IFN-α in the inhibition of telomerase in T cells underscores the importance of

this process in the regulation of T cell function *in vivo.* Future work is required to establish potential mechanistic links among the various signaling pathways orchestrated by IFN-α to inhibit telomerase in T cells.

Chapter IV: p38 activation in T cells: Challenging the paradigm

4.1 Background and rationale

The finding that IFN-α inhibited T cell telomerase via p38 signalling was supported by recent data from our group indicating a spontaneous yet unexplained activation of p38 that directly inhibited telomerase and proliferative potential in both senescent human $CD4^+$ and $CD8^+$ T cells (Henson et al., 2014, 2015; Di Mitri et al., 2011). Conversely, others reported that p38 activation promoted T cell proliferation (Zhang et al., 1999) that could be explained by either differences in downstream substrate-specificity or different activation pathways upstream of p38, or both. Thus a more selective intervention (that is, to block p38 signalling only in senescent T cells) may represent a better strategy for boosting T cell function during ageing than indiscriminate p38 inhibition in all T cells.

As discussed, there are two (canonical and alternative) independent pathways in T cells that can activate p38 in response to various events (Ashwell, 2006). Because inflammatory signalling can activate p38 by the canonical MAPK cascade (Chang and Karin, 2001) and because the inflammatory cytokine IFN-α accelerates human T cell differentiation towards senescence in part through p38 activation, one prediction would be that p38 is potently activated by the canonical MAPK cascade in senescent T cells. However inflammation also induces loss of co-stimulatory receptor expression in T cells (Libri et al., 2011) that are important for canonical MAPK activation (Rincón and Davis, 2007), raising the question of whether this pathway was actually inactive in senescent T cells that lose both CD27 and CD28 receptors as a result of differentiation related events. Nevertheless because

continuous episodes of T cell activation drive human T cell differentiation (Weng et al., 2009), it was possible that p38, activated by the alternative TCR-related activation pathway, occurred in senescent T cells. To determine the mechanism of spontaneous p38 activation in senescent T cells, both canonical and alternative pathways were studied in primary populations of human $CD4^+$ T cells at the different stages of relative CD27/CD28 differentiation, directly *ex vivo*.

4.2 Spontaneous p38 activation in senescent $CD27^-$ $CD28^-$ $CD4^+$ T cells.

To study p38 signalling and related upstream events in highly differentiated T cells, the relative expression of CD27 and CD28 receptors was used as a gating strategy for cells at different stages of differentiation. By flow cytometry, the proportion of highly differentiated/senescent $CD27^-$ $CD28^-$ $CD4^+$ T cells ranged between 0.5-5 % of total human $CD4^+$ T cells (**Figure 18 a,** representative staining). Flow-cytometry enabled signaling studies in very small populations of cells directly *ex vivo*. To confirm increased p38 phosphorylation in human senescent $CD4^+$ T cells, total $CD4^+$ T cells were isolated from blood by positive selection and immediately surface stained for CD27 and CD28 receptors, then fixed, permabilized and incubated with a fluorocrome labeled antibody to phosphorylated p38 at Thr180-Tyr182 that are the sites phosphorylated within the activation loop of the molecule. **Figure 18 b** shows that p38 MAPK signalling is spontaneously increased in $CD27^-$ $CD28^-$ $CD4^+$ T cells, by 2-2.5 fold versus the less differentiated $CD27^+$ $CD28^+$ $CD4^+$ T cells and $CD27^-$ $CD28^+$ $CD4^+$ T cells. These data are derived from 9 separate individuals.

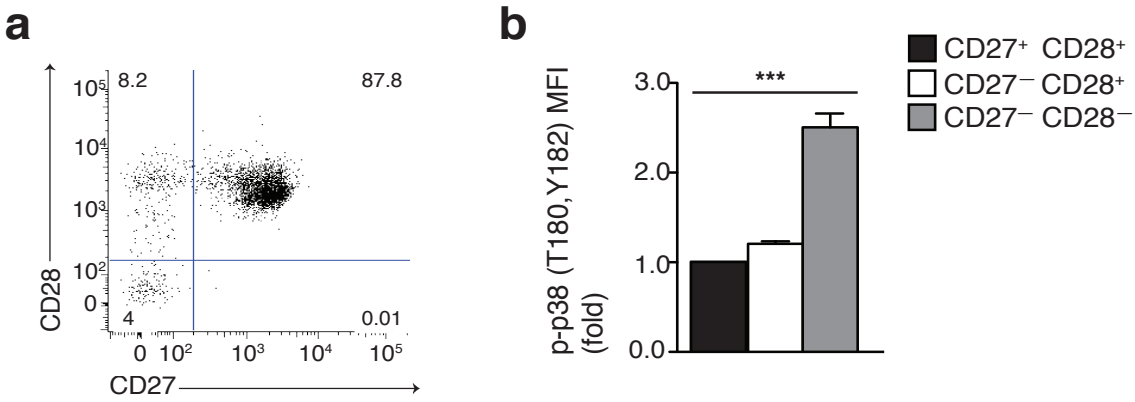

Figure 18. Spontaneous p38 activation in human senescent CD4$^+$ T cells. (**a**) The relative expression of CD27 and CD28 receptors in primary human CD4$^+$ T cells, directly ex vivo, representative of 9 separated donors. (**b**) Phospho-flow data (*n = 9*) showing endogenous activation of p38 MAPK in subsets of human CD4$^+$ T cells gated as in (a).

4.3 p38 activation without canonical pathway in senescent human $CD4^+$ T cells

As all other MAP kinases, p38 is mainly activated by the canonical MAPK cascade in all cell types, including T cells (Ashwell, 2006). To assess if the endogenous activation of p38 in human senescent $CD4^+$ T cells was linked with upstream signalling by the canonical MAPK cascade, both expression and activation of MKK3 and MKK6 that directly phosphorylate p38 in this signalling pathway (Chang and Karin, 2001) were assessed by Western Blot. The subsets of human $CD4^+$ T cells defined by relative CD27/CD28 expression were isolated as described, immediately lysed and endogenous MKK expression and activation were measured using antibodies to total MKK3 and MKK6 and to phosphorylated MKK3/MKK6 at Ser189/Ser206, respectively. GAPDH expression was measured to assess equal protein loading throughout and to determine the relative ratio of MKK activation. **Figure 19 a** shows that progressive CD27/CD28 differentiation in human $CD4^+$ T cells is associated with the down-regulation of MKK3/6 expression and activation until a maximum extent at which highly differentiated $CD27^-$ $CD28^-$ $CD4^+$ T cells do not synthetize or activate MKK molecules. These result were confirmed in 4 independent experiments (**Figure 19 b**). Thus the spontaneous activation of p38 in senescent human $CD4^+$ T cells occurs in the absence of upstream MKK3/6 signalling. This raised the question of whether p38 in senescent T cells would be unresponsive to canonical MAPK re-activation by a specific agonist. Thus human $CD4^+$ T cells were isolated, labelled for CD27/CD28 expression, activated for 1 hour by the canonical MAPK cascade agonist phorbol ester PMA (Alam et al., 2014), and p38 activation was measured by phospho-flow. Despite higher basal p38 activity, PMA treatment did not further increase p38

(T180/Y182) phosphorylation in highly differentiated $CD4^+$ T cells (**Figure 19 c**); conversely p38 was potently phosphorylated in response to PMA in relatively undifferentiated $CD4^+$ T cells that express MKK molecules (**Figure 19 c**). The cumulative data from 3 different experiments are shown in **Figure 19 d**. These data show that despite the constitutive increase in p38 activity, human senescent $CD27^-$ $CD28^-$ $CD4^+$ T cells did not regulate p38 signalling by the canonical MAPK cascade. Of note, since the representative shift depicting increased p38 activity in $CD27^-$ $CD28^-$ $CD4^+$ T cells is not absolute (for instance, as compared with the PMA-induced activation of p38 in the non-senescent population), it suggests that only part of this senescent population exhibits endogenous activity of the kinase. This does not alter the conclusion that endogenous p38 activity in senescent human $CD4^+$ T cells occurs independently of canonical MAPK signaling.

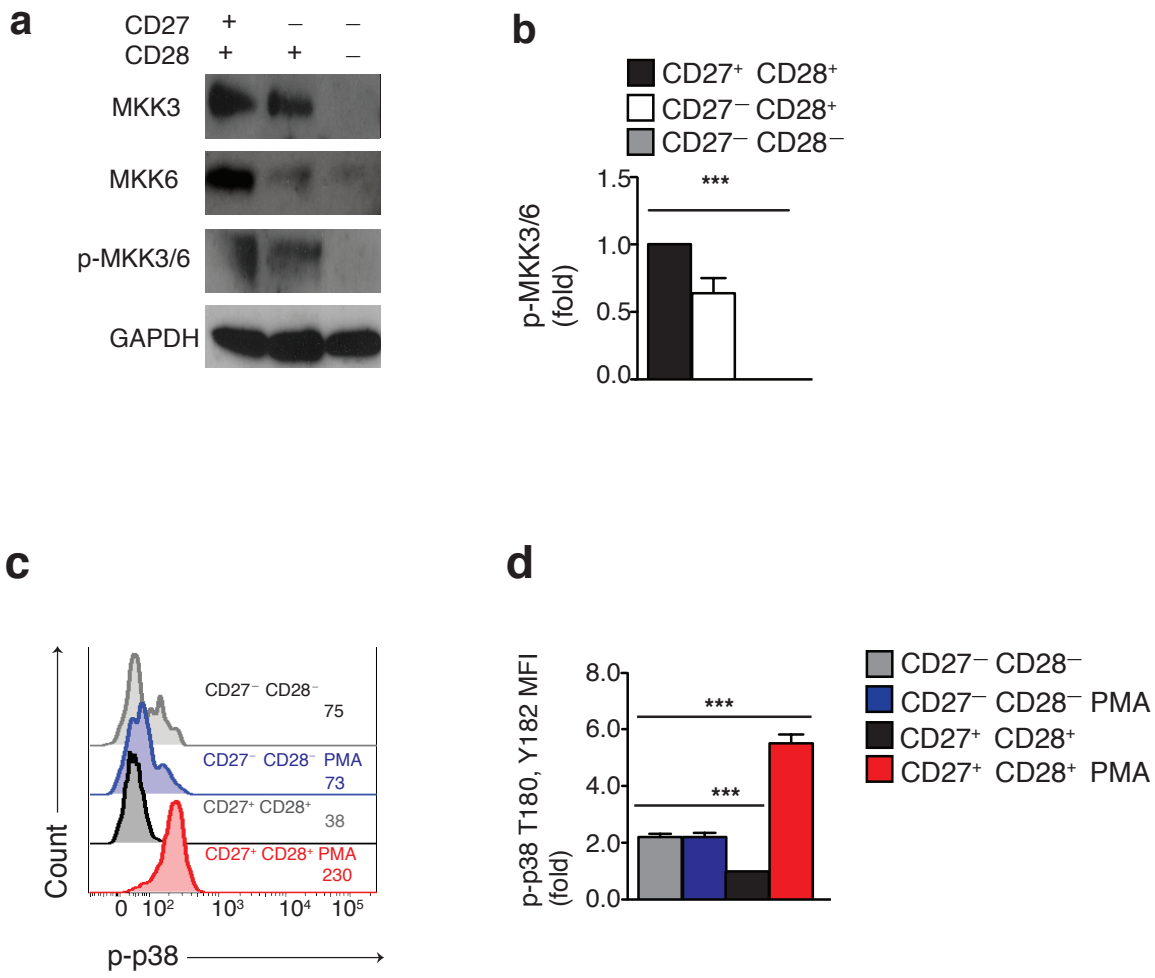

Figure 19: Loss of canonical p38 activation pathway in human senescent CD4$^+$ T cells. (**a**) Immunoblots of MKK3, MKK6 or phosphorylated MKK3/6 (Ser189/Ser206) in the CD27/28 related populations of human CD4$^+$ T cells. Untouched CD4$^+$ T cell were isolated by an immunomagnetic based 'negative' selection followed by further purification in CD27$^+$ CD28$^+$, CD27$^-$ CD28$^+$ and CD27$^-$ CD28$^-$ T cells directly *ex vivo*. Cell populations were immediately harvested without activation and endogenous signalling responses are shown. (**b**) The pooled results of band intensity from 3 different donors showing endogenous activation of MKK3/6 assessed by ratio of MKK3/6 versus total GAPDH, presented as relative to MKK activation in relatively undifferentiated CD27$^+$ CD28$^+$ CD4$^+$ T cells, set as 1. (**c**) Measurement of p38 activity by phospho-flow in relatively undifferentiated (as a positive control) or highly differentiated T cells either before or after short activation with the canonical MAPK agonist PMA (20 ng/mL) for 1 hour. (**d**) The pooled results of 3 separate experiments performed as in (c) and presented as relative to that of unstimulated CD27$^+$ CD28$^+$, set as 1. In (**b**, **d**) a one-way analysis of variance (ANOVA) for repeated-measures with a Bonferroni post-test correction. ****p< 0,01.* Error bars indicate s.e.m.

4.4 p38 activation without alternative pathway in senescent human $CD4^+$ T cells

T cells possess an alternative pathway downstream of TCR activation in which p38 is phosphorylated on Tyr323 by the TCR related kinases LCK and ZAP70 (Salvador et al., 2005), followed by p38 auto-phosphorylation on Thr180-Tyr182 (Salvador et al., 2005). The scaffold molecule DLG1 coordinates this process (Round et al., 2007). Because this pathway does not require co-stimulatory signalling and because human T cell differentiation occurs in response to repeated episodes of TCR activation, I studied the potential involvement of the alternative pathway in the constitutive activation of p38 found in senescent human $CD4^+$ T cells. To determine if alternative p38 signalling can occur in senescent human $CD4^+$ T cells, p38 (Y323) phosphorylation was measured by Western Blot both before and after αCD3 activation in either senescent $CD27^-$ $CD28^-$ $CD4^+$ T cells or nonsenescent $CD27^+$ $CD28^+$ $CD4^+$ T cells (as a control). These experiments showed that unlike relatively undifferentiated $CD4^+$ T cells in which p38 was abundantly phosphorylated on Tyr323 upon TCR activation (**Figure 20 a**), senescent human $CD4^+$ T cells did not phosphorylate p38 on Tyr323 either before or after TCR ligation (**Figure 20 a**), suggesting that the alternative pathway was inactive in this sub-population of human T cells. In fact, Western Blot-based experiments revealed that $CD27^-$ $CD28^-$ $CD4^+$ T cells lacked LCK, ZAP70 and DLG1, essential TCR signalosome components that mediate alternative p38 activation (Ashwell, 2006) (**Figure 20 b**). Conversely, both $CD27^+$ $CD28^+$ and $CD27^-$ $CD28^+$ $CD4^+$ T cells expressed high levels of TCR signalling molecules (**Figure 20 b**). This loss of TCR signalosome components was confirmed in four

different donors (**Figure 20 c**). Together, these data show that the alternative TCR dependent pathway does not activate p38 in senescent human $CD4^+$ T cells.

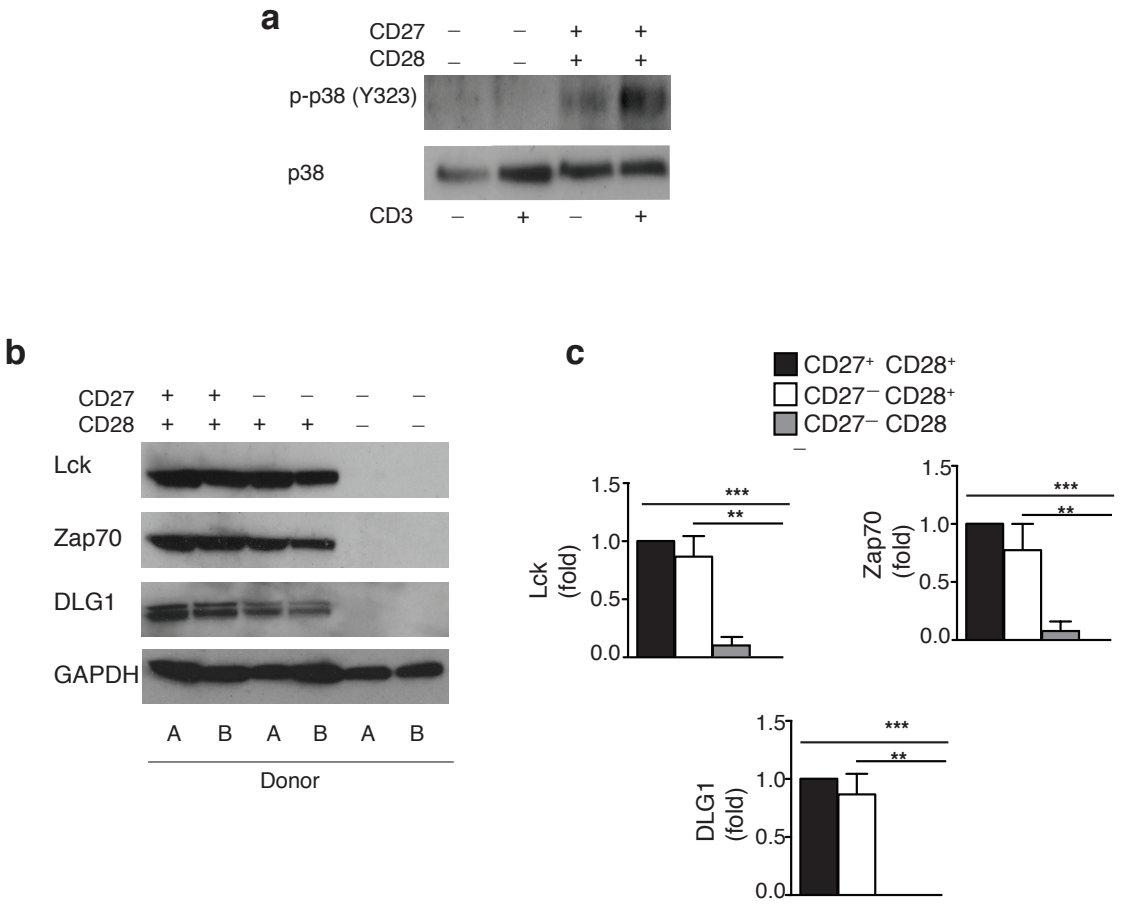

Figure 20: Loss of alternative p38 activation pathway in human senescent CD4$^+$ T cells. (**a**) Immunoblots of phosphorylated p38 at Tyr323 and total p38 in relatively undifferentiated CD27$^-$ CD28$^-$ or highly differentiated CD27$^-$ CD28$^-$ CD4$^+$ T cells either before or after short-term activation (30', 10 μg/mL) with antibody to invariant CD3 chain. (**b**) Immunoblots of total LCK, ZAP70, DLG1 and GAPDH (as a loading control) in purified subsets of human CD27$^+$ CD28$^+$, CD27$^-$ CD28$^+$ and CD27$^-$ CD28$^-$ CD4$^+$ T cells directly *ex vivo*. (**c**) Pooled data of band intensity for 3 separate experiments performed as in (b) and presented as relative to relatively undifferentiated CD27$^+$ CD28$^+$ CD4$^+$ T cells, set as 1. In (**c**) a one-way analysis of variance (ANOVA) for repeated-measures with a Bonferroni post-test correction. ***p< 0,01*, ****p< 0,01.* Error bars indicate s.e.m.

4.5 The loss of TCR signalosome is associated with defective Calcium signalling

The loss of TCR signalling components in highly differentiated, senescent human $CD4^+$ T cells was unexpected. To further characterize this process, the expression of other molecules that are essential for optimal TCR signalling was assessed. Human $CD4^+$ T cells were purified by relative CD27/CD28 expression, immediately lysed and then immune-blotted for LAT, SLP76 and PLC-γ1 expression using specific signalling antibodies; GAPDH was used to assess equal protein loading and to measure relative expression of LAT, SLP76 and PLC-γ1 throughout. **Figure 21 a** shows that $CD27^-$ $CD28^-$ $CD4^+$ T cells do not express LAT and SLP76 molecules and show very low expression of PLC-γ1 that are important to trigger calcium dependent signalling cascades upon TCR stimulation. The cumulative data from 3 different donors are shown in **Figure 21 b**. Because intracellular calcium-flux is essential for optimal T cell activation and proliferation, loss of TCR signalling machinery and proliferative potential in senescent T cells might be related to defective calcium signalling (in addition to lack of telomerase activity). To explore this possibility, human $CD4^+$ T cell subsets were isolated and activated by αCD3 for 5' and intracellular calcium abundance was measured by flow-cytometry using Fluo-4 AM dye. This probe that emits fluorescence excitation proportional to intracellular calcium concentration showed that levels of calcium in activated senescent $CD27^-$ $CD28^-$ $CD4^+$ T cells were much lower than those in relatively undifferentiated $CD27^+$ $CD28^+$ $CD4^+$ T cells upon activation (**Figure 21 c**). These observations were confirmed in 3 independent experiments (**Figure 21 d**). Thus, the loss of TCR signalosome is a novel feature of human T cell differentiation that is associated with defective intracellular calcium signals.

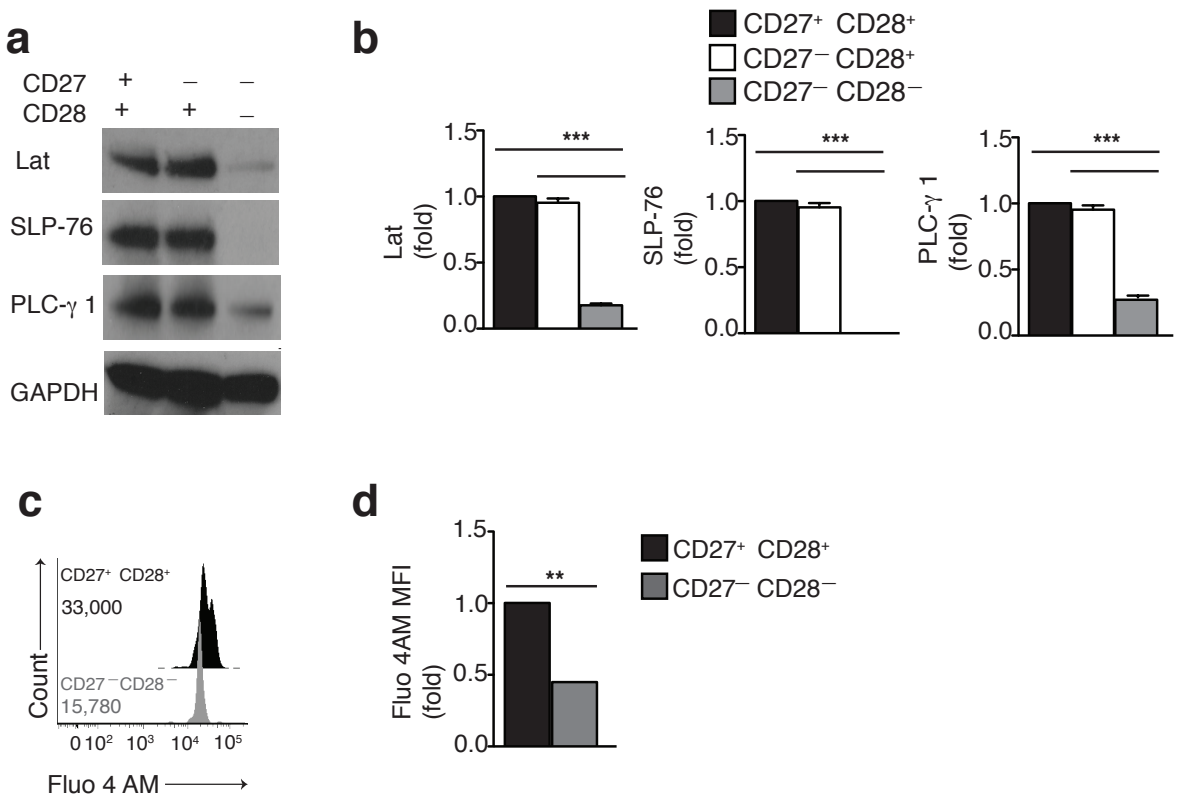

Figure 21: Loss of TCR signalosome in senescent CD4⁺ T cells.

(**a**) Immunoblot of total LAT, SLP-76 and PLC-γ 1 expression in freshly isolated human $CD4^+$ CD27/CD28 defined subsets. GAPDH was used as a loading control. (**b**) The relative expression of LAT, SLP-76 and PLC-γ 1 *vs.* total GAPDH in the $CD4^+$ CD27/CD28 defined subsets from 3 different individuals. (**c**) Representative overlay and (**d**) pooled Fluo-4 AM data from 3 independent experiments showing intracellular calcium influx after αCD3 activation (10 μg/mL, 5') in $CD27^+$ $CD28^+$ and $CD27^-$ $CD28^-$ $CD4^+$ T cells, as measured by flow-cytometry. In (**b**) a one-way analysis of variance (ANOVA) for repeated-measures with a Bonferroni post-test correction. In (**d**) a paired Student's t test. *$p< 0,05$, **$p<0.01$, and ***$p< 0.001$. Error bars depict SEM throughout.

4.6 Summary and conclusions

In T cells, P38 can be activated by either the canonical or alternative pathway in response to either environmental stress or TCR activation, respectively (Rincón and Davis, 2007). Here I provide evidence to challenge this paradigm and to imply the existence of a third, unrecognized mode for the activation of p38 in senescent T cells that potently activate the kinase in the absence of both canonical and alternative related pathways.

Although inflammation can activate p38 through the canonical MAPK cascade (Chang and Karin, 2001) (**Chapter 3**), resulting in loss of telomerase and accelerated T cell differentiation, it was unlikely that the canonical MAPK cascade, that requires co-stimulatory receptor engagement, would be active in senescent T cells that are $CD27^-$ $CD28^-$ lymphocytes. Indeed there was a progressive loss of upstream (canonical) MKK signalling during human $CD4^+$ T cell differentiation. The loss of canonical MAPK activation of p38 was not compensated by alternative TCR mediated p38 activation and instead there was an unexpected loss of TCR signalosome components in senescent human $CD4^+$ T cells, leaving the activation of p38 in these cells unexplained.

Because human senescent $CD4^+$ T cells also had defective calcium influx upon TCR activation, it suggests that loss of TCR signalling machinery in $CD27^-$ $CD28^-$ $CD4^+$ T cells may cause TCR hypo-responsiveness resulting in loss of TCR driven proliferation. Reduced capacity for TCR activation has been already described in aged naïve T cells from both mice and humans but it was linked with defective tuning of TCR calibration due to reduced ERK signalling and altered microRNA signature (Li et al., 2012). Together with loss of co-stimulatory receptor expression

and down-regulation of telomerase and proliferative potential (Akbar and Henson, 2011), the loss of TCR signalling machinery represents a novel feature of human T cell differentiation. Whether it is reversible is not clear at present.

In conclusion the results presented here challenge the current paradigm for activation of p38 in T cell populations and introduce an unrecognized characteristic of human T cell senescence. However the proximal signals that activate p38 in senescent human T cells remained to be identified. In the next chapter of this work the mechanism that spontaneously activates p38 in these cells will be unveiled.

Chapter V: p38 is activated by AMPK/TAB1 in senescent human $CD4^+$ T cells

5.1 Background and rationale

Another MKK independent mechanism for p38 activation was described in HEK293 cells using a yeast two hybrid screening assay to identify p38 binding-partners. The mechanism relied on the scaffold molecule TAB1 that was previously found to constitutively bind to and activate the MAPKK kinase TAK1 activated in turn by various cytokine receptors (Ge et al., 2002). Thus TAB1 was initially thought to provide a link between cytokine signalling and downstream p38 activation through the canonical MAPK cascade. However sub-sequent findings that both TAK1 and MKK-negative mutants did not prevent activation of the p38 bound to TAB1 revealed that the process occurred independently of the canonical MAPK pathway (Ge et al., 2002). Instead it relied on the intrinsic kinase activity of p38 itself because inactivating mutations within the p38 kinase catalytic domain or addition of the ATP competitive p38 inhibitor SB-203580 prevented the phosphorylation of p38 mediated by TAB1 (Ge et al., 2002) (that is, auto-phosphorylation of p38). The fact that TAB1 activates p38 independently of TAK1 was further corroborated by the discovery of a naturally occurring splicing variant of TAB1 (namely TAB1-β) that lack the C-term domain for interaction with TAK1 but that still potently activates p38 through the same auto-phosphorylation dependent mechanism (Ge et al., 2003).

The physiological relevance for TAB1 mediated activation of p38 has remained elusive as the pathway responded in HEK293 cells to stimuli such as inflammation, sorbitol and UV radiation that generally activate p38 via the canonical MAPK cascade (Ashwell, 2006). Among the upstream regulators of TAB1 dependent auto-phosphorylation of p38, the ubiquitin ligase TRAF6 was found to co-immunoprecipitate with both TAB1 and p38 in response to TNF-α activation in HEK293 (Ge et al., 2002) and also in monocyte-derived immature dendritic cells in response to discoidin domain receptor 1 (DDR1) engagement (Matsuyama et al., 2003), indicating that the mechanism could have important yet still poorly characterized physiological implications for tuning of immune cell function.

TAB1 dependent activation of p38 was also proposed to be important for p38 auto-phosphorylation in mouse ischemic cardiomyocytes. Li *et al.* reported that the process occurred in both wild type and MKK3 knockout ischemic hearts indicating that the process met the MKK-independence requirement for alternative TAB1 mediated p38 activation (Li et al., 2005). Importantly the mechanism was defective in AMPK knockout hearts, indicating involvement of the energy sensor AMPK (Li et al., 2005). However two sub-sequent studies rejected these conclusions by showing that perturbation of AMPK signalling by either gene knockdown or negative dominant mutant overexpression failed to prevent TAB1 dependent activation of p38 in the same experimental conditions and proposed instead that AMPK lay downstream of TAB1-p38 (Jacquet et al., 2007; Jaswal et al., 2007).

Here I tested the hypothesis that TAB1 dependent p38 signalling could compensate for the loss of both canonical and alternative p38 activation pathways observed in senescent human $CD4^+$ T cells.

5.2 Alternative TAB1 expression in senescent human $CD4^+$ T cells is associated with spontaneous AMPK activation

There are two splicing variants of TAB1 (of 60 and 50 kDA, respectively) that bind to and activate p38 through the same mechanism that is based on auto-phosphorylation (Ge et al., 2002, 2003). To begin to evaluate if TAB1 was involved in the spontaneous activation of p38 observed in senescent T cells, TAB1 expression was studied in the subsets of human $CD4^+$ T cells defined by relative CD27 and CD28 expression as above described, directly *ex vivo*. Western Blot based experiments showed that TAB1 was expressed in human $CD4^+$ T cells at all stages of differentiation however only senescent $CD27^-$ $CD28^-$ $CD4^+$ T cells expressed the alternative splicing 50 kDA-variant of TAB1 that does not bind nor activate the kinase TAK1 (Ge et al., 2003), its binding partner (**Figure 22 a**). Indeed these cells also did not express TAK1 itself (**Figure 22 a**). Because TAB1 signalling has been shown to require upstream activation by the ubiquitin ligase TRAF6 to in turn down-stream activate p38 (Ge et al., 2002), the expression of TRAF6 was investigated in the same experiments. Membranes were stripped and re-probed with anti-TRAF6, which showed that this molecule was lost in $CD27^-$ $CD28^-$ $CD4^+$ T cells (**Figure 22 a**). Conversely, non-senescent $CD27^+$ $CD28^-$ or $CD27^+$ $CD28^+$ $CD4^+$ T cells expressed abundant TRAF6 protein (**Figure 22 a**). Thus, if TAB1 was involved in the activation of p38 in senescent $CD4^+$ T cells, it

would have to be activated by a different upstream mechanism, independently of the TRAF6-TAK1 axis.

AMPK is a low energy sensor that is a TAB1 binding partner (Li et al., 2005). Activated AMPK is phosphorylated on its catalytic α sub-unit in response to either catabolic conditions (that is, when AMP levels increase over those of ATP) or oxidative stress (Cardaci et al., 2012; Hardie et al., 2012). Although it was shown that AMPK activation blocks anabolic mTOR dependent signalling in T cells (Rolf et al., 2013), it is not known if AMPK can activate p38 in these or other immune cells. To study if AMPK was involved in p38 activation via TAB1 in senescent T cells, both AMPK expression and activation were evaluated in Western Blot-based experiments. Human $CD4^+$ T cells defined by relative CD27 and CD28 expression were isolated, immediately lysed and immunoblotted with antibodies to AMPK-α and phosphorylated AMPK-α at Thr172. These experiments showed that although all human $CD4^+$ T cells had abundant AMPK-α expression only the senescent $CD27^-$ $CD28^-$ population spontaneously activated the kinase (**Figure 22 b**). To begin to probe if AMPK could act upstream of T cell p38, AMPK was pharmacologically activated by A-769662, a selective AMPK agonist (Goransson et al., 2007). $CD27^+$ $CD28^+$ $CD4^+$ T cells that normally exhibit very low spontaneous p38 phosphorylation in the absence of AMPK activity were activated either by DMSO vehicle control or A-769662 for 1 hour, followed immediately by analysis of p38 phosphorylation by phospho-flow. The representative overlay in **Figure 22 c** shows that agonist driven activation of AMPK induces p38 phosphorylation on T180/Y182, which indicates that AMPK acts upstream of p38 in T cells. The results from 3 separate experiments confirmed these findings (**Figure 22 d**). However the potential link with TAB1 remained to be determined.

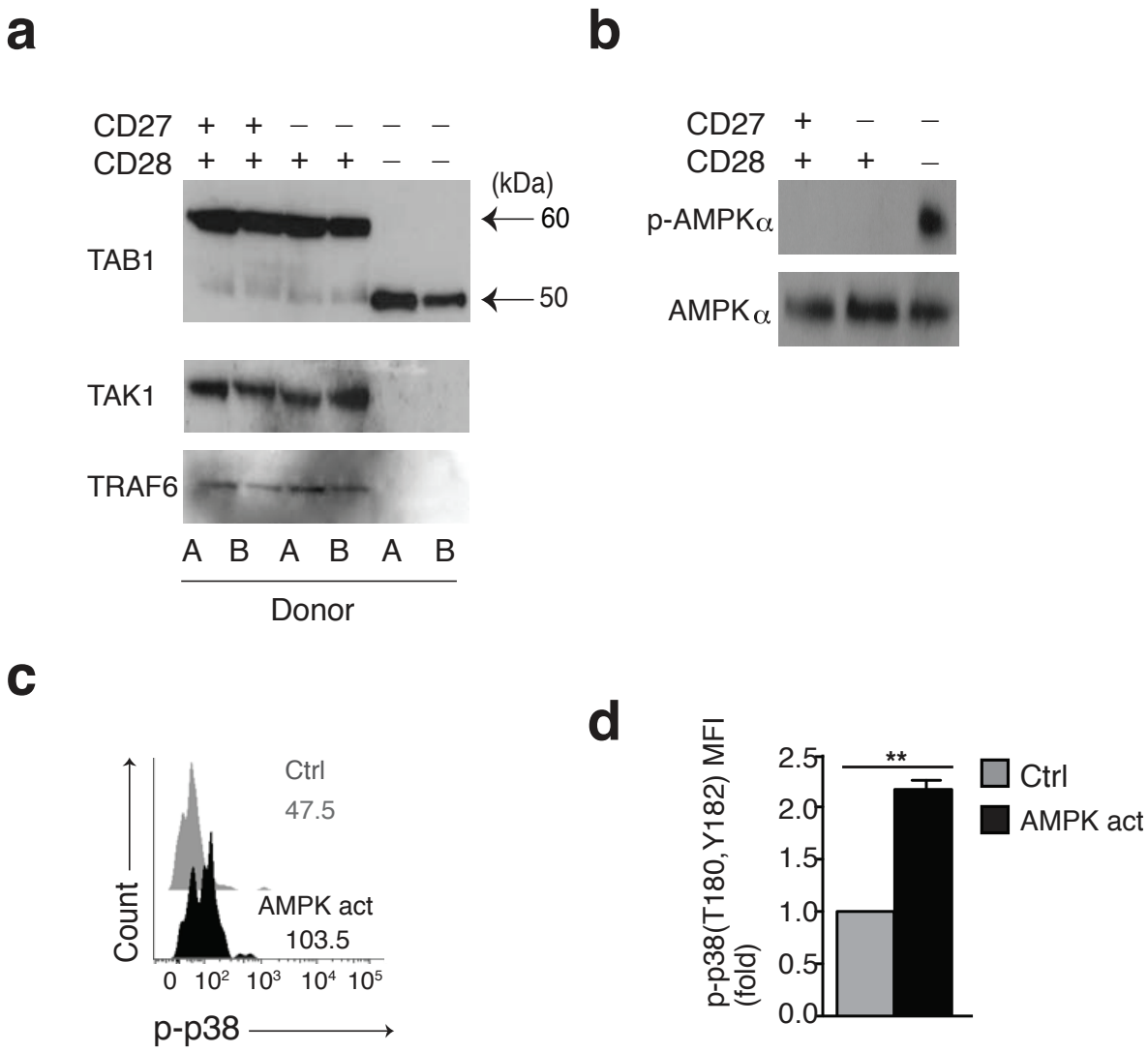

Figure 22: Senescent CD4$^+$ T cells spontaneously activate AMPK and express an alternative TAB1 variant. (**a**) Immunoblots from 2 separate donors (A and B) of TAB1, TAK1 and TRAF6 in freshly isolated human CD4$^+$ CD27/CD28 defined T cell subsets. Alternative TAB1 variants (60 and 50 k-DA respectively) are indicated by black arrows. (**b**) Endogenous phosphorylation of AMPK-α at Thr172 and expression of total AMPK-α assessed by western blotting in subsets of human CD4 T cells gated as in (a). (**c**) Phosphorylation of T cell p38 at Thr180/Tyr182 assessed by phospho-flow after incubation with either the AMPK agonist A-769662 (150 μM) for 1 hour or DMSO as vehicle control. Human CD4$^+$ T cells were isolated from peripheral blood by 'positive' selection, and, after pharmacological AMPK activation, surface-stained with antibody to CD27 and CD28 receptors; p38 activity was then studied in the CD27$^+$ CD28$^+$ population. (**d**) Pooled phospho-flow data of p38 activity from 3 separate experiments performed as in (c) and presented as relative to that of DMSO vehicle control, set as 1. In (**d**) a paired Student's t test was used. ***p<0.01*. Error bars depict sem.

5.3 Silencing AMPK and TAB1 in senescent human $CD4^+$ T cells by lentiviral vectors

Lentiviral vectors are HIV-1 derived systems used to manipulate gene expression of both dividing and non dividing target cells by permanent integration of a gene cassette into the host genome, a process known as gene transduction (Vigna and Naldini). The delivered gene cassette may encode for either a transgene, to enforce gene expression, or a short-hairpin RNA (shRNA), for gene knockdown studies based on activation of the RNA interference pathway (RNAi) (Wilson and Doudna, 2013). We used lentiviral vectors enconding shRNAs to either AMPK (shAMPK-α) or TAB1 (shTAB1) genes and studied the role of AMPK-TAB1 signaling in primary human senescent $CD4^+$ T cells. An irrelevant (nonsilencing) shRNA was used as control (shCTRL). These specific shRNAs were cloned (as described in Materials and Methods) into a p-SIREN HIV-1 derived lentiviral vector backbone, kindly provided by Dr. David Escors (a schematic representation of the vector is provided in **Figure 23 a**). These vectors were co-transfected in HEK293 cells by liposomes (Fugene 6) together with env and gag-pol plasmids to generate specific lentiviral particles (the procedure is described in Materials and Methods). These particles were then titrated in HEK293 cells (described in Materials and Methods) and finally transduced (with an MOI of 10) into purified human $CD27^-$ $CD28^-$ $CD4^+$ T cells, after activation for 48 hours by αCD3 and rh-IL2. Using this strategy of gene manipulation of primary human senescent $CD4^+$ T cells, potent knockdown (about 60-80% protein down-regulation) of either T cell AMPK-α (**Figure 23 b**) or TAB1 (**Figure 23 c**) in comparison to scrambled control transduced cells was achieved, as assessed by either RT-PCR or Western Blot analysis, 96 hours after transduction.

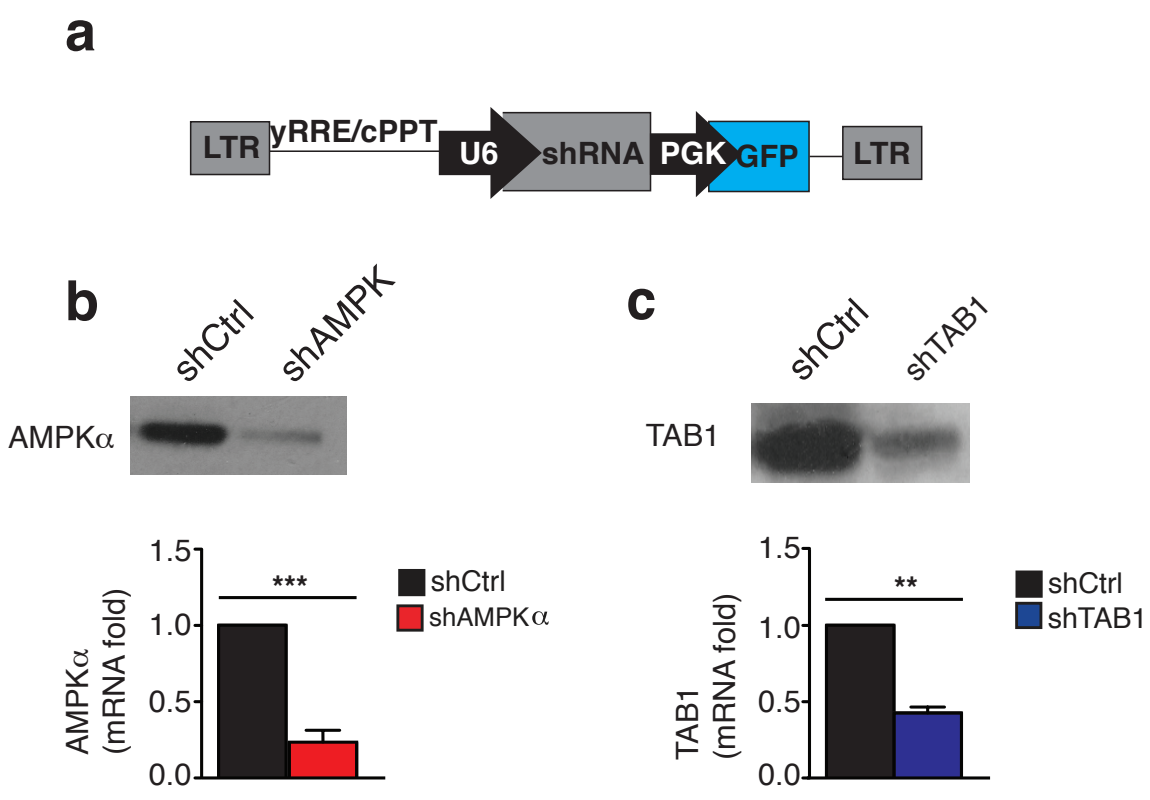

Figure 23: Validation of lentiviral vector knockdown of AMPK-α and TAB1 in senescent human CD4⁺ T cells. (**a**) Schematic representation of the p-Siren HIV lentiviral vector system used for gene knock-down. The vector encodes a shRNA for interference studies that is coupled to a GFP reporter gene (under control of a PGK promoter). LTR, long terminal repeats. Measurement of (**b**) AMPK-α or (**c**) TAB1 expression in human $CD27^-$ $CD28^-$ $CD4^+$ T cells by either immunoblot (*top*) or RT-PCR (*bottom*). Human $CD4^+$ T cells were purified by 'negative selection' followed by CD27 and CD28 sorting; and highly differentiated $CD27^-$ $CD28^-$ $CD4^+$ T cells were activated by αCD3 plus rh-IL2 for 48 hours. Cells were then transduced with lentiviral particles encoding shRNAs to either AMPK-α or TAB1. A scrambled shRNA was used as internal control. Four days post-transduction AMPK-α or TAB1 expression was assessed in shAMPK-α or shTAB1 transduced populations as above described by comparison to that of shCTRL transduced cells. Immunoblots are representative of 3 independent experiments. Samples for quantitative PCR were analyzed from 4 different donors and normalized against housekeeping GAPDH. Knockdown efficiency was evaluated 96 hours post-transduction (day 7). $^{**}p<0.01$ and $^{***}p< 0.001$ values were assessed by a paired Student's t test. Errors bars depict s.e.m.

5.4 Both AMPK and TAB1 act upstream of p38 in human senescent $CD4^+$ T cells

In addition to shRNA expression, the lentiviral vectors used for gene knockdown also encode for a green fluorescent protein (GFP) reporter gene. Thus detection of GFP^+ expression by flow-cytometry enabled the identification of effectively transduced cells in which gene knockdown was active. To study signalling events at the single cell level in the reporter GFP^+ populations, phospho-flow analysis was used. Human $CD27^-$ $CD28^-$ $CD4^+$ T cells were purified from peripheral blood of healthy volunteers, activated for 48 hours by αCD3 and rh-IL2, transduced with lentiviral particles using an MOI of 10, and the effect of either AMPK-α or TAB1 knockdown on p38 activity was studied in the GFP^+ compartments (**Figure 24 a**) using APC-labelled antibody to p-p38 (T180/Y182), 96 hours post-transduction. These experiments showed that under-steady state conditions both AMPK-α and TAB1 silenced cells showed a significant reduction of p38 activity versus scrambled control cells (by 40-50% kinase activity down-regulation; **Figure 24 b**). The pooled data from 3 independent experiments are shown in **Figure 24 c**. Thus both AMPK and TAB1 act upstream of p38 activation in senescent human $CD4^+$ T cells.

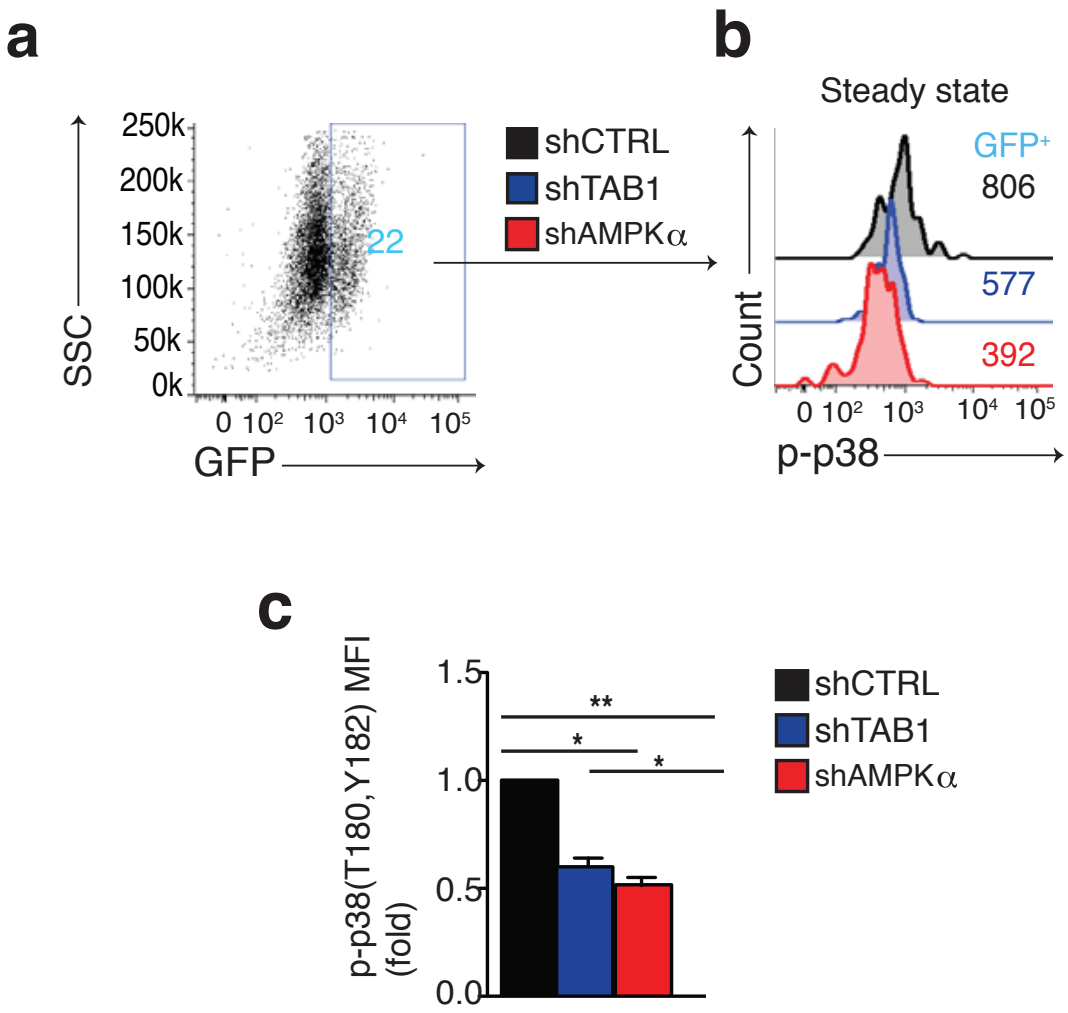

Figure 24: Both AMPK and TAB1 act upstream of p38. (**a**) Measurement of the reporter GFP gene expression in transduced purified $CD27^-$ $CD28^-$ $CD4^+$ T cells (staining of shCTRL lentivector is shown; this is representative of shTAB1 and shAMPK-α vectors too). Cells were purified, activated and transduced as in **figure 23** and analyzed by flow-cytometry 96 hours post-transduction. (**b**) Overlay from the same experiment and (**c**) pooled phospho-flow data from 3 separate experiments showing steady-state p38 (Thr^{180},Tyr^{182}) phosphorylation within the reporter GFP^+ populations of $CD27^-$ $CD28^-$ $CD4^+$ T cells transduced with lentiviral vectors encoding either shAMPKa, shTAB1 or shCtrl. Cells were fixed immediately ex-culture without further activation, permeabilized and incubated with APC-conjugated antibody to p38 phosphorylated at (Thr180-Tyr182), followed by analysis by flow-cytometry. Data are presented as relative to the transduced control population, set as 1. In (**c**) a one-way analysis of variance (ANOVA) for repeated-measures with a Bonferroni post-test correction was used. *$p< 0,05$, **$p<0.01$, and ***$p< 0.001$. Error bars depict SEM throughout.

5.5 AMPK activates p38 via TAB1 in senescent human $CD4^+$ T cells

To study the reliance of AMPK on TAB1 to induce p38 signalling, senescent human $CD4^+$ T cells were isolated, activated and transduced as above described and p38 signalling was studied in response to AMPK activation by A-769662 for 1 hour using APC-labelled antibody to p-p38 (T180/Y182). Phospho-flow analysis of GFP^+ cells showed that agonist driven activation of AMPK elevated p38 signalling in shCTRL transduced $CD27^-$ $CD28^-$ $CD4^+$ T cells but not in those transduced with shAMPK-α (**Figure 25 a**), confirming that the process was AMPK dependent. Importantly, the AMPK-agonist mediated activation of p38 was also impaired in shTAB1 transduced $CD27^-$ $CD28^-$ $CD4^+$ T cells (**Figure 25 a**), indicating that AMPK activation required TAB1 expression for optimal downstream activation of p38. I confirmed these observations in 3 separate experiments (**Figure 25 b**). To corroborate these data, the activity of a downstream target of p38, namely transcription factor ATF-2 phosphorylated at Thr71, was assessed by phospho-flow in the same experimental conditions. ATF2 activation driven by A-769662 was impaired in both shAMPK-α and shTAB1 transduced $CD27^-$ $CD28^-$ $CD4^+$ T cells, compared to scrambled control cells (**Figure 25 c**). The cumulative data are shown in **Figure 25 d**. Thus upon activation, AMPK induces p38 signalling in a TAB1 dependent way in senescent human $CD4^+$ T cells.

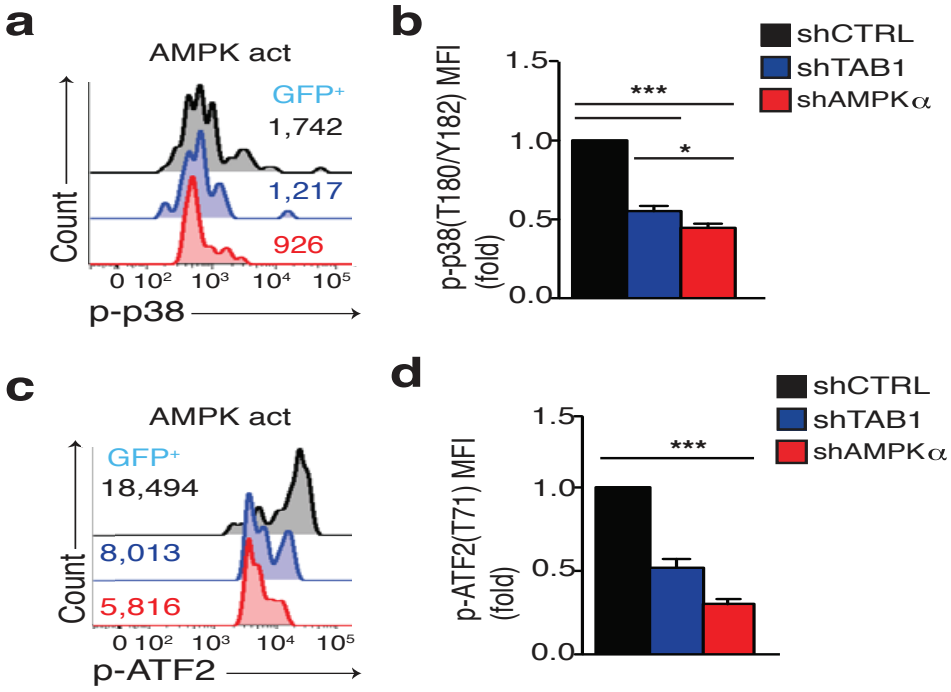

Figure 25: AMPK activates p38 via TAB1. (**a**) Phospho flow analysis and (**b**) pooled data from 3 separate experiments of purified human CD27$^-$ CD28$^-$ CD4$^+$ T cells activated and transduced as in **figure 24.** Cells were treated using the AMPK agonist (150 μM) for 1 hour followed by immediate analysis of p38 activity in the GFP$^+$ by intracellular-flow citometry. (**c**) Upon pharmacological AMPK activation (as in (**a**)), transduced CD27$^-$ CD28$^-$ CD4$^+$ T cells were analyzed by phospho-flow using anti-p-ATF2 (Thr71). (**d**) Pooled data from 3 separate experiments performed as in (**c**) and presented as relative to ATF2 phosphorylation in shCTRL transduced cells, set as 1. In (**c**), (**d**) a one-way analysis of variance (ANOVA) for repeated-measures with a Bonferroni post-test correction was used. ***$p< 0.001$. Error bars depict SEM throughout.

5.6 AMPK is activated in response to endogenous DNA damage in senescent human CD4$^+$ T cells

The spontaneous activity of AMPK in senescent human CD4$^+$ T cells was unexplained and understanding the signals that regulate AMPK activity in senescent T cells would be important to determine the physiological significance of this pathway. AMPK is activated generally in response to low nutrient sensing in the cell, when the AMP levels rise over those of ATP (Hardie, 2007). However, there was not a significant reduction of ATP levels in CD4$^+$ T cells at all stages of differentiation (**Supplementary Figure 2**).

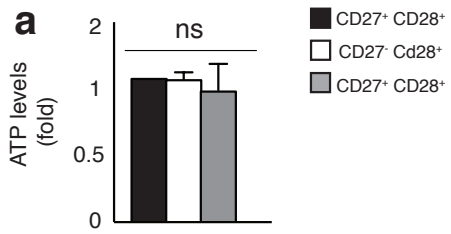

Figure S2: Endogenous ATP levels in CD27/CD28 subsets of CD4$^+$ T cells.

(**a**) ATP levels from 2 donors were measured by ELISA directly *ex vivo*.

We therefore tested whether spontaneous AMPK activation in CD27$^-$ CD28$^-$ CD4$^+$ T cells was a biochemical manifestation of senescence. When CD27$^-$ CD28$^-$ CD4$^+$ T cells were analysed by either phospho-flow or western blotting, evidence of endogenous, active DNA damage related signalling was found (Campisi and d'Adda di Fagagna, 2007), such as spontaneous phosphorylation of the apical kinase ATM at S1961 (representative overlay in **Figure 26 a** and pooled data from 3 separate experiments in **Figure 26 b**) and of its downstream target H2A-X at

T169 (representative overlay**, Figure 26 c** and pooled data in **Figure 26 d**). These features were previously used to probe active DNA damage foci. Conversely non-senescent $CD27^-$ $CD28^+$ or $CD27^+$ $CD28^+$ $CD4^+$ T cells did not spontaneously activate either ATM (**Figure 26 a**) or H2AX (**Figure 26 b**), confirming that the process occurred in a T cell compartment specific way. To investigate if ATM could in turn downstream activate both AMPK and p38, $CD27^-$ $CD28^-$ $CD4^+$ T cells were isolated from peripheral blood and immediately treated for 1 hour with the selective ATM inhibitor Ku-55933 (Hickson et al., 2004), to block endogenous ATM kinase activity directly *ex vivo*, followed by measurement of both AMPK and p38 phosphorylation by intracellular specific flow-cytometry. Treatment with Ku-55933 impaired activation of both AMPK (**Figure 26 e**) and p38 (**Figure 26 g**). These findings were confirmed in 3 separate experiments for both AMPK (**Figure 26 f**) and p38 (**Figure 26 h**). Together these data showed that ATM endogenously acted upstream of both AMPK and p38 *in vivo*. Thus endogenous AMPK-p38 activity in senescent human $CD4^+$ T cells occurred in response to ATM dependent, DNA damage related signalling.

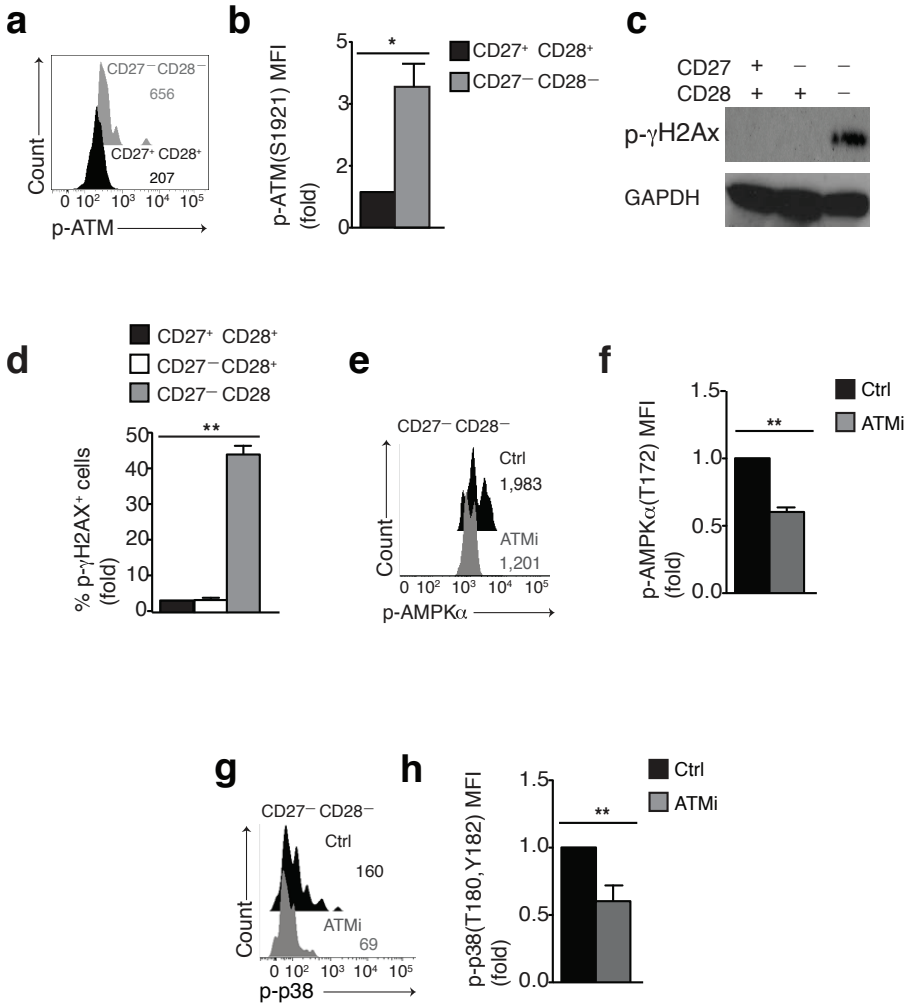

Figure 26: AMPK-p38 signalling is activated downstream of ATM. (**a**) Phosphorylation of ATM at Ser1981 by phospho-flow analysis and (**b**) pooled results from 3 separate experiments performed as in (a) in $CD27^-$ $CD28^-$ and $CD27^+$ $CD28^+$ $CD4^+$ T cells, directly *ex vivo*. Human $CD4^+$ T cells were purified by 'positive selection' and then immediately surface-stained for CD27 and CD28 expression, followed by intracellular staining for p-ATM. (**c**) Immunoblots of γ-H2A-x phosphorylated at Ser139 in CD27/CD28 defined $CD4^+$ T cell subsets directly *ex vivo*. GAPDH, loading control. (**d**) Endogenous phosphorylation of γ-H2AX at Ser139 in CD27/CD28 defined $CD4^+$ T cell subsets assessed by phospho-flow. (**e**) Representative overlay and (**f**) pooled phospho-flow data showing the effect of the selective ATM inhibitor KU-55933 (60', 10 μM) on constitutive AMPK-α (Thr^{172}) phosphorylation in $CD27^-$ $CD28^-$ $CD4^+$ T cells. Highly differentiated $CD4^+$ T cells were isolated by 'negative selection' and immediately treated with the ATM inhibitor KU-55933, followed by incubation with anti p-AMPK-α. A DMSO vehicle solution was used as a control. (**g**) Representative overlay and (**h**) pooled phospho-flow data of p38 (Thr^{180},Tyr^{182}) phosphorylation from 3 separate experiments performed as described in (e,f).

5.7 Elevated oxidative stress endogenously activates ATM, AMPK and p38

Because DNA damage by reactive oxidative species (ROS) is associated with cell senescence (Passos et al., 2013) and because ROS are known activator of AMPK (Cardaci et al., 2012), it was possible that oxidative stress (hence a telomere-independent pathway of senescence) was linked with activation of ATM, AMPK and p38 signalling in $CD27^-$ $CD28^-$ $CD4^+$ T cells. Indeed intracellular (cytosolic) ROS levels were elevated in these cells as compared to relatively undifferentiated $CD27^+$ $CD28^+$ $CD4^+$ T cells (measured by the dye indicator Dihydroethidium, DHE; **Figure 27 a**). To evaluate the effect of ROS signalling, $CD27^-$ $CD28^-$ $CD4^+$ T cells were isolated directly *ex vivo* and either left untreated or treated for 1 hour with the ROS scavenger Super-oxide dismutase (SOD) that catalyses the permutation of superoxide into oxygen and peroxide hydrogen and is therefore involved in anti-oxidant defence. This treatment reduced ATM, AMPK and p38 activity in $CD27^-$ $CD28^-$ $CD4^+$ T cells (about 50% of kinase activity down-regulation; **Figure 27 b**). The pooled data from 3 separate experiments are shown in **Figure 27 c.** These results indicate that oxidative stress by ROS can endogenously activate ATM, AMPK and p38 in senescent human $CD4^+$ T cells.

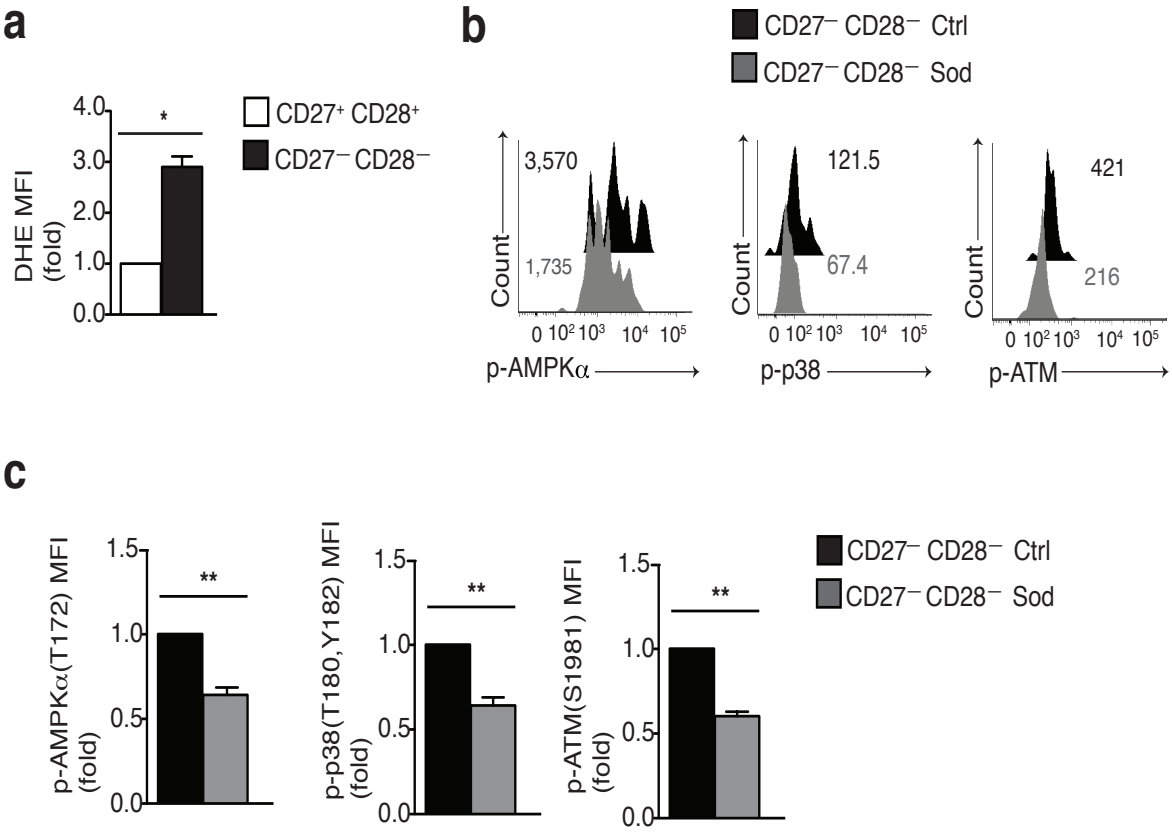

Figure 27: ROS endogenously activate ATM, AMPK and p38 in senescent CD27$^-$ CD28$^-$ CD4$^+$ T cells. (**a**) Intracellular ROS levels by Dihydroethidium (DHE) in CD27$^+$ CD28$^+$ and CD27$^-$ CD28$^-$ CD4$^+$ T cells directly *ex vivo*, as measured by flow cytometry. Data are pooled from 4 independent experiments. (**b**) Representative overlays and (**c**) pooled phospho-flow data from 3 different donors showing the effect of the ROS scavenger superoxide-dismutase (SOD; 100 U, 60') on AMPKa (Thr^{172}), p38 (Thr^{180},Tyr^{182}) and ATM (Ser^{1921}) phosphorylation in senescent CD27$^-$ CD28$^-$ CD4$^+$ T cells. All *$p< 0,05$, **$p<0.01$, and ***$p< 0.001$ values were calculated by a paired Student's t test. Error bars depict s.e.m

5.8 Evidence for p38-dependent checkpoint regulated by glucose in T cells

Because AMPK is a low-glucose sensor that is activated in response to glucose withdrawal (Rolf et al., 2013) and because spontaneous AMPK activation induces p38 signalling via TAB1 in senescent human $CD4^+$ T cells (**Figure 25**), it was possible that glucose deficiency would trigger p38 activity in non-senescent $CD4^+$ T cells that do not spontaneously activate AMPK and have very low endogenous phosphorylation of p38. A first clue that this was possible came from culturing non-senescent $CD27^+$ $CD28^+$ $CD4^+$ T cells, activated by αCD3 plus αCD28 for 48 hours, either in the presence or absence of glucose (25 mM). Glucose is essential for T cell growth (Frauwirth et al., 2002) and in the absence of a valid carbon-source alternative (for example, galactose) T cells should not become activated and die instead (Chang et al., 2013). To link p38 activation to nutrient sensing and to study its role in T cell activation, T cells were activated either in the presence or absence of the selective p38 inhibitor BIRB-796 in media either with or without glucose. Culturing T cells in the presence of glucose resulted in robust T cell clusters, hallmark of optimal lymphocyte activation (**Figure 28, *top left panel***). This process was impaired by the addition of BIRB-796 (**Figure 28, *top right panel***), indicating that p38 signalling supports T cell activation in the presence of glucose. In the absence of glucose, T cell clustering was completely abrogated (**Figure 28, *bottom left panel***). However the addition of BIRB-796 to glucose-deprived T cells partially enforced T cell clustering (**Figure 28, *bottom right panel***), suggesting that when p38 is activated in response to glucose withdrawal, it negatively regulates T cell activation instead. These data are consistent with p38 being activated in non-senescent T cells in response to glucose deprivation, a well-recognized condition leading to AMPK activation (Rolf et al., 2013).

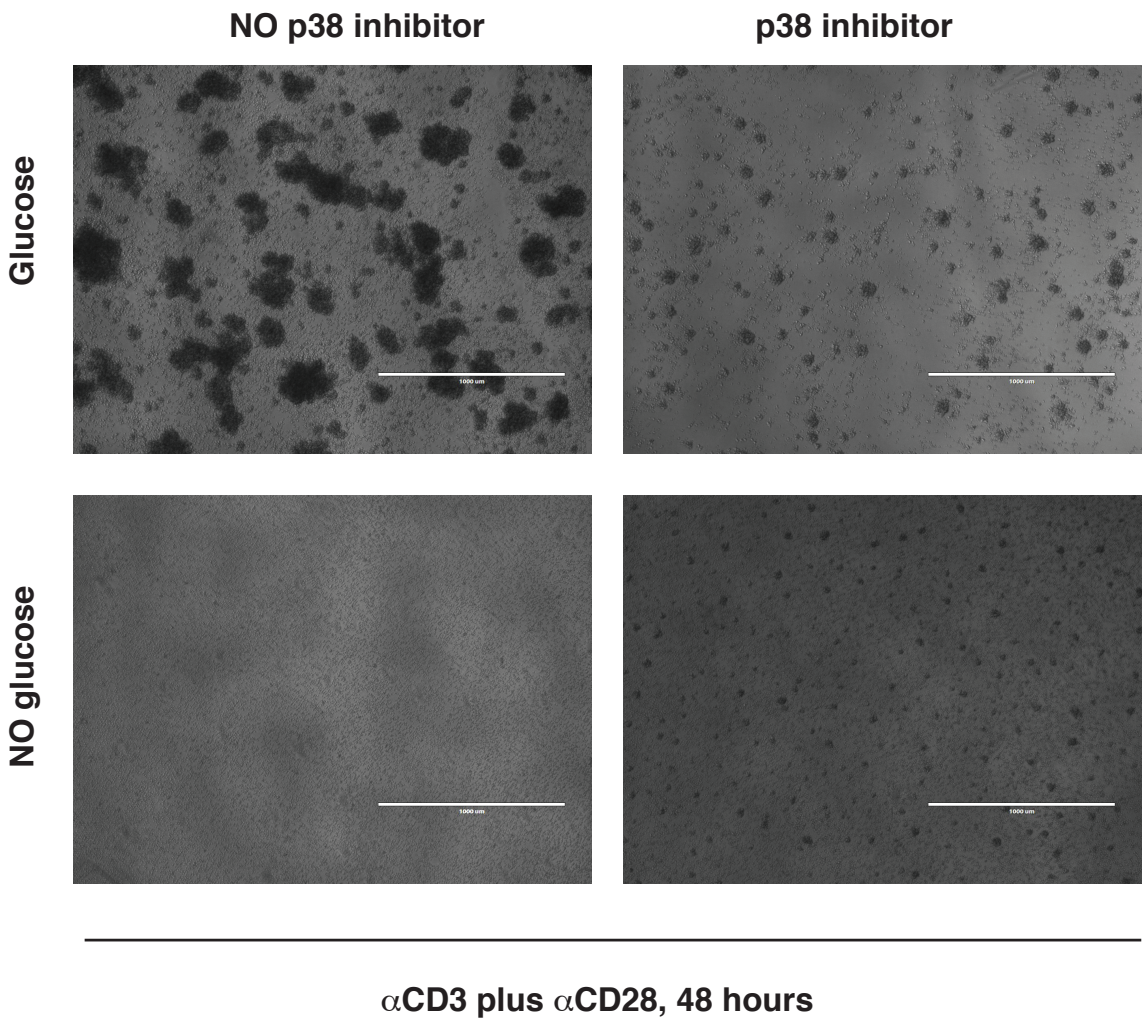

Figure 28: Evidence for a p38-dependent T cell activation checkpoint regulated by glucose. Microscopy of relatively undifferentiated human $CD27^+$ $CD28^+$ $CD4^+$ T cells activated by αCD3 plus αCD28 and cultured either in the presence or absence of glucose (25mM); p38 activity was direclty blocked through the addition of the selective p38 inhibitor BIRB 796 (500 nM) before activation; and a DMSO vehicle solution was used as a control.

5.9 Glucose deficiency activates p38 via AMPK-TAB1 in T cells

To rigorously validate that p38 was activated in response to glucose deprivation, non-senescent $CD27^+$ $CD28^+$ $CD4^+$ T cells were isolated and either rested in full-glucose or glucose-starved for 18 hours, followed by measurement of p38 activity by phospho-flow using APC-labelled antibody to p-p38 (Thr180/Tyr182). These experiments showed that glucose deprivation induced p38 phosphorylation by 1.5-2 folds in T cells (**Figure 29 a**). The cumulative data from 3 separate experiments are shown in **Figure 29 b**. To investigate if the increase in T cell-p38 activity under glucose starvation was dependent on upstream AMPK-TAB1 signalling, $CD27^+$ $CD28^+$ $CD4^+$ T cells were isolated, activated by αCD3 plus αCD28 and 48 hours later transduced with lentiviral particles to silence either AMPK-α or TAB1 gene expression. Four days post-transduction, $CD27^+$ $CD28^+$ $CD4^+$ T cells were glucose-starved for 18 hours and p38 activity was measured in the GFP^+ T cell compartment by phospho-flow, which showed that p38 phosphorylation was impaired in $CD27^+$ $CD28^+$ $CD4^+$ T cells transduced with either shAMPK-α or shTAB1 versus those transduced with shCTRL lentivector (**Figure 29 c**). These observations were confirmed in 3 independent experiments (**Figure 29 d**). Thus the activation of T cell-p38 in response to glucose starvation relies on AMPK-TAB1. Together with endogenous DNA damage activating AMPK in senescent T cells (**Figure 26**), these data support a model in which both low nutrient sensing and senescence related signalling converge on AMPK to downstream activate p38 via the scaffold molecule TAB1 in both senescent and non-senescent T cells.

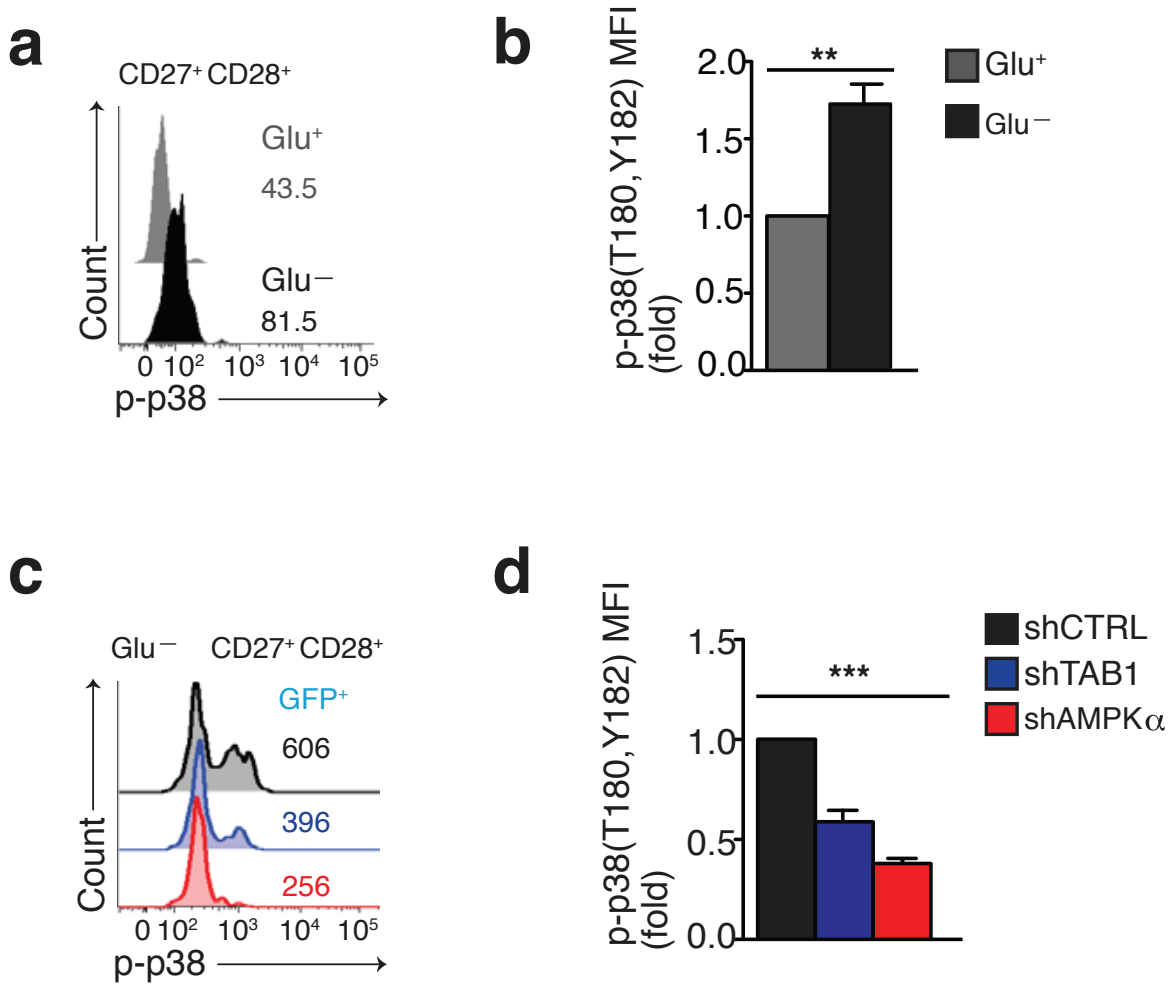

Figure 29: Glucose deficiency activates T cell p38 via AMPK-TAB1.

(**a**) Measurement and (**b**) pooled data from 3 separate donors showing p38 phosphorylation at Thr180-Tyr182 by phospho-flow in relatively undifferentiated $CD27^+$ $CD28^+$ $CD4^+$ T cells rested in the presence or absence of glucose for 18 hours. (**c**) Phosphorylation of p38 under glucose starvation in relatively undifferentiated $CD27^+$ $CD28^+$ $CD4^+$ T cells that have been transduced with lentiviral particles expressing either shCTRL, shAMPK-α or TAB1. Cells were activated by αCD3 plus αCD28 for 48 hours and then transduced 48 hours later. Four days post-transduction, GFP^+ cells were analysed by phospho-flow for p38 activity. In (**b**) a Student's t test was used; in (**d**) a one-way analysis of variance (ANOVA) for repeated-measures with a Bonferroni post-test correction.**p<0.05 ***$p< 0.001$. Error bars depict s.e.m.

5.10 AMPK activation induces p38 binding to TAB1 in T cells

Our data described a system in which there were three components: a sensor (AMPK), a scaffold (TAB1) and an effector kinase (p38). To further dissect the mechanistic details of the AMPK-TAB1 pathway of p38 activation, immunoprecipitation studies were performed in non-senescent $CD27^+$ $CD28^+$ $CD4^+$ T cells that were either left untreated or activated for 2 hours using the AMPK agonist A-769662. Cells were lysed, immunoprecipitated with antibody to TAB1, extensively washed and analysed by western blotting, which showed that agonist driven activation of AMPK induced p38 binding to TAB1 (**Figure 30 a**). The densitometric analysis to total TAB1 from 4 separate experiments demonstrated an increase in p38 binding to TAB1 in response to AMPK activation up to 3 fold (**Figure 30 b**). Furthermore TAB1 immunoprecipitates from AMPK agonist treated $CD27^+$ $CD28^+$ $CD4^+$ T cells were enriched for both phosphorylated AMPK and p38, indicating the existence of an active complex (**Figure 30 a**). These results were consistent with p38 being activated in response to AMPK activation through TAB1 binding.

It was possible that in senescent $CD27^-$ $CD28^-$ $CD4^+$ T cells in which the AMPK-TAB1 pathway for p38 activation is spontaneously active, the p38 binding to TAB1 was constitutive. To verify this prediction, either $CD27^-$ $CD28^-$ or $CD27^+$ $CD28^+$ $CD4^+$ T cells (as a negative control) were isolated, immediately lysed and immunoprecipated with antibody to TAB1, followed by western blotting analysis. These experiments showed that indeed both phosphorylated AMPK and p38 were bound to the shorter 50-kDa variant of TAB1 expressed senescent human $CD4^+$ T cells (**Figure 30 c**); conversely non-senescent human $CD4^+$ T cells expressed the 60-kDA variant of TAB1 and did not show constitutive binding of either

phosphorylated AMPK or p38 (**Figure 30 c**). Collectively these data indicate that in response to AMPK activation, p38 is phosphorylated and is bound to the scaffold TAB1 in both senescent and non-senescent T cells.

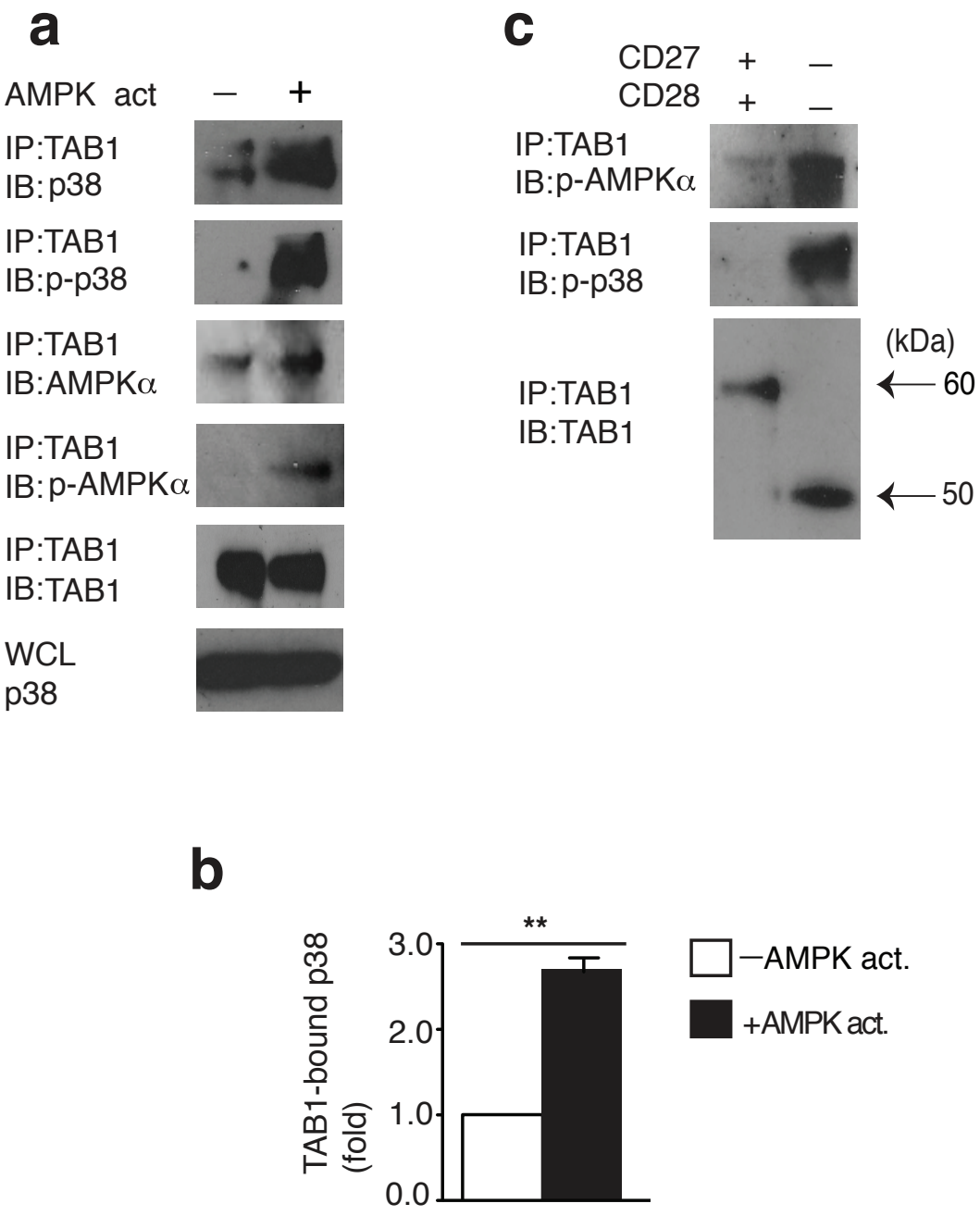

Figure 30: AMPK activation recruits T cell p38 to TAB1. (**a**) Immunoblots of total p38, phospho-p38 (Thr180/Tyr182), total AMPK-α, phospho-AMPK-α (Thr172) and TAB1 in $CD27^+$ $CD28^+$ $CD4^+$ T cells activated with DMSO control or the AMPK agonist A-769662 (150 mM) for 2 hours, followed by immunoprecipitation with anti-TAB1. Data are representative of 4 separate donors. Immunoblot of total p38 from whole cell lysate (WCL) served as input control. (**b**) The relative binding of p38 to TAB1 upon AMPK activation as determined by 4 independent experiments performed as described in (a), and presented as relative to control cells (-AMPK act), set as 1. (**c**) Freshly-isolated $CD27^+$ $CD28^+$ or $CD27^-$ $CD28^-$ $CD4^+$ T cells were immunoprecipitated with anti-TAB1 and analysed by immunoblot, as indicated (alternative TAB1 isoforms depicted by black arrows). Data are representative of 2 separate experiments (for the minor $CD4^+$ $CD27^-$ $CD28^-$ T cell fraction, cells were pooled together from 2 different donors to achieve sufficient cell number to perform the assay). In (**b**) a Student's t test was used.**p<0.05 ***$p< 0.001$. Error bars depict s.e.m.

5.11 AMPK triggered p38 recruitment to TAB1 causes p38 auto-phosphorylation.

The biochemical means by which TAB1 bound p38 became activated was still unclear. But because TAB1 was reported to mediate p38 auto-phosphorylation, a modification that relies on the intrinsic activity of the kinase (Ge et al., 2002), and because p38 is not a direct substrate for AMPK, the data suggested that AMPK may have induced p38 auto-phosphorylation via eliciting its binding to TAB1. Thus p38 was immunoprecipitated from AMPK agonist-activated $CD27^+$ $CD28^+$ $CD4^+$ T cells that had been transduced with either shTAB1 or shAMPKα and the kinase activity of p38 was assessed in the absence of an added substrate *in vitro* as described, to determine p38 auto-phosphorylation (Salvador et al., 2005). Using this assay, activated p38 was detected in immunoprecipitates from scrambled control-transduced $CD27^+$ $CD28^+$ $CD4^+$ T cells, and this activity was enhanced by the addition of ATP *in vitro* (**Figure 31 a**). Conversely adding ATP to p38 immunoprecipitates from shTAB1 or shAMPKα-transduced $CD27^+$ $CD28^+$ $CD4^+$ T cells did not increase p38 activity *in vitro* (**Figure 31 a**). This indicates that p38 auto-phosphorylation requires both AMPK-TAB1 with which p38 interacts in response to AMPK activation**.** To confirm that the above experiment was indicative of p38 auto-phosphorylation (and not an event mediated by an unrelated co-immunoprecipitated kinase), an inhibitor of p38 that is an ATP-competitor (SB-203580) was added directly to the *in vitro* kinase reaction itself. SB-203580 prevented the enhanced p38 phosphorylation *in vitro* in response to exogenous ATP, but not the baseline kinase activation within the cells, in TAB1 immunoprecipitates after AMPK activation (**Figure 31 b**). Similar results were

obtained with a different inhibitor of p38 activity (BIRB 796, data not shown). Thus, the p38 recruited at the AMPK-TAB1 complex auto-phosphorylates.

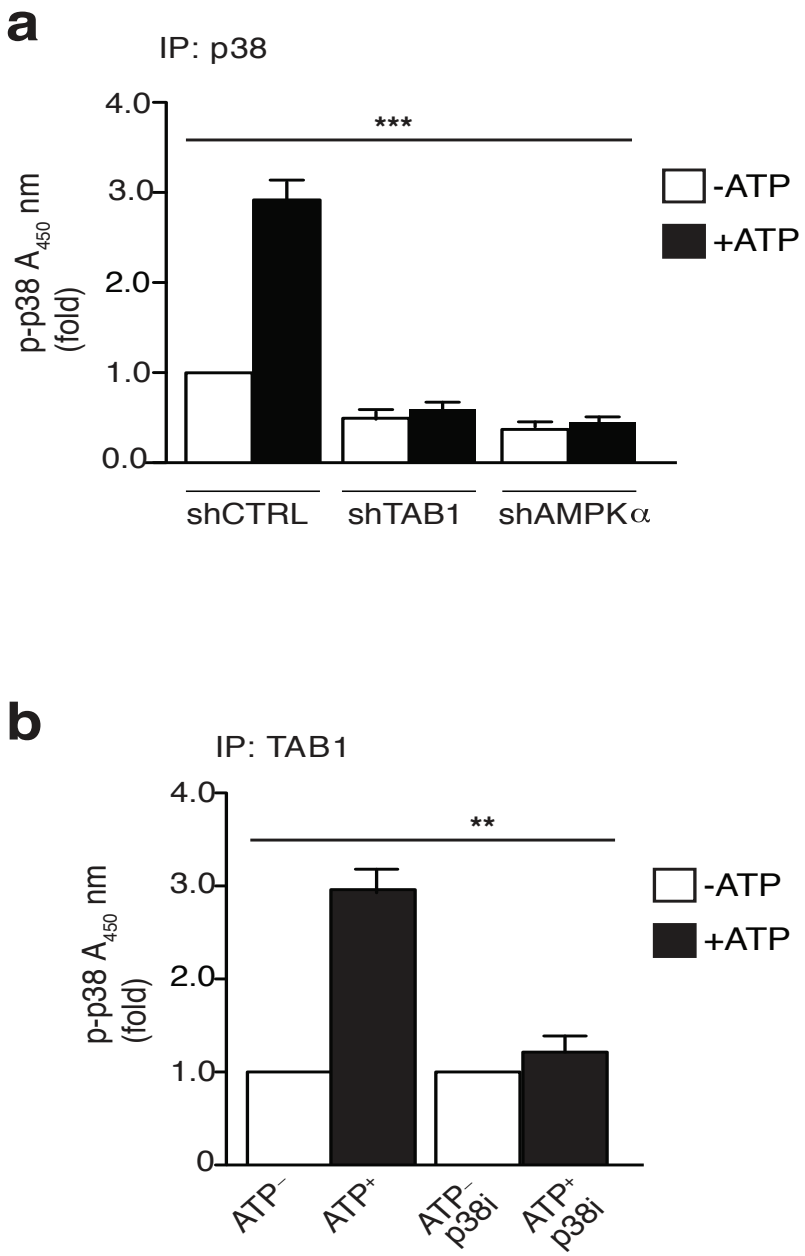

Figure 31: AMPK-TAB1 bound T cell p38 auto-phosphorylates. (**a**) Measurement of p38 auto-phosphorylation by ELISA-based *in vitro* kinase assay of p38 immunoprecipitates from transduced purified $CD27^+$ $CD28^+$ $CD4^+$ T cells reactivated with the AMPK agonist A-769662 (150 μM) for 2 hours. Immunoprecipitates were left untreated or incubated for 30 min with ATP (200 μM). Data are pooled from 3 different donors and are presented as relative to the shCTRL transduced populations that was not treated with ATP (-ATP), set as 1. (**e**) Measurement of p38 auto-phosphorylation of TAB1 immunoprecipitates from $CD4^+$ $CD27^+$ $CD28^+$ T cells activated with the AMPK agonist A-769662 (150 μM) for 2 hours. The assay was performed as described in (a) in the presence or absence of the p38 inhibitor SB-203580 (10 μM). Data are pooled from 3 separate donors and presented as relative to the control cells without ATP (-ATP). In (**a**), (**b**) a one-way analysis of variance (ANOVA) for repeated-measures with a Bonferroni post-test correction. ***p<0.01*, and ****p< 0.001.* Error bars depict s.e.m.

5.12 Summary and Conclusions

Here a previously unrecognized mode for the activation of T cell p38 is described. This relies on upstream activation by the metabolic master regulator AMPK and is mediated by the scaffolding molecule TAB1, leading to p38 MAPK auto-phosphorylation. In senescent $CD4^+$ T cells the pathway is spontaneously active because of endogenous activation of the DDR related kinase ATM, in response to genotoxic stress. However, glucose starvation can also trigger AMPK and lead to p38 activation via the scaffold TAB1 in non-senescent $CD4^+$ T cells that have no DNA damage. Thus, signalling through this AMPK-TAB1 pathway for p38 activation can be induced in undifferentiated T cells by low nutrient availability or in senescent T cells by DNA damage. This defines an 'intra-sensory' pathway for p38 activation in T cells that, unlike the canonical or alternative pathways that respond to external cues (Ashwell, 2006)(for example, cytokines or TCR activation), senses intracellular changes such as nutrient deprivation and genotoxic stress. Thus, intra-sensory p38 signalling is characterized by the integration of two very separate physiological processes namely low nutrient signalling and senescence through activation of the energy sensor AMPK and downstream MAPK activation. Whether this mode may also be important for the non-canonical activation of other MAP kinases (such as the JNKs or the ERKs) remains to be determined.

Auto-phosphorylation is important for intra-sensory activation of p38. Nevertheless auto-phosphorylation of p38 was previously shown to characterize both alternative DLG1 (Round et al., 2007) and TAB1 (Ge et al., 2002) mediated activation of the kinase, indicating that possibly all non-canonical mechanisms for p38 activation rely on the intrinsic activity of the kinase itself. The reason for the evolution of

various (canonical, alternative and the newly identified intra-sensory) modes for the activation of p38 is not clear, but our findings suggest that they may enable the same signalling molecule to exert opposite effects on T cell function. This may involve phosphorylation of completely different subsets of transcription factors and other effector molecules downstream of p38 as it has been recently suggested for the differential regulation of NFAT activity by canonical versus alternative phosphorylated T cell p38 (Alam et al., 2014). One possibility is that the binding of p38 to TAB1 will direct the kinase towards a different subsets of biochemical targets, which would explain the different physiological functions of differentially activated p38. In the future, it would be interesting to identify the specific downstream targets by which intra-sensory activated p38 acts, using mass spectrometry analysis.

The crystal structure of the docking site for TAB1 on p38 has been solved and is conserved in both the 60-kDa and 50-kDa variants of TAB1 that activate p38 through the same mechanism based on auto-phosphorylation (De Nicola et al., 2013). Targeting this restricted, MKK-independent interaction may reveal useful to dampen p38 activity, as it would spare ubiquitous activation by the MAPK cascade. TAB1 may be therefore a very promising target for selective tuning of p38 activity, in a T cell compartment specific way (that is, to reduce p38 signalling only in senescent T cells). In the light of the different roles ascribed to p38 signalling in T cell biology that are linked with different upstream activation pathways, this would offer important pharmacological opportunities to design selective strategies for tuning of T cell function. This may be particularly interesting in the case of p38 blocking since all the available p38 inhibitors that have been

developed for treating disease with inflammatory aetiology exhibited disappointing side effects due to the ubiquitous expression of p38 and related unselective p38 blockade in off-target tissues (Hammaker and Firestein, 2010).

The cross talk between AMPK and MAPK signalling is an important, so-far unrecognized property of immunological networks, showing that the metabolic changes that accompany nutrient deprivation and senescence (that is, when T cell function has to be constrained) do not just rely on the blocking of anabolic routes such as mTOR yet also involve the activation of dedicated downstream signalling cascades. However because AMPK is a central regulator of cell metabolism and homeostasis in many different tissues, direct intervention to block AMPK signalling in order to reduce p38 activity may not be an optimal solution. This further reinforces the idea that TAB1 inhibition may be a more interesting interventional target for tuning of intra-sensory MAPK signalling.

Chapter VI: Consequences of AMPK/TAB1 activated p38 signalling in T cells

6.1 Background and rationale

The activation of p38 regulates pleiotropic functions in T cells (Ashwell, 2006). Nevertheless the existence of different activation pathways upstream of p38 that regulate its kinase activity in opposite physiological conditions may explain the different biochemical and functional properties of the molecule.

Previous studies reported that T cell telomerase and proliferation are actively inhibited in senescent T cells by spontaneous p38 activation (Di Mitri et al., 2011). Importantly the observation that p38 blockade restores both proliferative potential and telomerase activity in senescent T cells raised the question of whether these effects could be reproduced in principle via tuning p38 activity by silencing either AMPK or TAB1 that are upstream of p38.

Therefore the aim of this chapter was to examine the effects of AMPK and TAB1 inhibition on T cell function and to link this with the downstream down-regulation of p38 activity in senescent human $CD4^+$ T cells.

6.2 Silencing AMPK or TAB1 restores telomerase in senescent $CD4^+$ T cells

To investigate the functional outcomes of AMPK or TAB1 inhibition, $CD27^-$ $CD28^-$ $CD4^+$ T cells were isolated from peripheral blood, activated by αCD3 plus rh-IL2 and 48 hours later transduced with lentiviral particles (using an MOI of 10) encoding either shAMPK-α, shTAB1 or shCTRL. Cells were maintained in activation medium (replaced every 2-3 days) and examined for functional readouts either four days post-transduction, when hTERT expression, telomerase activity and short-term proliferation were measured, or after up-to 1 month in culture, when long-term proliferation and telomere length were assessed. In case of long-term culture, cells were reactivated every 10 days (the procedure is further described in Material and Methods; see also **Figure 32**).

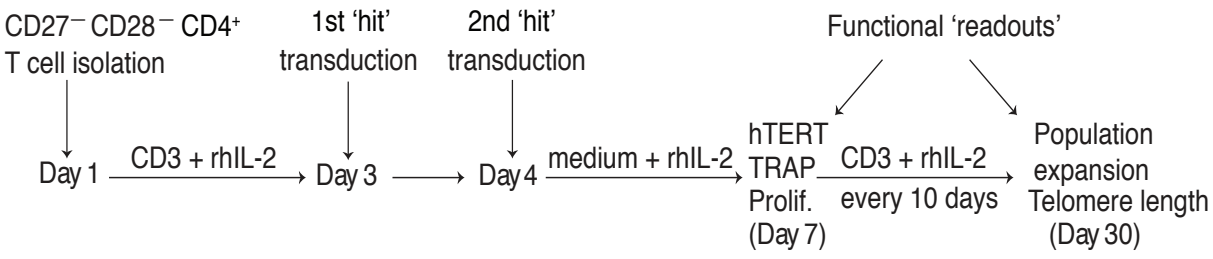

Figure 32: Experimental design. The experimental settings to manipulate gene expression in primary human senescent $CD4^+$ T cells are shown and further discussed in the text.

Firstly, the effect of AMPK-TAB1 signalling on T cell telomerase was examined. As discussed, the up-regulation of the catalytic sub-unit of telomerase hTERT is essential for telomerase activity and reduced hTERT expression is a feature of human senescent T cells that have defective telomerase activity (Akbar and Vukmanovic-Stejic, 2007). When activated $CD27^-$ $CD28^-$ $CD4^+$ T cells were transduced with lentiviral particles and then examined by Western Blot using antibody to hTERT, the protein was found to be abundantly expressed in both TAB1 and AMPK-α silenced cells versus scrambled control cells, one week after activation (**Figure 33 a, *left panel***). This was also true when hTERT mRNA was examined from transduced cells by RT-PCR under the same experimental conditions (**Figure 33 a, *right panel***). Thus, silencing AMPK-α or TAB1 restored hTERT expression in senescent human $CD4^+$ T cells.

To investigate if enhanced hTERT expression in both AMPK-α and TAB1 silenced cells would result in telomerase activity up-regulation, activated $CD27^-$ $CD28^-$ $CD4^+$ T cells were analysed by TRAP assay at the same time point. There was a significant induction of telomerase activity (by 2-3 fold) one week after transduction, upon silencing of either TAB1 or AMPK-α versus scrambled control cells (**Figure 33 b**). These data indicate that AMPK-TAB1 signalling inhibited T cell telomerase activity in part through active hTERT down-modulation.

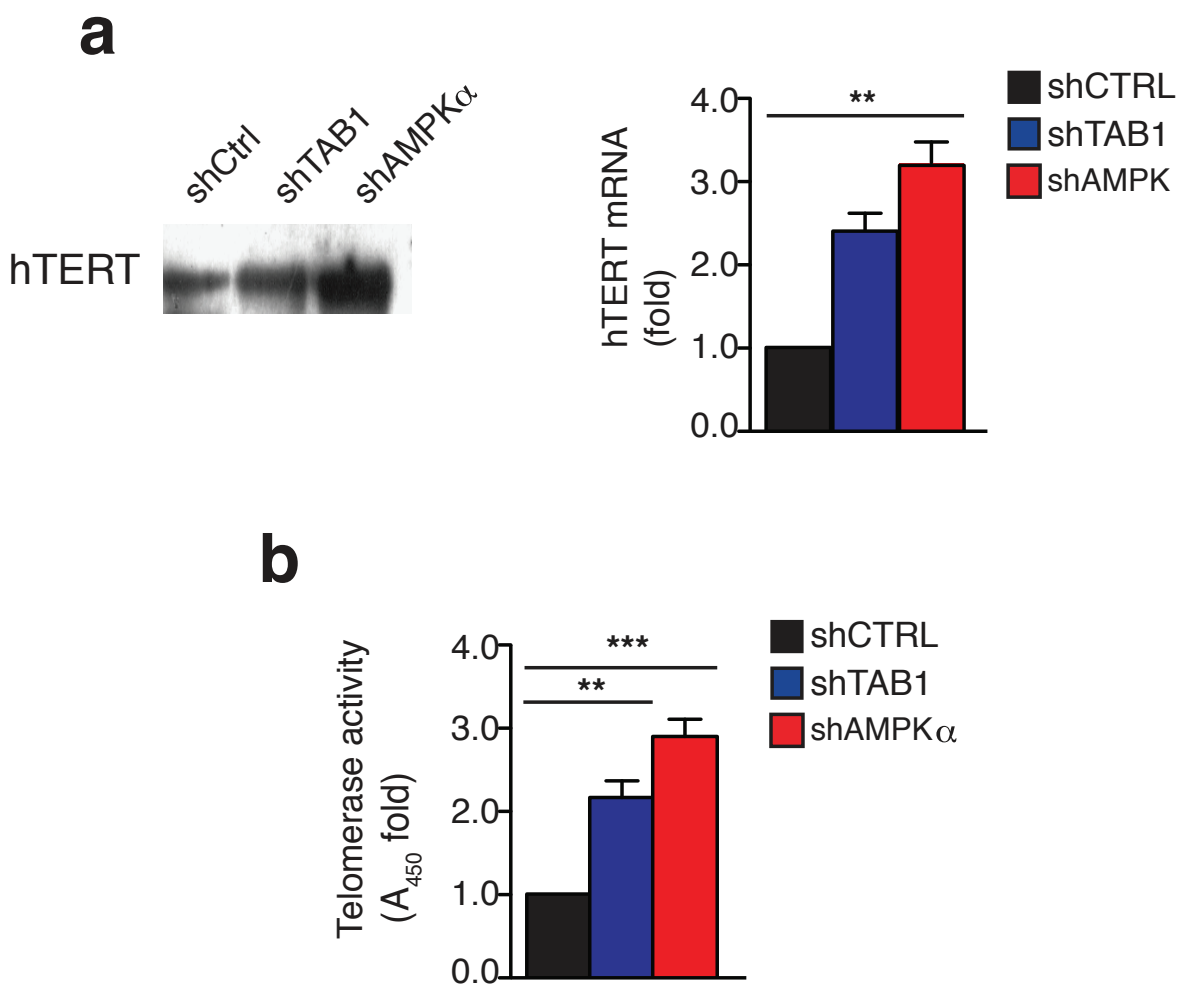

Figure 33: Silencing AMPK or TAB1 restores T cell telomerase. (**a**) Measurement of hTERT expression by both immunoblot (*left*) or RT-PCR (*right*) in purified human $CD27^-$ $CD28^-$ $CD4^+$ T cells. Cells were activated by αCD3 and rh-IL2 and transduced with the indicated lentiviral particles 48 hours later, followed by assessment of hTERT levels 96 hours post-transduction. Immunoblot is representative of 2 separate experiments; hTERT mRNA were measured from 3 different donors, and presented as relative to those of shCTRL transduced cells, set as 1. (**b**) Pooled data from 3 different donors showing measurement of telomerase activity by an ELISA-based non radioactive TRAP assay in purified human $CD27^-$ $CD28^-$ $CD4^+$ T cells activated and transduced as in (a). Results are from 3 separate donors and are presented as relative to control transduced cells, set as 1. In (**a**) and (**b**) a one-way analysis of variance (ANOVA) for repeated measures with a Bonferroni post-test correction. ***p<0.01*, and ****p< 0.001.* Error bars depict s.e.m.

6.3 Silencing AMPK or TAB1 restores telomere length and proliferation in senescent $CD4^+$ T cells

As discussed, loss of telomerase activity in senescent T cells results in telomere shortening, leading to proliferative arrest and replicative senescence (Plunkett et al., 2007). Thus to explore the *in vivo* effect of enhanced telomerase activity in AMPK and TAB1 silenced cells, telomere length was assessed. Purified $CD27^-$ $CD28^-$ $CD4^+$ T cells were activated and transduced as above described, reactivated every 10 days, and after 4 weeks in culture telomere abundance was determined using the flow-fish protocol described in Materials and Methods. These experiments showed that enhanced telomerase activity in senescent human $CD4^+$ T cells was biologically important and led to an effective telomere elongation by 0.5-0.7 kb in the GFP^+ compartments of both AMPK-α and TAB1 silenced cells, versus scrambled control cells (**Figure 34 a**). The pooled data from 3 independent experiments are shown in **Figure 34 b**.

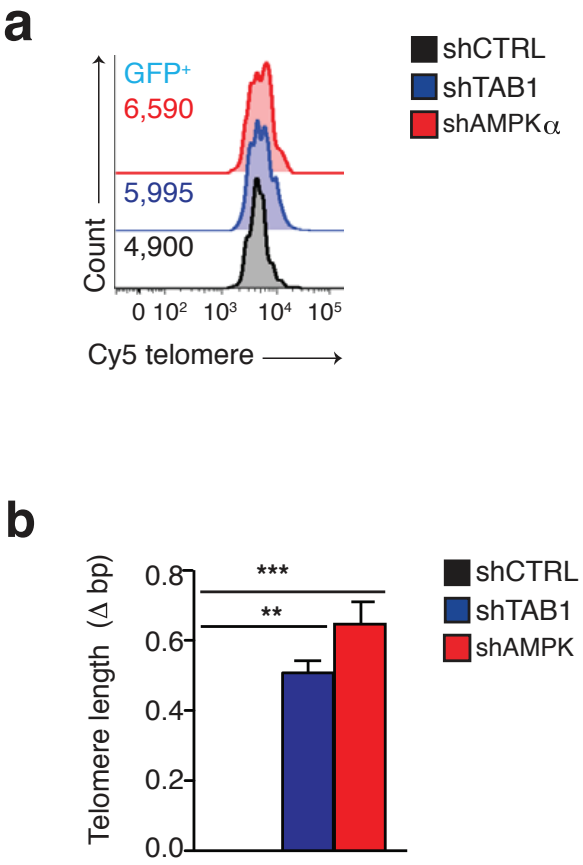

Figure 34: Silencing AMPK or TAB1 elongates T cell telomeres. (**a**) Abundance of telomeres in the GFP$^+$ population of CD27$^-$CD28$^-$ CD4$^+$ T cells transduced as in a, assessed by fluorescent *in situ* hybridization coupled to flow cytometry with a telomere-specific probe conjugated to indodicarbocyanine (Cy5 telomere). (**b**) Change in telomere length (Δbp) in CD27$^-$CD28$^-$ CD4$^+$ T cells transduced as in (a) and subjected to two rounds of activation with anti-CD3 and rh-IL2 during culture and assessed after 30 d (experimental design, **figure 32**), as in (a) and presented relative to that of cells transduced with shCTRL, set as 0.

Next the effects of either AMPK or TAB1 knockdown on both short and long-term proliferation of $CD27^-$ $CD28^-$ $CD4^+$ T cells were assessed. When transduced $CD27^-$ $CD28^-$ $CD4^+$ T cells were labelled using the cell-trace violet dye to determine T cell proliferation, multiple cell generations resulting in progressive dye dilution were observed in either AMPK-α or TAB1 silenced cells versus scrambled control transduced cells, one week after activation (**Figure 35 a**). This increase in short-term T cell proliferation was also confirmed by overnight ^{3}H-thymidine incorporation (to measure rate of active DNA synthesis) in activated transduced $CD27^-$ $CD28^-$ $CD4^+$ T cells. Silencing either AMPK-α or TAB1 enhanced ^{3}H-thymidine incorporation rates (by 3-4 fold) versus scrambled control transduced cells (**Figure 35 b**). Collectively these data demonstrate that AMPK-TAB1 signalling inhibits human T cell proliferation.

To assess if restored telomerase and proliferative potential in senescent human $CD4^+$ T cells may be associated with increased long-term expansion, activated transduced $CD27^-$ $CD28^-$ $CD4^+$ T cells were counted and their population doublings (PD) were measured, according to the equation described in Materials and Methods. There was a constant growth advantage (by 2-3 fold) for both AMPK and TAB1 silenced cells over scrambled control cells that was evident at both 96 hours post-transduction (**Figure 35 c**) and also throughout the four weeks of culture (**Figure 35 d**). Altogether these data suggested that active AMPK-TAB1 signalling enforced a status of replicative senescence in human $CD27^-$ $CD28^-$ $CD4^+$ T cells. However cells could re-elongate their telomeres and re-acquire some proliferative activity thus escaping senescence when either molecule was silenced.

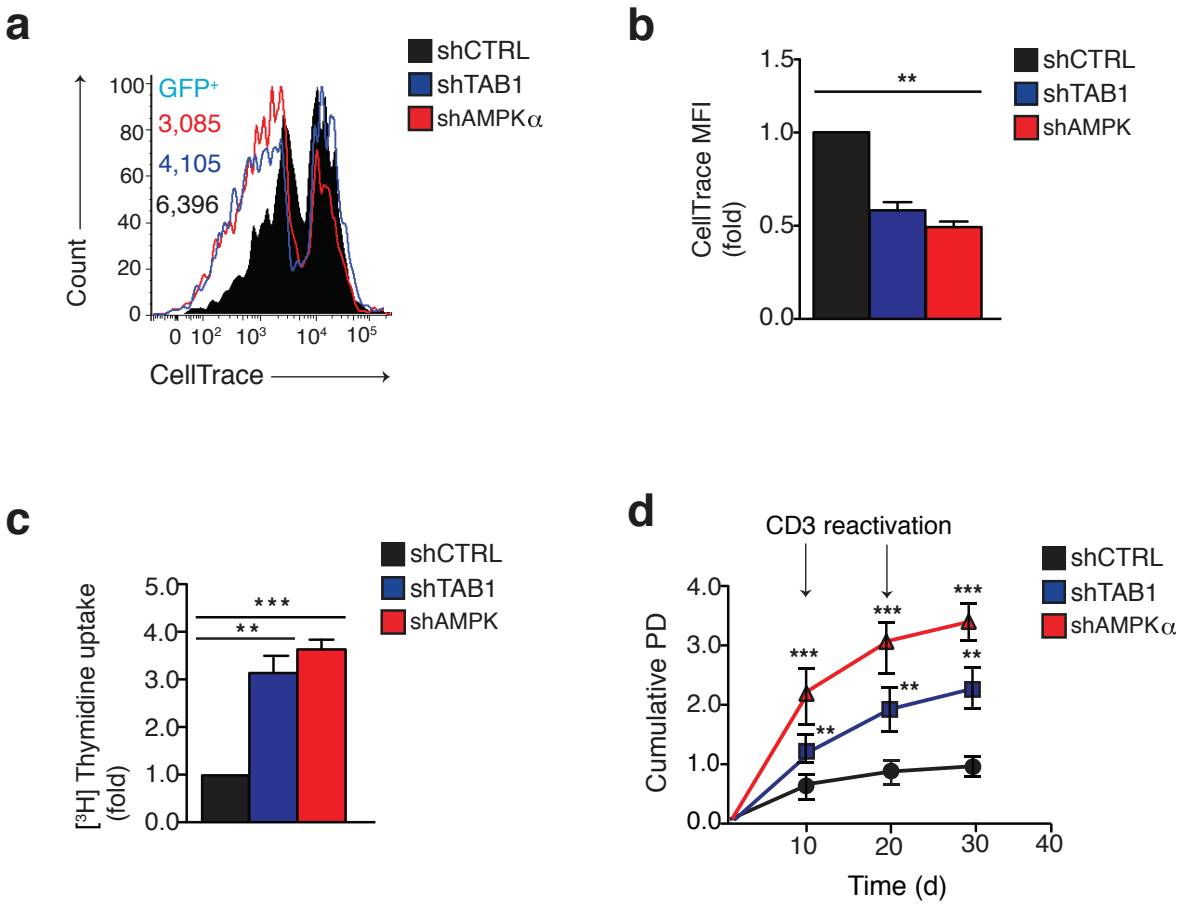

Figure 35: Silencing AMPK or TAB1 restores T cell proliferation.

(**a**) Multi-generation measurement of cell divisions by dye dilution analysis in activated $CD27^-$ $CD28^-$ $CD4^+$ T cells transduced as indicated and analyzed 96 hours later (see also experimental design, **figure 32**). (**b**) The pooled results from 3 separate experiments performed as in (a), and presented as relative to the shCTRL transduced population, set as 1. (**c**) Pooled data from 3 separate donors of rate of DNA synthesis by [^{3}H] thymidine incorporation assay (n=3) in activated $CD27^-$ $CD28^-$ $CD4^+$ T cells transduced as indicated and analyzed 96 hours post-transduction. (**d**) Replicative lifespan by cumulative population doublings (PD) of long-term cultured $CD27^-$ $CD28^-$ $CD4^+$ T cells, transduced as indicated (see also experimental design, **figure 32**). Data are from 3 separate donors. Cumulative PD were calculated by total cell number enumeration as described in Materials and Methods. All *$p< 0,05$, **$p<0.01$, and ***$p< 0.001$ values were calculated using a one-way analysis of variance (ANOVA) for repeated-measures with a Bonferroni post-test correction. Error bars depict s.e.m.

6.4 Silencing p38 reproduces the effects of AMPK-TAB1 knockdown

Because silencing either AMPK-α or TAB1 that are upstream of p38 restored telomerase and proliferative activity in senescent T cells, silencing p38 should produce similar effects. Thus $CD27^-$ $CD28^-$ $CD4^+$ T cells were purified, activated, transduced as described with lentiviral particles encoding either shP38 or shCTRL and functional outcomes were measured at the indicated time points. To confirm p38 knockdown, $CD27^-$ $CD28^-$ $CD4^+$ T cells were lysed four days post transduction and analysed by both RT-PCR and Western blotting to measure p38 levels in both shP38 and shCTRL expressing cells. $CD27^-$ $CD28^-$ $CD4^+$ T cells transduced with shP38 vector had much lower p38 mRNA and protein levels than those of shCTRL transduced cells (**Figure 36 a**), which showed that the knockdown was effective. To study the effect of reduced p38 expression on telomerase, activated transduced $CD27^-$ $CD28^-$ $CD4^+$ T cells were analysed by TRAP assay, which showed that p38 silencing up-regulated telomerase activity more than 2 fold (**Figure 36 b**). This effect was similar to that was similar to that achieved by shTAB1 or shAMPK-α transduction in these cells (**Figure 33**). P38 knockdown produced an analogous up-regulation to that induced by either AMPK-α or TAB1 knockdown, of both short (**Figure 36 c**) and long-term proliferation of $CD27^-$ $CD28^-$ $CD4^+$ T cells (overlay in **Figure 36 d** and pooled data in **Figure 36 e**), as assessed by overnight ^{3}H-thymidine incorporation and cell-trace dye violet analysis respectively. In line with increased proliferation, senescent T cells depleted of either AMPK or TAB1 expanded in culture much more than control cells as assessed by population doublings enumeration (**Figure 36 f**). Together these data indicate that the AMPK-TAB1 'intra-sensory' pathway for p38 activation inhibits T cell proliferative activity.

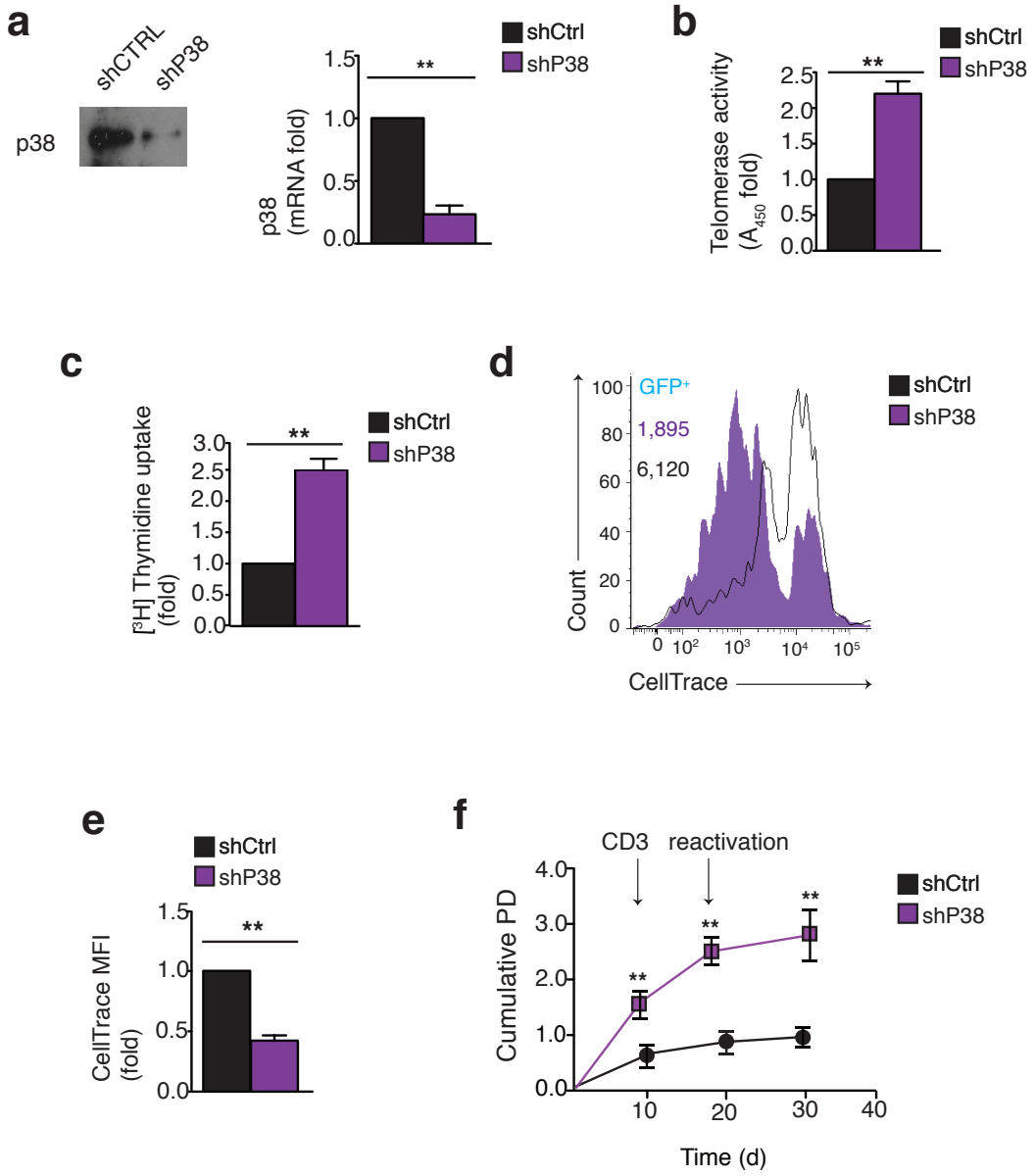

Figure 36: Silencing p38 restores T cell telomerase and proliferation (**a**) Measurement of p38 expression by both immunoblot (left) and quantitative PCR (right) in highly differentiated $CD4^+$ $CD27^-$ $CD28^-$ T cells, transduced as indicated. Immunoblot is representative of 2 independent experiments. Samples for quantitative PCR were analyzed in triplicate from 3 different donors and normalized against housekeeping GAPDH. Knockdown efficiency was evaluated 96 hours post-transduction (day 7). (**b**) Telomerase activity by TRAP assay in $CD4^+$ $CD27^-$ $CD28^-$ T cells transduced as indicated. Experiments were performed in triplicate from 3 separate donors, 96 hours post-transduction. Proliferative activity by either (**c**) ^3H thymidine incorporation or (**d**) dye dilution assay in $CD4^+$ $CD27^-$ $CD28^-$ T cells, transduced as indicated. Experiments were performed in triplicate from 3 separate donors, 96 hours after transduction. (**e**) The pooled results of 3 separate experiments performed as in (d). MFI values of a representative experiment are shown in **(**d**)**. (**f**) Replicative lifespan by cumulative PD of long-term cultured $CD4^+$ $CD27^-$ $CD28^-$ T cells, transduced as indicated. Cumulative PD were assessed by absolute cell number enumeration, in triplicate, from 3 separate donors. All *$p< 0,05$, **$p<0.01$, and ***$p< 0.001$ values were calculated by a paired Student's t test. Error bars depict s.e.m

6.5 p38 mediated modulation of cell cycle machinery in senescent $CD4^+$ T cells

To explore biochemical events that may be related to restored telomerase and proliferative potential in senescent T cells upon p38 blockade, the effects of p38 inhibition on the cell-cycle machinery of $CD27^-$ $CD28^-$ $CD4^+$ T cells were examined. In proliferating cells, there are two separate important cell-cycle regulatory checkpoints, at both the G1-S and G2-M boundaries (Giacinti and Giordano, 2006). But because senescent T cells are blocked at the G1-phase to avoid DNA replication under persistent DDR signaling (Fumagalli and d'Adda di Fagagna, 2009) and because p38 inhibition increased S-phase cycling in senescent T cells as assessed by increased ^{3}H-thymidine incorporation, only known regulators of the G1-S transition were studied. $CD27^-$ $CD28^-$ $CD4^+$ T cells were purified from peripheral blood, activated for 36 hours by αCD3 and rh-IL2 either in the presence or absence of the p38 inhibitor BIRB 796, and the levels of D1-cyclins, cell-cycle inhibitors p21 and p27, RB phosphorylation and p53 activation were examined by intracellular flow-cytometry using specific PE-conjugated antibodies. Blocking p38 signalling down-modulated the expression of the cell cycle inhibitor p27 (**Figure 37 a**), that was confirmed in 3 indepdent experiments (**Figure 37 b**); and it up-regulated the levels of D1-cyclin (representative overlay in **Figure 37 c**, pooled data in **Figure 37 d**). Inhibiton of p38 also lowered the expression of under-phosphorylated Rb (**Figure 37 e**), the active variant of the protein that acts as a cell cycle suppressor. This observation was confirmed in 3 separate experiments (**Figure 37 f**). The relative levels of phosphorylated RB (the inactive variant of the enzyme, associated with cell cycle progression) did not change when blocking p38 (data not shown) however the ratio to dephosphorylated RB-protein expression,

showed enhanced RB inactivation by BIRB-796 (**Figure 37 f**). Finally, p38 inhibtion diminished activation of p53 at the regulatory S46 residue that is directly phosphorylated by p38 (**Figure 37 h**). These changes are known to promote the G1-S transition (Campisi and d'Adda di Fagagna, 2007), which suggested that spontaneous p38 activity in senescent $CD4^+$ T cells enforces G1-phase occupancy.

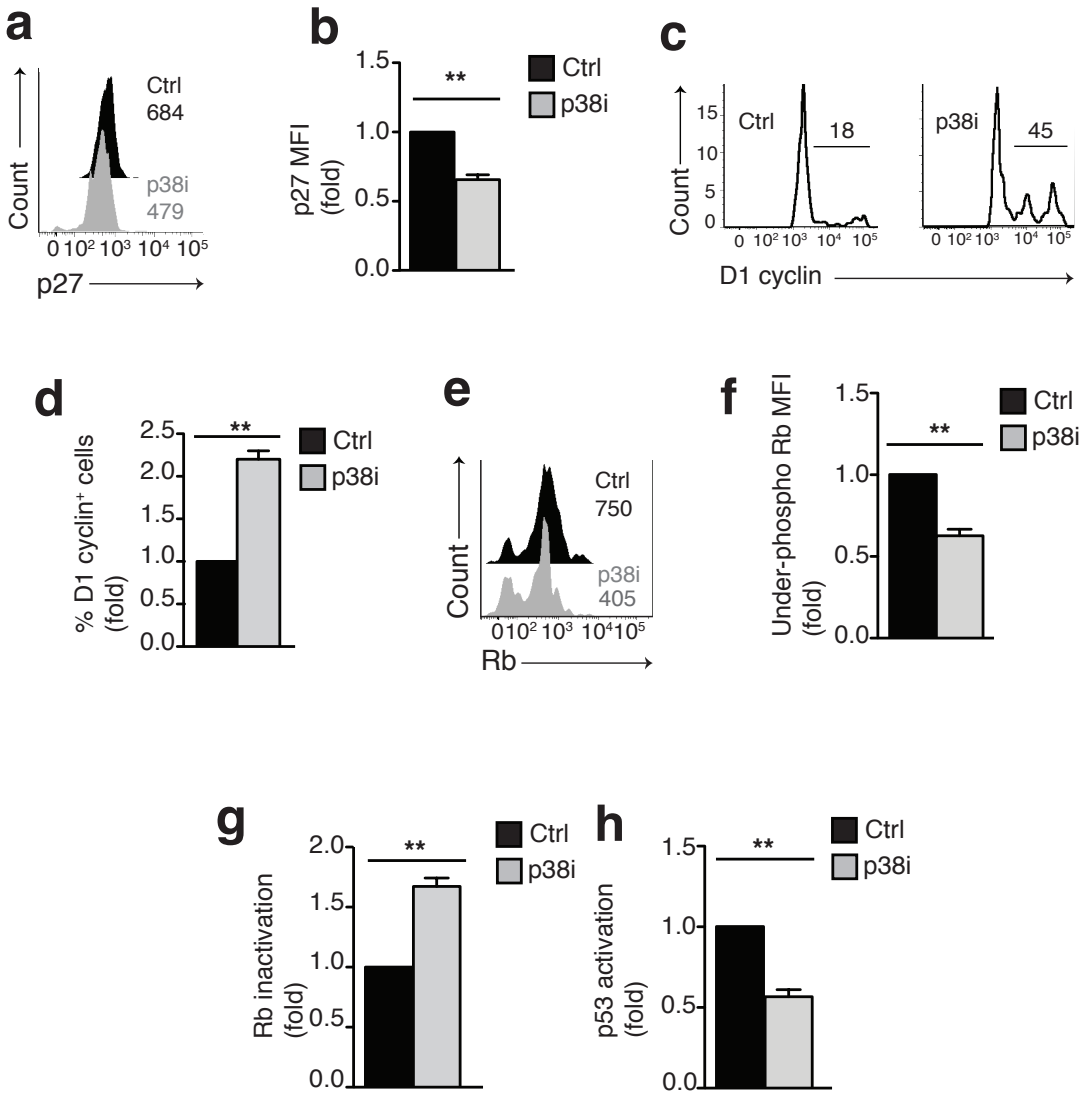

Figure 37: Blocking p38 down-regulates G1 inhibitory cell cycle machinery.
(**a, c, e, g**) Representative overlays and (**b, d, f, h**) pooled data from 3 independent experiments using purified human highly differentiated $CD4^+$ $CD27^-$ $CD28^-$ T cells, activated in the presence or absence of the selective p38 inhibitor BIRB (500 nM) for 36 hours, then analyzed by flow-citometry with the indicated antibodies; Rb inactivation was calculated as fold increase of the inhibitory Ser807/811 phosphorylation to the active, under-phosphorylated species; and p53 activation was calculated as phosphorylation at Ser46. All ***p<0.01* values were calculated by a paired Student's t test. Error bars depict s.e.m.

6.6 AMPK inhibits T cell telomerase and proliferation via p38 MAPK

Thus far the data showed that blocking either AMPK, TAB1 or p38 itself restored telomerase and proliferative activity in senescent human $CD4^+$ T cells in which the AMPK-TAB1 pathway for p38 activation is spontaneously active but the reliance on p38 signalling had to be formally proved. To mechanistically demonstrate that changes in p38 activity by upstream AMPK-TAB1 signalling are directly linked with the tuning of T cell function, AMPK was pharmacologically activated by A-769662 in non-senescent $CD27^+$ $CD28^+$ $CD4^+$ T cells either in the presence or absence of the p38 inhibitor BIRB 796. Agonist driven activation of AMPK inhibited both the short-term proliferation and telomerase activity (96 hours post-activation) and completely abrogated the population expansion of $CD27^+$ $CD28^+$ $CD4^+$ T cells (up to 4 weeks in culture) activated by αCD3 plus αCD28 while the addition of BIRB 796 restored these functions (**Figure 38 a-b**).

To robustly validate these findings (that is, to exclude off-target effects due to the simultaneous addition of two drugs targeting two different kinases in cell), p38 signalling was also blocked by lentiviral-vector knockdown. Purified $CD27^+$ $CD28^+$ $CD4^+$ T cells were activated as above described and transduced 48 hours later with lentiviral particles (using an MOI of 10) expressing either shP38 or shCTRL. Four days post transduction, either the AMPK agonist A-769662 or DMSO vehicle solution control was added in culture and both cell proliferation and telomerase activity were assessed by ^{3}H-thymidine incorporation and TRAP assay respectively, after additional 36 hours in culture. The AMPK agonist A-769662 (but not the DMSO vehicle control) inhibited both proliferation and telomerase activity of activated non-senescent human $CD4^+$ T cells in shCTRL expressing cells but not in those transduced with shP38 lentiviral vector (**Figure 38 c**). Silencing p38

also slightly inhibited the proliferation (but not the telomerase activity) of activated $CD27^+$ $CD28^+$ $CD4^+$ T cells in the presence of DMSO vehicle control, in accordance with the published observation that alternative activated p38 downstream of TCR signalosome promotes the proliferation of non-senescent T cells (Salvador et al., 2005) (**Figure 38 d**). Altogether these data show that AMPK activation inhibits the telomerase and proliferation of human T lymphocytes via downstream activation of p38 signalling, a process that requires p38 allosteric binding to the scaffold molecule TAB1, followed by p38 MAPK auto-phosphorylation ('intra-sensory' p38 activation).

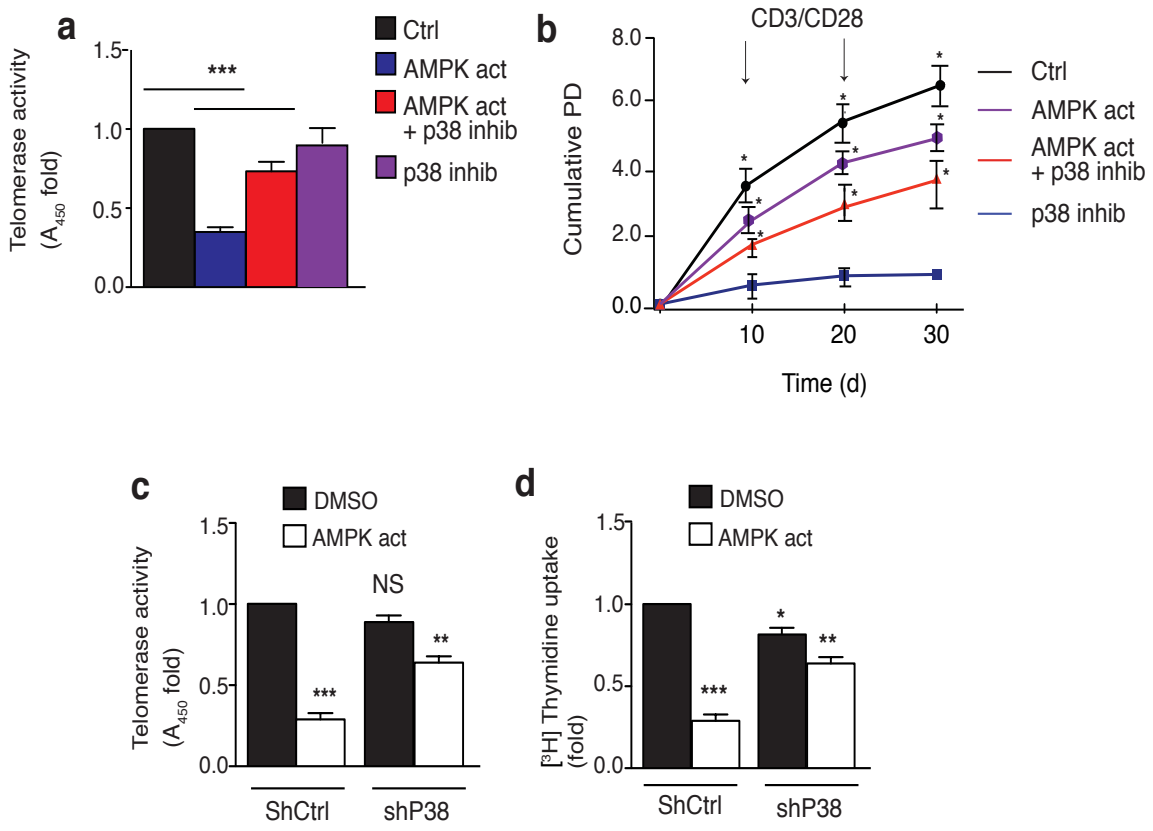

Figure 38: AMPK inhibits T cell telomerase and proliferation via p38. (**a**) Measurement of telomerase activity by an ELISA-based non-radioactive TRAP assay in purified relatively undifferentiated $CD27^+$ $CD28^+$ $CD4^+$ T cells activated by αCD3 plus αCD28 for 72 hours either in the presence or absence of the AMPK activator A-769662 (150 μM) and/or the p38 inhibitor BIRB 796 (500 nM). A DMSO vehicle solution was used as a control. Data are pooled from 3 separate experiments and presented as relative to telomerase in the control activated population, set as 1. (**b**) Replicative lifespan by cumulative PD of $CD27^+$ $CD28^+$ $CD4^+$ T cells activated and cultured over 4 weeks as in (a). Data are from 3 separate donors. (**c**) Undifferentiated $CD4^+$ $CD27^+$ $CD28^+$ T cells were activated by αCD3/CD28 antibodies and transduced 48 hours later with either shCTRL or shP38. Subsequently, cells were maintained in activation medium in the presence of the AMPK agonist A-769662 (150 μM) or DMSO vehicle control solution. Four days post-transduction, telomerase activity was assessed by an ELISA based non radioactive TRAP assay. (**d**) Proliferative activity in $CD4^+$ $CD27^+$ $CD28^+$ T cells activated and transduced as in (c) was measured by ^3H thymidine incorporation assays. All *$p< 0,05$, **$p<0.01$, and ***$p< 0.001$ values were calculated by a one-way analysis of variance (ANOVA) for repeated-measures with a Bonferroni post-test correction. Error bars depict s.e.m

6.7 Glucose starvation inhibits T cell telomerase and proliferation via p38 MAPK

Because glucose withdrawal was found to activate p38 via AMPK-TAB1 signalling, the effect of p38 activity in glucose starved T cells was studied. Non-senescent human $CD27^+$ $CD28^+$ $CD4^+$ T cells that do not spontaneously activate AMPK were activated as above described either in full glucose (as a positive control) or in the absence of glucose and any other valid carbon-source alternative (that is, to elevate AMPK signalling); either the p38 inhibitor BIRB 796 or vehicle DMSO control was added in culture to glucose starved T cells, since day 0. In accordance with the T cell activation status observed by cell-microscopy (**Figure 28**), glucose deprivation completely abolished human $CD4^+$ T cell proliferation as assessed by strong down-regulation of the nuclear antigen Ki67 that is associated with active cell cycling, compared to cells cultured in full-glucose (**Figure 39 a**). This inhibitory effect on cell cycle and related proliferation was in part mediated by p38 activation because addition of BIRB 796 enforced Ki67 up-regulation (by 10-12 fold) by glucose deprived T cells (**Figure 39 a**). These observations were confirmed in 3 separate experiments (**Figure 39 b**). Importantly the enhanced T cell proliferation upon p38 blockade was also associated with increased telomerase activity of $CD27^+$ $CD28^+$ $CD4^+$ T cells activated by αCD3 plus αCD28 under glucose starvation (**Figure 39 c**), which indicated that low-energy related activation of p38 (by AMPK-TAB1) is- at least in part- directly responsible for shutting-off T cell function. However cells did not survive the prolonged absence of glucose after 5 days even when blocking p38 (**Figure 39 d**) , in agreement with previous studies (Chang et al., 2013).

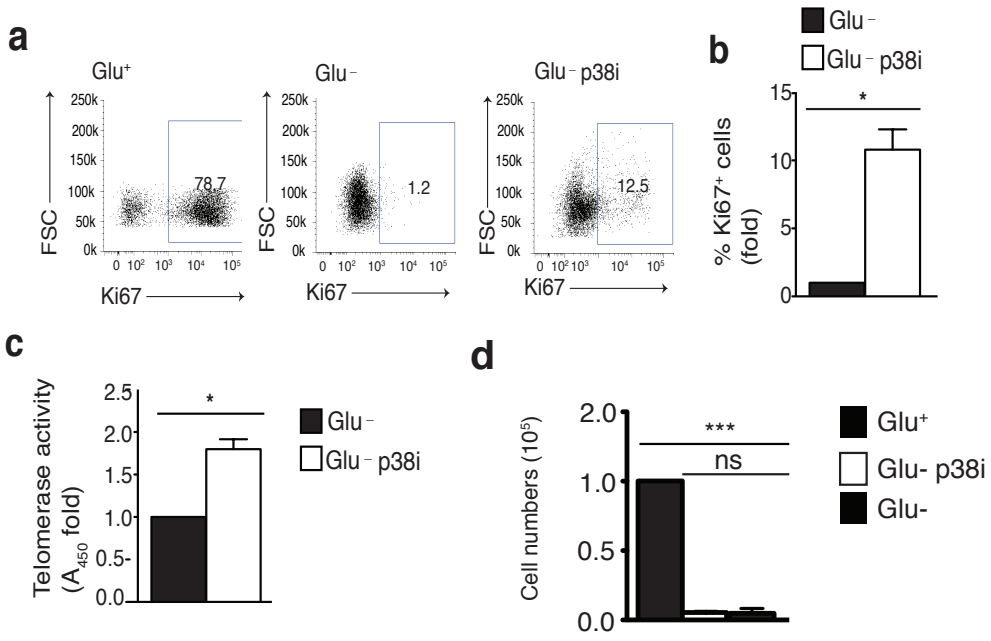

Figure 39: Glucose deprivation inhibits T cell proliferation and telomerase via p38. (**a**) Glucose starved $CD27^+$ $CD28^+$ $CD4^+$ T cells were activated and cultured as described in (a) for 48 hours and proliferation was assessed by intracellular staining for the nuclear antigen Ki67. $CD4^+$ $CD27^+$ $CD28^+$ T cells grown in the presence of glucose [20mM] served as positive proliferation control. (**b**) The pooled data from 3 independent experiments, performed as described in (a). (**c**) Telomerase activity of relatively undifferentiated $CD27^+$ $CD28^+$ $CD4^+$ T cells under glucose starvation either in the presence or absence of the small molecule p38 inhibitor BIRB 796 (500 nM). Cells were activated by αCD3/CD28, in the absence of glucose. Telomerase activity was determined after 48 hours by TRAP assay. (**d**) Viability of cells as in (c) after 5 days in culture. Cells activated in full glucose served as an internal control. In (**b**, **c**) *$p< 0,05$ calculated by a paired Student's t test. Error bars depict s.e.m

6.8 AMPK activation mediates loss of TCR signalling molecules via p38.

The loss of TCR signalling components is a novel feature of human T cell senescence. Because AMPK activation was found here to drive other important senescence characteristics of T cells such as loss of proliferative and telomerase activity, it was possible that AMPK signalling was involved in the down-regulation of TCR signalling machinery. To study a potential albeit so-far unrecognized link between the metabolic master regulator AMPK and TCR signalling, non-senescent human $CD27^+$ $CD28^+$ $CD4^+$ T cells that possess a functional TCR signalosome were activated by αCD3 plus αCD28 in the presence of either DMSO vehicle control or increasing dosages of the AMPK activator A-769662. Four days post-activation, cells were counted, lysed and immunoblotted using antibodies to total Zap70, LCK and SLP-76 that are all essential components of the TCR signalling machinery. Agonist driven activation of AMPK induced a dose-dependent loss of TCR signalling molecules (**Figure 40 a)** that resembles that found in *ex-vivo* isolated senescent human $CD4^+$ T cells in which AMPK is spontaneously active (**Figure 20**). Thus AMPK activation inhibits TCR function. To explore if AMPK activation mediated loss of TCR signalosome relied on downstream activation of p38 (similarly to the documented loss of T cell proliferative and telomerase potential), $CD27^+$ $CD28^+$ $CD4^+$ T cells were activated by αCD3 plus αCD28 either in the presence or absence of the AMPK activator A-769662, with or without the p38 inhibitor BIRB-796. After four days, cells were analysed by intracellular flow-cytometry for expression of the TCR signalling molecules LAT and SLP-76. These experiments showed that AMPK activation potently down-regulated LAT and SLP-76 expression however the addition of BIRB-796 partially antagonized this process (**Figure 40 b**). Conversely blocking p38 in DMSO control treated cells did not

significantly modulate either LAT or SLP-76 expression (**Figure 40 b**). These observations were confirmed in 3 separate experiments (**Figure 40 c**). Further studies using the glycolysis inhibitor 2DG, that potently activates AMPK (Rolf et al., 2013), are in due course. These data show that p38 activation downstream of AMPK is in part involved in the loss of the TCR signalosome in glucose-deprived lymphocytes discovered here.

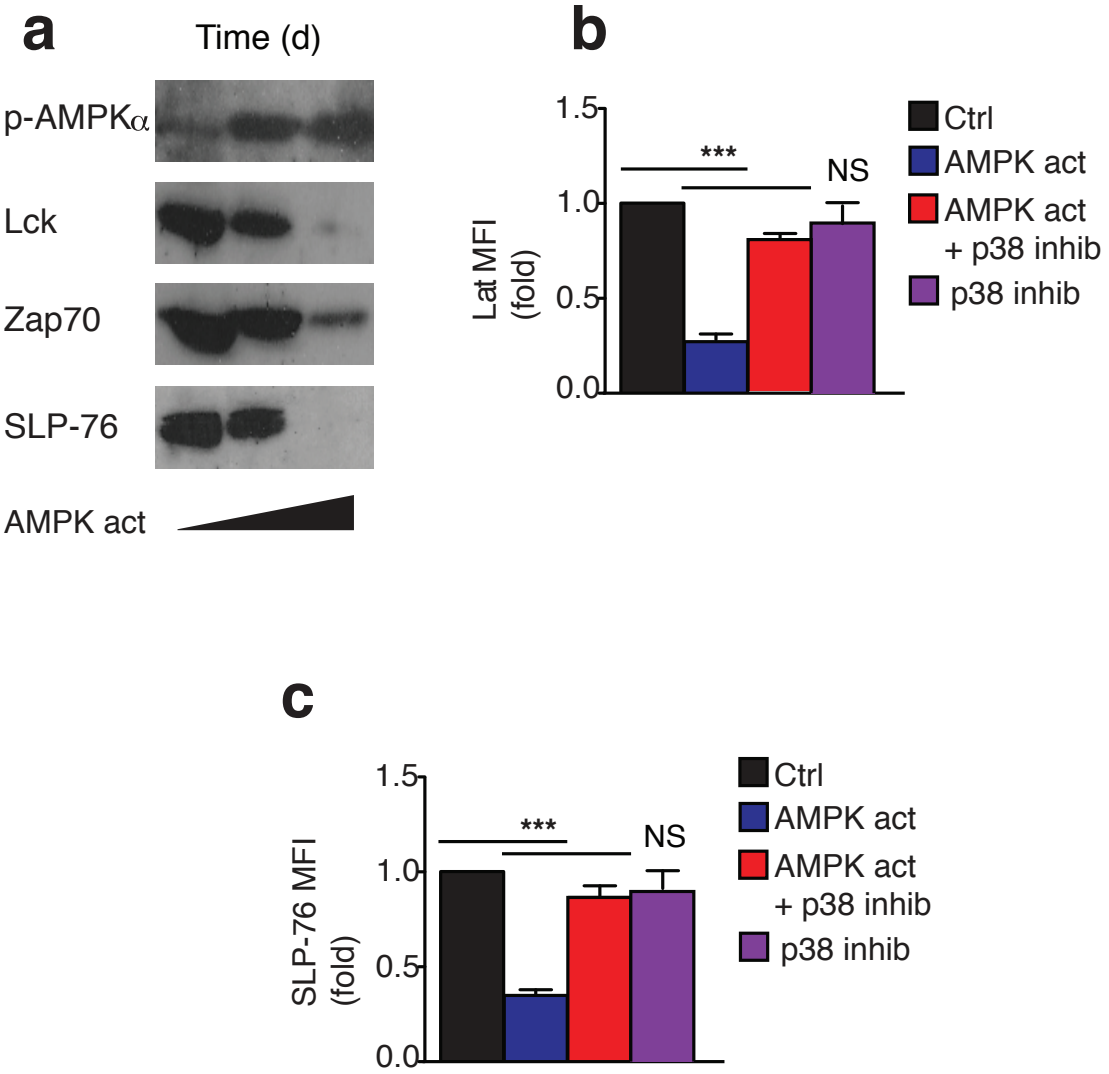

Figure 40: Loss of TCR machinery regulated by AMPK-p38 signalling.

(**a**) Immunoblots of p-AMPK-α at Thr172 (as a pharmacological activation control), LCK, Zap70 and SLP76 in relatively undifferentiated $CD27^+$ $CD28^+$ $CD4^+$ T cells activated by αCD3 plus αCD28 for 4 days either in the absence or presence of increasing concentrations of the AMPK agonist A-769662 (100 or 150 μM respectively). (**b**) Pooled MFI data from 3 different experiments of Lat and SLP-76 expression in relatively undifferentiated $CD27^+$ $CD28^+$ $CD4^+$ T cells activated as in (a) either in the presence or absence of the AMPK activator A-769662 (150 μM) or the p38 inhibitor BIRB 796 (500 nM), assessed by intracellular flow-citometry. In (**b**) a one-way analysis of variance (ANOVA) for repeated-measures with a Bonferroni post-test correction. *$p< 0,05$, **$p<0.01$, and ***$p< 0.001$. Error bars depict s.e.m

6.9 Summary and Conclusions

Here I investigated the consequences of AMPK-TAB1 ('Intra-sensory') activated p38 signalling and found that this pathway maintains the senescence of human T lymphocytes. There are at least three known different senescent features in T cells, namely loss of telomerase and proliferative activity and the here-identified loss of TCR signalosome components. Here I showed that AMPK, activated in response to either glucose deprivation or senescence-associated DNA damage, in turn promotes the onset of all these features of T cell senescence in part through downstream activation of p38, a process that requires TAB1 expression. This provides a mechanistic link between nutrient sensing and senescence signalling pathways in human T cells. Indeed, intra-sensory p38 activation was found here to inhibit the function of both senescent and non-senescent T cells, regardless of the upstream trigger activating AMPK.

Further studies are needed to fully understand how 'intra-sensory' activated p38 constrains human T cell proliferation and telomerase activity however our data highlighted an active role for T cell p38 during senescence through the inhibition of various elements that promote the G1-S cell cycle transition (Mathon and Lloyd, 2001). But because previous studies reported instead that p38 activity promoted cell proliferation and active cell cycling (Alam et al., 2014), different mechanisms downstream of p38 have to be engaged to either promote or inhibit cell proliferation.

There is a tremendous number of molecules that lie downstream of p38 (Shi and Gaestel, 2002) and different tissue expression profiles for the various p38

biological substrates may explain the opposite functional outcomes regulated by p38, however our data suggests this not to be the case. Opposite effects were indeed observed in non-senescent T cells when blocking p38, activated downstream of either AMPK or TCR signalosome, which indicates that even within the same cell-type and timing p38 activation differentially regulates T cell function. Thus multiple pathways upstream of p38 that activate the molecule under opposite physiological conditions provide a more robust answer.

The tuning of T cell function by the metabolic master regulator AMPK indicates that there are important yet poorly understood biochemical networks linking T cell metabolism and T cell signalling. However whether p38 can directly modulate T cell metabolism downstream of AMPK remains elusive. Also, although p38 activity is in part involved in the loss of TCR signalosome downstream of AMPK, blocking p38 did not restore TCR signalosome expression in senescent T cells (data not shown), indicating the existence of other mechanisms.

Enhancing human T cell proliferation through direct inhibition of the AMPK-TAB1 pathway for p38 activation described here may represent a novel way to boost immune cell function *in vivo*. One caveat is that the enhancement of telomerase and proliferation in senescent T cells that have evidence of DNA damage may be tumorigenic (Akbar and Henson, 2011). The risk versus possible benefit of selective therapeutic 'tuning' of telomerase in human T lymphocytes *in vivo* remains to be determined.

Chapter VII: General discussion

The Hayflick limit dictates that the extent at which mammalian cells can proliferate is constrained by mechanisms of telomere erosion, which regulate the onset of replicative senescence (HAYFLICK and MOORHEAD, 1961). The activation of the enzyme telomerase extends mammalian cell life span by telomere elongation however in most adult somatic cells telomerase activity is repressed (Hodes et al., 2002). Conversely cancer cells and stem cells up-regulate the telomerase by virtue of their indefinite proliferative potential (Cong et al., 2002).

Unlike other somatic cells, lymphocytes can potently induce telomerase activity upon antigenic challenge that is essential to regulate the rapid expansion of antigen specific lymphocytes followed by their contraction when the immune challenge is cleared (Akbar and Vukmanovic-Stejic, 2007).

The mechanisms regulating telomerase in both immune and non-immune cells are poorly characterized and this PhD project investigated mechanisms of telomerase down-regulation in primary human T lymphocytes. There is progressive inhibition of telomerase activity during the differentiation of T cells towards senescence, which limits T cell proliferative potential (Goronzy and Weyand, 2013). Here I set up a strategy to restore both telomerase and proliferative activity in naturally occurring senescent human T cells. These cells that have lost expression of both the co-stimulatory receptors CD27 and CD28 can be found in peripheral blood since relatively young age and accumulate during ageing, chronic viral infections and auto-immune disease probably because of differentiation related events, when

repeated episodes of cell activation occurs, and tissue inflammation (Weng et al., 2009).

Boosting T cell proliferation during ageing may be therefore essential to restore immune protection towards a 'healthy ageing' and to prevent the onset of age-associated concerns such as elevated cancer incidence and low responsiveness to vaccination that is essential to modulate immunity in humans (Boraschi et al., 2013). However it is presently unknown if the accumulation of low proliferative, senescent T cells actively contributes to defective immunity in old humans, neither is known if restoring the proliferation of senescent T cells that have evidence of irreversibly-damaged DNA by means of telomerase up-regulation may be a safe therapeutic intervention. But because very little is known about end-stage specific mechanisms that regulate life span in humans, these studies are important to understand the biology of human ageing.

There is very little and controversial information about the mechanisms that regulate human ageing although the causative link with cell senescence is relatively well accepted. In humans, senescence is most studied in fibroblast models where it is induced upon modifications *in vitro* such as aberrant oncogene activation, UV radiation, growth factor withdrawal or repeated cell passages (Campisi and d'Adda di Fagagna, 2007). Thus although such studies have provided important insights into the basic mechanisms regulating senescence, whether the same processes might also be active *in vivo* remains to be determined. Also, it is not clear how senescence is regulated in different human cell types, nor the *in vivo* phenotype of most human senescent cells is known.

T cell senescence is a relatively unexplored field of study. However the identification and isolation of blood highly differentiated $CD27^-$ $CD28^-$ T lymphocytes with very short telomeres, low telomerase activity, loss of proliferative potential and the here identified loss of TCR signalosome expression, provide a unique model for studying mechanisms of immune-senescence directly *ex vivo*, in humans. This is the first study investigating spontaneous signalling processes in primary populations of human highly differentiated (senescent) T cells, followed by their *in vitro* manipulation, thus linking endogenous mechanisms of immune-senescence to the tuning of human T cell function.

Caution should be taken to evaluate biochemical data generated by *in vitro* manipulation of human samples. Here when human T cells were activated in the presence of the inflammatory cytokine IFN-α, this was found to activate p38 MAPK signalling resulting in telomerase down-regulation, similarly to what spontaneously occurs in senescent T cells (Di Mitri et al., 2011), which raised the question of whether the underlying biochemical mechanism of p38 activation was identical. However p38 signalling in senescent T cells was then found to be unrelated to upstream activation by the canonical MAPK cascade that links inflammation to downstream MAPK activation (Chang and Karin, 2001). Instead it relied on an unrecognized AMPK-TAB1 dependent mechanism integrating endogenous DNA damage and low-nutrient sensing ('Intra-Sensory' pathway, Chapter V). Indeed inflammatory signals did not even activate AMPK-TAB1 in T cells (data not shown). While these data suggest that *in vitro* and *in vivo* biochemical processes are not necessarily linked, it would be interesting to assess if highly differentiated T cells induced in culture by IFN-α would also lose canonical MAPK cascade and

activate p38 by AMPK-TAB1 signalling, thus behaving as their endogenously generated counter-parts.

The previous link between AMPK and senescence was tenuous. In a study conducted on fibroblasts, replicative senescence was shown to be associated with spontaneous AMPK activation *in vitro* (Wang et al., 2003). Subsequently, aberrant activation of fibroblast AMPK by either metformin or genetic manipulation was shown to enforce cell cycle arrest at the G1-phase via a p53-dependent mechanism (Jones et al., 2005). Because both TAB1 and p38 lie downstream of AMPK that is important to activate p53 (Jones et al., 2005), it is possible that the 'intra-sensory' AMPK-TAB1 mechanism of p38 activation described here in senescent T cells would be also active in fibroblasts. If so, it would be interesting to understand whether a conserved signature that regulates senescence in multiple cell types may exist, as this would offer a common mechanism to reverse the detrimental effects of ageing. Nevertheless there are important biochemical clues that this may be the case. Firstly, all senescent cells are characterized by the upstream activation of persistent DDR signalling and rely on potent activation of p53 to enforce proliferative arrest (Campisi and d'Adda di Fagagna, 2007). Secondly, DNA damage is well-recognized trigger of AMPK activity in many different cell types (Sanli et al., 2010). Thirdly, it has been recently reported that telomere shortening in fibroblasts from TERT knockout mice (a modification required to induce replicative senescence in mice whose telomeres are significantly longer than humans) triggers spontaneous activation of AMPK leading to enhanced energetic demands (Missios et al., 2014). Albeit this would represent a provocative scenario- set by a unique signature for mammalian senescence

whose manipulation may reveal a potent tool to either attenuate or reverse ageing-blocking such a mechanism may bear risks of uncontrolled cell proliferation and malignancy. Nevertheless this concern is linked with the pleiotropic antagonistic nature of senescence itself (Campisi and d'Adda di Fagagna, 2007).

Because AMPK and mTOR activation are antagonistic processes, these data appear incompatible with previous reports indicating a pro-ageing role for active mTOR signalling, possibly due to the generation of aberrant oxidative stress (Lee et al., 2010). There is indeed robust, evidence-based belief that mTOR inhibition extends life span in mammals (Johnson et al., 2013). Furthermore, mTOR inhibition has been very recently shown to improve T cell function in old humans (Mannick et al., 2014). Paradoxically enough both senescent human $CD4^+$ and $CD8^+$ T cells do not even express mTOR (Henson et al., 2014). How can these data be re-conciliated together? Most likely the core-question may be due to a semantic issue; even among researchers the terms ageing and senescence are often used interchangeably. Although senescent cells accumulate during ageing and probably accounts for the overall progressive loss of cell function characterizing ageing, considering a whole tissue or an unfractionated cell population from an aged animal or individual as entirely senescent *per se* may give rise to important misunderstandings. Also, the exact time-point of intervention (throughout either age or differentiation) should be homogenous to make different studies comparable, because the mechanisms that drive senescence (that is, before entering senescence) and those that actively maintain senescence (that is, to enforce G1-phase occupancy) do not necessarily overlap. I propose that mTOR inhibition would delay human T cell differentiation and the onset of senescence

however restoring function in senescent T cells requires inhibition of AMPK signalling and down-stream TAB1 dependent activation of p38.

The existence of multiple pathways for the activation of p38 in T cells that respond to opposite physiological stimuli indicates that the same effector molecule can regulate opposite functions by engaging different downstream mechanisms. It is not clear at present if such pathways are also active in other immune or even in non-immune cell types, although it seems that alternative activation pathway of p38 that was initially ascribed only to activated T cells may also occur in activated B cells. Also, we note that end-stage differentiated human NK cells exhibit spontaneously activation of AMPK and show elevated p38 phosphorylation suggesting that the 'intra-sensory' pathway of p38 activation may not be a prerogative of T lymphocytes (Durovic Muller B, Lanna A & Akbar AN, unpublished findings). If so, it would be important to investigate the effect of blocking AMPK-TAB1-p38 signalling in these cells. As discussed, one tempting yet unsupportive speculation is that the proliferative defects of various senescent cells is maintained in part via intra-sensory p38 signalling in response to endogenous DNA damage.

Signal integration is a well-recognized property of biochemical networks identified by numerous cross talks among separate signalling cascades. Yet it is not clear how the same signalling molecule can respond to contrasting physiological stimuli. Why would mammalian cells use convergent mechanisms to tune opposite cellular functions rather than completely separate processes? I propose that the convergence of opposite physiological inputs on the same effector molecule may be important to ensure functional output variability through a limited number of

biochemical processes. In such a model, different scaffolding molecules would be important to tune downstream specificity of the same effector kinase towards separate subsets of biochemical substrates, which induce in turn robust, non-ambiguous physiological responses. An integrated biochemical network would be of easier regulation rather than a system in which various physiological cues downstream activate a multitude of different pathways (**Figure 41**). In this post-genomic era of high-throughput screening, logic may therefore reveal a more useful tool to understand biochemical complexity.

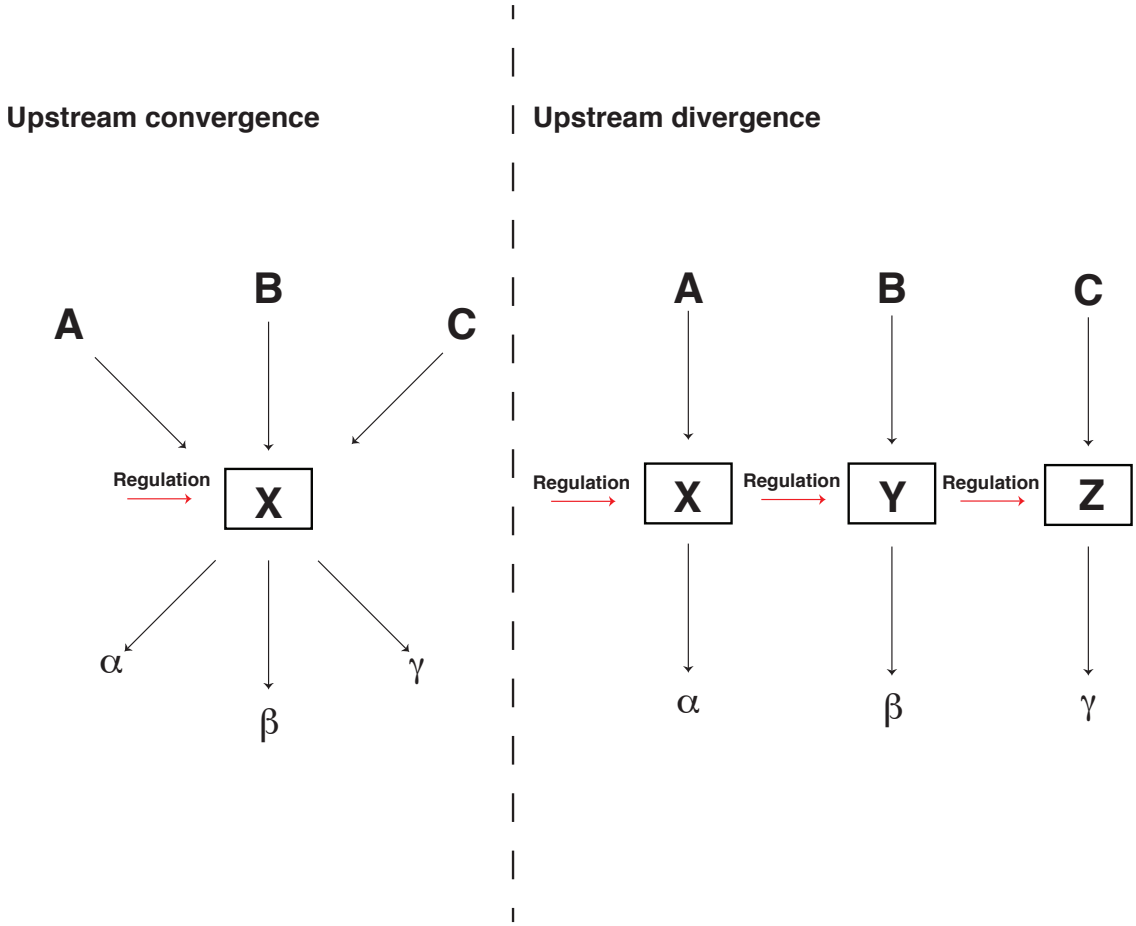

Figure 41: The advantage of upstream signalling convergence over divergence. Different stimuli triggering separate pathways (**A**, **B**, **C**) may converge on the same effector molecule (**X**) to induce non-ambiguous physiological responses (**α**, **β**, **γ**; *left*). This is the case for p38 signalling in T cells. This model allows multiple, non-reduntant responses through a limited number of biochemical effectors, hence restricting regulatory checkpoints compared to a system in which different upstream triggers signal via separate biochemical effectors (**X**, **Y**, **Z**; *right*).

Chapter VIII: Future Perspectives

8.1 How does metabolism regulate TCR signalling?

One unexpected observation was that several components of the TCR signalosome such as LCK, ZAP70, DLG1, LAT and SLP-76 are spontaneously lost in senescent human $CD4^+$ T cells that also lose expression of both co-stimulatory receptors CD27 and CD28. The collective loss of these signalling molecules will exacerbate the inhibition of proliferation in these cells by decreasing their capacity for TCR activation. It is not clear if TCR machinery can be restored in senescent T cells however our data linking TCR signalosome down-modulation to the upstream activation of the energy sensor AMPK suggests the existence of metabolic programs within the T cells that directly regulate TCR responsiveness. It is well recognized that important metabolic changes occur downstream of TCR activation in T cells (Pearce et al., 2013; Sinclair et al., 2013) and these data provide evidence that inhibitory feedback mechanisms exist linking changes in T cell metabolism to TCR function. Because AMPK activates catabolic metabolism, it is tempting to speculate that enforcing anabolic metabolism would restore TCR function in senescent T cells, in an antagonistic way. It would be important to identify the specific metabolic programs that may exert TCR control and the related downstream mechanism, as it may provide interventional targets for boosting TCR responsiveness that is impaired during ageing. Importantly, TCR down-modulation may also be an unrecognized way by which non-senescent T cells become unresponsive during an immune response *in vivo*, when nutrient supply may not be optimal (O'Sullivan and Pearce, 2015).

8.2 Towards an Intra-Sensory MAPK cascade?

Another important standing question is a possible involvement of ERK and JNK, in addition to p38, during T cell senescence and whether they may also be activated downstream of AMPK. Unlike p38, non-canonical pathways for ERK or JNK activation have not been reported. The possible existence of an intra-sensory mode for multiple MAPK activation driven by AMPK may unveil MAP kinases as important biochemical effectors of unrecognized signalling networks.

References:

Abbas, A.K., Lohr, J., Knoechel, B., and Nagabhushanam, V. (2004). T cell tolerance and autoimmunity. Autoimmun. Rev. *3*, 471–475.

Acosta, J.C., O'Loghlen, A., Banito, A., Guijarro, M. V, Augert, A., Raguz, S., Fumagalli, M., Da Costa, M., Brown, C., Popov, N., et al. (2008). Chemokine signaling via the CXCR2 receptor reinforces senescence. Cell *133*, 1006–1018.

Acuto, O., Di Bartolo, V., and Michel, F. (2008). Tailoring T-cell receptor signals by proximal negative feedback mechanisms. Nat. Rev. Immunol. *8*, 699–712.

Akbar, A.N., and Fletcher, J.M. (2005). Memory T cell homeostasis and senescence during aging. Curr. Opin. Immunol. *17*, 480–485.

Akbar, A.N., and Henson, S.M. (2011). Are senescence and exhaustion intertwined or unrelated processes that compromise immunity? Nat. Rev. Immunol. *11*, 289–295.

Akbar, A.N., and Vukmanovic-Stejic, M. (2007). Telomerase in T Lymphocytes: Use It and Lose It? J. Immunol. *178*, 6689–6694.

Akbar, A.N., Beverley, P.C.L., and Salmon, M. (2004). Will telomere erosion lead to a loss of T-cell memory? Nat. Rev. Immunol. *4*, 737–743.

Akiyama, M., Hideshima, T., Hayashi, T., Tai, Y.-T., Mitsiades, C.S., Mitsiades, N., Chauhan, D., Richardson, P., Munshi, N.C., and Anderson, K.C. (2003). Nuclear factor-kappaB p65 mediates tumor necrosis factor alpha-induced nuclear translocation of telomerase reverse transcriptase protein. Cancer Res. *63*, 18–21.

Alam, M.S., Gaida, M.M., Ogawa, Y., Kolios, A.G.A., Lasitschka, F., and Ashwell, J.D. (2014). Counter-regulation of T cell effector function by differentially activated

p38. J. Exp. Med. *211*, 1257–1270.

Alarcon, B., Gil, D., Delgado, P., and Schamel, W.W.A. (2003). Initiation of TCR signaling: regulation within CD3 dimers. Immunol. Rev. *191*, 38–46.

Alarcón, B., Mestre, D., and Martínez-Martín, N. (2011). The immunological synapse: a cause or consequence of T-cell receptor triggering? Immunology *133*, 420–425.

Appay, V. (2004). The physiological role of cytotoxic CD4(+) T-cells: the holy grail? Clin. Exp. Immunol. *138*, 10–13.

Araki, K., Turner, A.P., Shaffer, V.O., Gangappa, S., Keller, S.A., Bachmann, M.F., Larsen, C.P., and Ahmed, R. (2009). mTOR regulates memory CD8 T-cell differentiation. Nature *460*, 108–112.

Ashwell, J.D. (2006). The many paths to p38 mitogen-activated protein kinase activation in the immune system. Nat. Rev. Immunol. *6*, 532–540.

Blackburn, E.H. (2000). The end of the (DNA) line. Nat. Struct. Biol. *7*, 847–850.

Blasco, M.A. (2005). Telomeres and human disease: ageing, cancer and beyond. Nat. Rev. Genet. *6*, 611–622.

Boraschi, D., Aguado, M.T., Dutel, C., Goronzy, J., Louis, J., Grubeck-Loebenstein, B., Rappuoli, R., and Del Giudice, G. (2013a). The gracefully aging immune system. Sci. Transl. Med. *5*, 185ps8.

Boraschi, D., Aguado, M.T., Dutel, C., Goronzy, J., Louis, J., Grubeck-Loebenstein, B., Rappuoli, R., and Del Giudice, G. (2013b). The gracefully aging immune system. Sci. Transl. Med. *5*, 185ps8.

Borden, E.C., Sen, G.C., Uze, G., Silverman, R.H., Ransohoff, R.M., Foster, G.R.,

and Stark, G.R. (2007). Interferons at age 50: past, current and future impact on biomedicine. Nat. Rev. Drug Discov. *6*, 975–990.

Brancho, D., Tanaka, N., Jaeschke, A., Ventura, J.-J., Kelkar, N., Tanaka, Y., Kyuuma, M., Takeshita, T., Flavell, R.A., and Davis, R.J. (2003). Mechanism of p38 MAP kinase activation in vivo. Genes Dev. *17*, 1969–1978.

Brassard, D.L., Grace, M.J., and Bordens, R.W. (2002). Interferon-{alpha} as an immunotherapeutic protein. J. Leukoc. Biol. *71*, 565–581.

Brownlie, R.J., and Zamoyska, R. (2013). T cell receptor signalling networks: branched, diversified and bounded. Nat. Rev. Immunol. *13*, 257–269.

Campisi, J., and d'Adda di Fagagna, F. (2007). Cellular senescence: when bad things happen to good cells. Nat. Rev. Mol. Cell Biol. *8*, 729–740.

Cardaci, S., Filomeni, G., and Ciriolo, M.R. (2012). Redox implications of AMPK-mediated signal transduction beyond energetic clues. J. Cell Sci. *125*, 2115–2125.

Chakraborty, A.K., and Weiss, A. (2014). Insights into the initiation of TCR signaling. Nat. Immunol. *15*, 798–807.

Chandler, H., and Peters, G. (2013). Stressing the cell cycle in senescence and aging. Curr. Opin. Cell Biol. *25*, 765–771.

Chang, L., and Karin, M. (2001). Mammalian MAP kinase signalling cascades. Nature *410*, 37–40.

Chang, C.-H., Curtis, J.D., Maggi, L.B., Faubert, B., Villarino, A. V, O'Sullivan, D., Huang, S.C.-C., van der Windt, G.J.W., Blagih, J., Qiu, J., et al. (2013a). Posttranscriptional control of T cell effector function by aerobic glycolysis. Cell *153*, 1239–1251.

Chang, C.H., Curtis, J.D., Maggi, L.B., Faubert, B., Villarino, A. V., O'Sullivan, D., Huang, S.C.C., Van Der Windt, G.J.W., Blagih, J., Qiu, J., et al. (2013b). XPosttranscriptional control of T cell effector function by aerobic glycolysis. Cell *153*, 1239–1251.

Chou, J.P., Ramirez, C.M., Wu, J.E., and Effros, R.B. (2013). Accelerated aging in HIV/AIDS: novel biomarkers of senescent human CD8+ T cells. PLoS One *8*, e64702.

Cong, Y.-S., Wright, W.E., and Shay, J.W. (2002). Human telomerase and its regulation. Microbiol. Mol. Biol. Rev. *66*, 407–425, table of contents.

Corse, E., Gottschalk, R.A., and Allison, J.P. (2011). Strength of TCR-peptide/MHC interactions and in vivo T cell responses. J. Immunol. *186*, 5039–5045.

Crespo, J., Sun, H., Welling, T.H., Tian, Z., and Zou, W. (2013). T cell anergy, exhaustion, senescence, and stemness in the tumor microenvironment. Curr. Opin. Immunol. *25*, 214–221.

Crowe, D.L. (2001). E2F-1 represses transcription of the human telomerase reverse transcriptase gene. Nucleic Acids Res. *29*, 2789–2794.

d'Adda di Fagagna, F., Reaper, P.M., Clay-Farrace, L., Fiegler, H., Carr, P., Von Zglinicki, T., Saretzki, G., Carter, N.P., and Jackson, S.P. (2003). A DNA damage checkpoint response in telomere-initiated senescence. Nature *426*, 194–198.

Delgoffe, G.M., Pollizzi, K.N., Waickman, A.T., Heikamp, E., Meyers, D.J., Horton, M.R., Xiao, B., Worley, P.F., and Powell, J.D. (2011). The kinase mTOR regulates the differentiation of helper T cells through the selective activation of signaling by mTORC1 and mTORC2. Nat. Immunol. *12*, 295–303.

DePinho, R.A., Schreiber-Agus, N., and Alt, F.W. (1991). myc family oncogenes in the development of normal and neoplastic cells. Adv. Cancer Res. *57*, 1–46.

van Deursen, J.M. (2014). The role of senescent cells in ageing. Nature *509*, 439–446.

Dong, C., Yang, D.D., Tournier, C., Whitmarsh, A.J., Xu, J., Davis, R.J., and Flavell, R.A. (2000). JNK is required for effector T-cell function but not for T-cell activation. Nature *405*, 91–94.

Dustin, M.L. (2014). What counts in the immunological synapse? Mol. Cell *54*, 255–262.

Ferrantini, M., Capone, I., and Belardelli, F. (2007). Interferon-alpha and cancer: mechanisms of action and new perspectives of clinical use. Biochimie *89*, 884–893.

Finlay, D., and Cantrell, D.A. (2011). Metabolism, migration and memory in cytotoxic T cells. Nat. Rev. Immunol. *11*, 109–117.

Finlay, D.K., Rosenzweig, E., Sinclair, L. V, Feijoo-Carnero, C., Hukelmann, J.L., Rolf, J., Panteleyev, A.A., Okkenhaug, K., and Cantrell, D.A. (2012a). PDK1 regulation of mTOR and hypoxia-inducible factor 1 integrate metabolism and migration of CD8+ T cells. J. Exp. Med. *209*, 2441–2453.

Finlay, D.K., Rosenzweig, E., Sinclair, L. V, Feijoo-Carnero, C., Hukelmann, J.L., Rolf, J., Panteleyev, A.A., Okkenhaug, K., and Cantrell, D.A. (2012b). PDK1 regulation of mTOR and hypoxia-inducible factor 1 integrate metabolism and migration of CD8+ T cells. J. Exp. Med. *209*, 2441–2453.

Fletcher, J.M., Vukmanovic-Stejic, M., Dunne, P.J., Birch, K.E., Cook, J.E.,

Jackson, S.E., Salmon, M., Rustin, M.H., and Akbar, A.N. (2005). Cytomegalovirus-Specific CD4+ T Cells in Healthy Carriers Are Continuously Driven to Replicative Exhaustion. J. Immunol. *175*, 8218–8225.

Frauwirth, K.A., Riley, J.L., Harris, M.H., Parry, R. V, Rathmell, J.C., Plas, D.R., Elstrom, R.L., June, C.H., and Thompson, C.B. (2002). The CD28 Signaling Pathway Regulates Glucose Metabolism. Immunity *16*, 769–777.

Freund, A., Patil, C.K., and Campisi, J. (2011). p38MAPK is a novel DNA damage response-independent regulator of the senescence-associated secretory phenotype. EMBO J. *30*, 1536–1548.

Fujii, H., Shao, L., Colmegna, I., Goronzy, J.J., and Weyand, C.M. (2009). Telomerase insufficiency in rheumatoid arthritis. Proc. Natl. Acad. Sci. U. S. A. *106*, 4360–4365.

Fumagalli, M., and d'Adda di Fagagna, F. (2009). SASPense and DDRama in cancer and ageing. Nat. Cell Biol. *11*, 921–923.

Fumagalli, M., Rossiello, F., Clerici, M., Barozzi, S., Cittaro, D., Kaplunov, J.M., Bucci, G., Dobreva, M., Matti, V., Beausejour, C.M., et al. (2012). Telomeric DNA damage is irreparable and causes persistent DNA-damage-response activation. Nat. Cell Biol. *14*, 355–365.

Ge, B., Gram, H., Di Padova, F., Huang, B., New, L., Ulevitch, R.J., Luo, Y., and Han, J. (2002a). MAPKK-independent activation of p38alpha mediated by TAB1-dependent autophosphorylation of p38alpha. Science *295*, 1291–1294.

Ge, B., Gram, H., Di Padova, F., Huang, B., New, L., Ulevitch, R.J., Luo, Y., and Han, J. (2002b). MAPKK-independent activation of p38alpha mediated by TAB1-dependent autophosphorylation of p38alpha. Science *295*, 1291–1294.

Ge, B., Xiong, X., Jing, Q., Mosley, J.L., Filose, A., Bian, D., Huang, S., and Han, J. (2003). TAB1beta (transforming growth factor-beta-activated protein kinase 1-binding protein 1beta), a novel splicing variant of TAB1 that interacts with p38alpha but not TAK1. J. Biol. Chem. *278*, 2286–2293.

Germain, R.N. (2002). T-cell development and the CD4-CD8 lineage decision. Nat. Rev. Immunol. *2*, 309–322.

Giacinti, C., and Giordano, A. (2006). RB and cell cycle progression. Oncogene *25*, 5220–5227.

Goransson, O., McBride, A., Hawley, S.A., Ross, F.A., Shpiro, N., Foretz, M., Viollet, B., Hardie, D.G., and Sakamoto, K. (2007). Mechanism of Action of A-769662, a Valuable Tool for Activation of AMP-activated Protein Kinase. J. Biol. Chem. *282*, 32549–32560.

Goronzy, J.J., and Weyand, C.M. (2013). Understanding immunosenescence to improve responses to vaccines. Nat. Immunol. *14*, 428–436.

Goronzy, J.J., Fang, F., Cavanagh, M.M., Qi, Q., and Weyand, C.M. (2015). Naive T Cell Maintenance and Function in Human Aging. J. Immunol. *194*, 4073–4080.

Greider, C.W., and Blackburn, E.H. (1985). Identification of a specific telomere terminal transferase activity in tetrahymena extracts. Cell *43*, 405–413.

Hammaker, D., and Firestein, G.S. (2010). “Go upstream, young man”: lessons learned from the p38 saga. Ann. Rheum. Dis. *69 Suppl 1*, i77–i82.

Hardie, D.G. (2007). AMP-activated/SNF1 protein kinases: conserved guardians of cellular energy. Nat. Rev. Mol. Cell Biol. *8*, 774–785.

Hardie, D.G., Ross, F.A., and Hawley, S.A. (2012). AMPK: a nutrient and energy

sensor that maintains energy homeostasis. Nat. Rev. Mol. Cell Biol. *13*, 251–262.

Hayday, A., and Tigelaar, R. (2003). Immunoregulation in the tissues by gammadelta T cells. Nat. Rev. Immunol. *3*, 233–242.

HAYFLICK, L., and MOORHEAD, P.S. (1961). The serial cultivation of human diploid cell strains. Exp. Cell Res. *25*, 585–621.

Henson, S.M., Franzese, O., Macaulay, R., Libri, V., Azevedo, R.I., Kiani-Alikhan, S., Plunkett, F.J., Masters, J.E., Jackson, S., Griffiths, S.J., et al. (2009). KLRG1 signaling induces defective Akt (ser473) phosphorylation and proliferative dysfunction of highly differentiated CD8+ T cells. Blood *113*, 6619–6628.

Henson, S.M., Lanna, A., Riddell, N.E., Franzese, O., Macaulay, R., Griffiths, S.J., Puleston, D.J., Watson, A.S., Simon, A.K., Tooze, S.A., et al. (2014). p38 signaling inhibits mTORC1-independent autophagy in senescent human $CD8^+$ T cells. J. Clin. Invest. *124*, 4004–4016.

Henson, S.M., Macaulay, R., Riddell, N.E., Nunn, C.J., and Akbar, A.N. (2015). Blockade of PD-1 or p38 MAP kinase signaling enhances senescent human CD8(+) T-cell proliferation by distinct pathways. Eur. J. Immunol. *45*, 1441–1451.

Herrero-Martín, G., Høyer-Hansen, M., García-García, C., Fumarola, C., Farkas, T., López-Rivas, A., and Jäättelä, M. (2009). TAK1 activates AMPK-dependent cytoprotective autophagy in TRAIL-treated epithelial cells. EMBO J. *28*, 677–685.

Hickson, I., Zhao, Y., Richardson, C.J., Green, S.J., Martin, N.M.B., Orr, A.I., Reaper, P.M., Jackson, S.P., Curtin, N.J., and Smith, G.C.M. (2004). Identification and characterization of a novel and specific inhibitor of the ataxia-telangiectasia mutated kinase ATM. Cancer Res. *64*, 9152–9159.

Ho, I.-C., Tai, T.-S., and Pai, S.-Y. (2009). GATA3 and the T-cell lineage: essential functions before and after T-helper-2-cell differentiation. Nat. Rev. Immunol. *9*, 125–135.

Hodes, R.J., Hathcock, K.S., and Weng, N. (2002). Telomeres in T and B cells. Nat. Rev. Immunol. *2*, 699–706.

Jacquet, S., Zarrinpashneh, E., Chavey, A., Ginion, A., Leclerc, I., Viollet, B., Rutter, G.A., Bertrand, L., and Marber, M.S. (2007). The relationship between p38 mitogen-activated protein kinase and AMP-activated protein kinase during myocardial ischemia. Cardiovasc. Res. *76*, 465–472.

Jaswal, J.S., Gandhi, M., Finegan, B.A., Dyck, J.R.B., and Clanachan, A.S. (2007). p38 mitogen-activated protein kinase mediates adenosine-induced alterations in myocardial glucose utilization via 5'-AMP-activated protein kinase. Am. J. Physiol. Heart Circ. Physiol. *292*, H1978–H1985.

Johnson, S.C., Rabinovitch, P.S., and Kaeberlein, M. (2013). mTOR is a key modulator of ageing and age-related disease. Nature *493*, 338–345.

Jones, R.G., Plas, D.R., Kubek, S., Buzzai, M., Mu, J., Xu, Y., Birnbaum, M.J., and Thompson, C.B. (2005). AMP-activated protein kinase induces a p53-dependent metabolic checkpoint. Mol. Cell *18*, 283–293.

Kang, S.S., Kwon, T., Kwon, D.Y., and Do, S.I. (1999). Akt protein kinase enhances human telomerase activity through phosphorylation of telomerase reverse transcriptase subunit. J. Biol. Chem. *274*, 13085–13090.

Kanhere, A., Hertweck, A., Bhatia, U., Gökmen, M.R., Perucha, E., Jackson, I., Lord, G.M., and Jenner, R.G. (2012). T-bet and GATA3 orchestrate Th1 and Th2 differentiation through lineage-specific targeting of distal regulatory elements. Nat.

Commun. *3*, 1268.

Kipling, D. (2001). Telomeres, replicative senescence and human ageing. Maturitas *38*, 25–37; discussion 37–38.

Ku, C.C. (2000). Control of Homeostasis of CD8+ Memory T Cells by Opposing Cytokines. Science (80-.). *288*, 675–678.

Kyo, S., Takakura, M., Fujiwara, T., and Inoue, M. (2008). Understanding and exploiting hTERT promoter regulation for diagnosis and treatment of human cancers. Cancer Sci. *99*, 1528–1538.

Laberge, R.-M., Sun, Y., Orjalo, A. V, Patil, C.K., Freund, A., Zhou, L., Curran, S.C., Davalos, A.R., Wilson-Edell, K.A., Liu, S., et al. (2015). MTOR regulates the pro-tumorigenic senescence-associated secretory phenotype by promoting IL1A translation. Nat. Cell Biol. *17*, 1049–1061.

de Lange, T. (2009). How Telomeres Solve the End-Protection Problem. Science (80-.). *326*, 948–952.

Laplante, M., and Sabatini, D.M. (2012). mTOR signaling in growth control and disease. Cell *149*, 274–293.

Lazarevic, V., Glimcher, L.H., and Lord, G.M. (2013). T-bet: a bridge between innate and adaptive immunity. Nat. Rev. Immunol. *13*, 777–789.

Lee, J.C., Kumar, S., Griswold, D.E., Underwood, D.C., Votta, B.J., and Adams, J.L. (2000). Inhibition of p38 MAP kinase as a therapeutic strategy. Immunopharmacology *47*, 185–201.

Lee, J.H., Budanov, A. V, Park, E.J., Birse, R., Kim, T.E., Perkins, G.A., Ocorr, K., Ellisman, M.H., Bodmer, R., Bier, E., et al. (2010). Sestrin as a feedback inhibitor

of TOR that prevents age-related pathologies. Science *327*, 1223–1228.

Li, G., Yu, M., Lee, W.-W., Tsang, M., Krishnan, E., Weyand, C.M., and Goronzy, J.J. (2012). Decline in miR-181a expression with age impairs T cell receptor sensitivity by increasing DUSP6 activity. Nat Med *18*, 1518–1524.

Li, H., Zhao, L.L., Funder, J.W., and Liu, J.P. (1997). Protein phosphatase 2A inhibits nuclear telomerase activity in human breast cancer cells. J. Biol. Chem. *272*, 16729–16732.

Li, J., Miller, E.J., Ninomiya-Tsuji, J., Russell, R.R., and Young, L.H. (2005). AMP-activated protein kinase activates p38 mitogen-activated protein kinase by increasing recruitment of p38 MAPK to TAB1 in the ischemic heart. Circ. Res. *97*, 872–879.

Libri, V., Azevedo, R.I., Jackson, S.E., Di Mitri, D., Lachmann, R., Fuhrmann, S., Vukmanovic-Stejic, M., Yong, K., Battistini, L., Kern, F., et al. (2011). Cytomegalovirus infection induces the accumulation of short-lived, multifunctional CD4+CD45RA+CD27+ T cells: the potential involvement of interleukin-7 in this process. Immunology *132*, 326–339.

Linton, P.J., Haynes, L., Klinman, N.R., and Swain, S.L. (1996). Antigen-independent changes in naive CD4 T cells with aging. J. Exp. Med. *184*, 1891–1900.

Liu, K., Hodes, R.J., and Weng, N. -p. (2001). Cutting Edge: Telomerase Activation in Human T Lymphocytes Does Not Require Increase in Telomerase Reverse Transcriptase (hTERT) Protein But Is Associated with hTERT Phosphorylation and Nuclear Translocation. J. Immunol. *166*, 4826–4830.

Liu, W., Chen, E., Zhao, X.W., Wan, Z.P., Gao, Y.R., Davey, A., Huang, E., Zhang,

L., Crocetti, J., Sandoval, G., et al. (2012). The scaffolding protein synapse-associated protein 97 is required for enhanced signaling through isotype-switched IgG memory B cell receptors. Sci. Signal. *5*, ra54.

Macintyre, A.N., Finlay, D., Preston, G., Sinclair, L. V, Waugh, C.M., Tamas, P., Feijoo, C., Okkenhaug, K., and Cantrell, D.A. (2011). Protein kinase B controls transcriptional programs that direct cytotoxic T cell fate but is dispensable for T cell metabolism. Immunity *34*, 224–236.

Mannick, J.B., Del Giudice, G., Lattanzi, M., Valiante, N.M., Praestgaard, J., Huang, B., Lonetto, M.A., Maecker, H.T., Kovarik, J., Carson, S., et al. (2014). mTOR inhibition improves immune function in the elderly. Sci. Transl. Med. *6*, 268ra179.

Mathon, N.F., and Lloyd, A.C. (2001). Cell senescence and cancer. Nat. Rev. Cancer *1*, 203–213.

Matsuyama, W., Faure, M., and Yoshimura, T. (2003). Activation of discoidin domain receptor 1 facilitates the maturation of human monocyte-derived dendritic cells through the TNF receptor associated factor 6/TGF-beta-activated protein kinase 1 binding protein 1 beta/p38 alpha mitogen-activated protein kina. J. Immunol. *171*, 3520–3532.

Meyer, O. (2009). Interferons and autoimmune disorders. Joint. Bone. Spine *76*, 464–473.

Missios, P., Zhou, Y., Guachalla, L.M., von Figura, G., Wegner, A., Chakkarappan, S.R., Binz, T., Gompf, A., Hartleben, G., Burkhalter, M.D., et al. (2014). Glucose substitution prolongs maintenance of energy homeostasis and lifespan of telomere dysfunctional mice. Nat. Commun. *5*, 4924.

Di Mitri, D., Azevedo, R.I., Henson, S.M., Libri, V., Riddell, N.E., Macaulay, R., Kipling, D., Soares, M.V.D., Battistini, L., and Akbar, A.N. (2011). Reversible senescence in human CD4+CD45RA+CD27- memory T cells. J. Immunol. *187*, 2093–2100.

Moiseeva, O., Mallette, F.A., Mukhopadhyay, U.K., Moores, A., and Ferbeyre, G. (2006). DNA damage signaling and p53-dependent senescence after prolonged beta-interferon stimulation. Mol. Biol. Cell *17*, 1583–1592.

Molnár, E., Swamy, M., Holzer, M., Beck-García, K., Worch, R., Thiele, C., Guigas, G., Boye, K., Luescher, I.F., Schwille, P., et al. (2012). Cholesterol and sphingomyelin drive ligand-independent T-cell antigen receptor nanoclustering. J. Biol. Chem. *287*, 42664–42674.

Moriggl, R., Kristofic, C., Kinzel, B., Volarevic, S., Groner, B., and Brinkmann, V. (1998). Activation of STAT proteins and cytokine genes in human Th1 and Th2 cells generated in the absence of IL-12 and IL-4. J. Immunol. *160*, 3385–3392.

Navarro, M.N., and Cantrell, D.A. (2014). Serine-threonine kinases in TCR signaling. Nat. Immunol. *15*, 808–814.

De Nicola, G.F., Martin, E.D., Chaikuad, A., Bassi, R., Clark, J., Martino, L., Verma, S., Sicard, P., Tata, R., Atkinson, R.A., et al. (2013). Mechanism and consequence of the autoactivation of p38α mitogen-activated protein kinase promoted by TAB1. Nat. Struct. Mol. Biol. *20*, 1182–1190.

O'Sullivan, D., and Pearce, E.L. (2015). Targeting T cell metabolism for therapy. Trends Immunol. *36*, 71–80.

Oh, H., and Ghosh, S. (2013). NF-κB: roles and regulation in different CD4(+) T-cell subsets. Immunol. Rev. *252*, 41–51.

Parijs, L. V., Perez, V.L., Biuckians, A., Maki, R.G., London, C.A., and Abbas, A.K. (1997). Role of Interleukin 12 and Costimulators in T Cell Anergy In Vivo. J. Exp. Med. *186*, 1119–1128.

Passos, J.F., Miwa, S., and von Zglinicki, T. (2013). Measuring reactive oxygen species in senescent cells. Methods Mol. Biol. *965*, 253–263.

Pearce, E.L., Mullen, A.C., Martins, G.A., Krawczyk, C.M., Hutchins, A.S., Zediak, V.P., Banica, M., DiCioccio, C.B., Gross, D.A., Mao, C.-A., et al. (2003). Control of effector CD8+ T cell function by the transcription factor Eomesodermin. Science *302*, 1041 – .

Pearce, E.L., Walsh, M.C., Cejas, P.J., Harms, G.M., Shen, H., Wang, L.-S., Jones, R.G., and Choi, Y. (2009). Enhancing CD8 T-cell memory by modulating fatty acid metabolism. Nature *460*, 103–107.

Pearce, E.L., Poffenberger, M.C., Chang, C.-H., and Jones, R.G. (2013a). Fueling immunity: insights into metabolism and lymphocyte function. Science *342*, 1242454.

Pearce, E.L., Poffenberger, M.C., Chang, C.-H., and Jones, R.G. (2013b). Fueling immunity: insights into metabolism and lymphocyte function. Science *342*, 1242454.

Platanias, L.C. (2005). Mechanisms of type-I- and type-II-interferon-mediated signalling. Nat. Rev. Immunol. *5*, 375–386.

Plunkett, F.J., Franzese, O., Belaramani, L.L., Fletcher, J.M., Gilmour, K.C., Sharifi, R., Khan, N., Hislop, A.D., Cara, A., Salmon, M., et al. (2005). The impact of telomere erosion on memory CD8+ T cells in patients with X-linked lymphoproliferative syndrome. Mech. Ageing Dev. *126*, 855–865.

Plunkett, F.J., Franzese, O., Finney, H.M., Fletcher, J.M., Belaramani, L.L., Salmon, M., Dokal, I., Webster, D., Lawson, A.D.G., and Akbar, A.N. (2007). The Loss of Telomerase Activity in Highly Differentiated CD8+CD28-CD27- T Cells Is Associated with Decreased Akt (Ser473) Phosphorylation. J. Immunol. *178*, 7710–7719.

Pollizzi, K.N., and Powell, J.D. (2014). Integrating canonical and metabolic signalling programmes in the regulation of T cell responses. Nat. Rev. Immunol. *14*, 435–446.

Quezada, S.A., Simpson, T.R., Peggs, K.S., Merghoub, T., Vider, J., Fan, X., Blasberg, R., Yagita, H., Muranski, P., Antony, P.A., et al. (2010). Tumor-reactive CD4(+) T cells develop cytotoxic activity and eradicate large established melanoma after transfer into lymphopenic hosts. J. Exp. Med. *207*, 637–650.

Reed, J.R., Vukmanovic-Stejic, M., Fletcher, J.M., Soares, M.V.D., Cook, J.E., Orteu, C.H., Jackson, S.E., Birch, K.E., Foster, G.R., Salmon, M., et al. (2004). Telomere erosion in memory T cells induced by telomerase inhibition at the site of antigenic challenge in vivo. J. Exp. Med. *199*, 1433–1443.

Riley, T., Sontag, E., Chen, P., and Levine, A. (2008). Transcriptional control of human p53-regulated genes. Nat. Rev. Mol. Cell Biol. *9*, 402–412.

Rincón, M., and Davis, R.J. (2007). Choreography of MAGUKs during T cell activation. Nat. Immunol. *8*, 126–127.

Rincón, M., Enslen, H., Raingeaud, J., Recht, M., Zapton, T., Su, M.S., Penix, L.A., Davis, R.J., and Flavell, R.A. (1998). Interferon-gamma expression by Th1 effector T cells mediated by the p38 MAP kinase signaling pathway. EMBO J. *17*, 2817–2829.

Rolf, J., Zarrouk, M., Finlay, D.K., Foretz, M., Viollet, B., and Cantrell, D.A. (2013). AMPKα1: a glucose sensor that controls CD8 T-cell memory. Eur. J. Immunol. *43*, 889–896.

Round, J.L., Humphries, L. a, Tomassian, T., Mittelstadt, P., Zhang, M., and Miceli, M.C. (2007). Scaffold protein Dlgh1 coordinates alternative p38 kinase activation, directing T cell receptor signals toward NFAT but not NF-kappaB transcription factors. Nat. Immunol. *8*, 154–161.

Rudd, C.E., and Schneider, H. (2003). Unifying concepts in CD28, ICOS and CTLA4 co-receptor signalling. Nat. Rev. Immunol. *3*, 544–556.

Sabatini, D.M., Erdjument-Bromage, H., Lui, M., Tempst, P., and Snyder, S.H. (1994). RAFT1: a mammalian protein that binds to FKBP12 in a rapamycin-dependent fashion and is homologous to yeast TORs. Cell *78*, 35–43.

Salvador, J.M., Mittelstadt, P.R., Guszczynski, T., Copeland, T.D., Yamaguchi, H., Appella, E., Fornace, A.J., and Ashwell, J.D. (2005). Alternative p38 activation pathway mediated by T cell receptor-proximal tyrosine kinases. Nat. Immunol. *6*, 390–395.

Sanli, T., Rashid, A., Liu, C., Harding, S., Bristow, R.G., Cutz, J.-C., Singh, G., Wright, J., and Tsakiridis, T. (2010). Ionizing radiation activates AMP-activated kinase (AMPK): a target for radiosensitization of human cancer cells. Int. J. Radiat. Oncol. Biol. Phys. *78*, 221–229.

Schamel, W.W.A., and Alarcón, B. (2013). Organization of the resting TCR in nanoscale oligomers. Immunol. Rev. *251*, 13–20.

Seddon, B., Legname, G., Tomlinson, P., and Zamoyska, R. (2000). Long-term survival but impaired homeostatic proliferation of Naïve T cells in the absence of

p56lck. Science *290*, 127–131.

Seddon, B., Tomlinson, P., and Zamoyska, R. (2003). Interleukin 7 and T cell receptor signals regulate homeostasis of CD4 memory cells. Nat. Immunol. *4*, 680–686.

Shaw, R.J., Kosmatka, M., Bardeesy, N., Hurley, R.L., Witters, L.A., DePinho, R.A., and Cantley, L.C. (2004). The tumor suppressor LKB1 kinase directly activates AMP-activated kinase and regulates apoptosis in response to energy stress. Proc. Natl. Acad. Sci. U. S. A. *101*, 3329–3335.

Shi, Y., and Gaestel, M. (2002). In the cellular garden of forking paths: How p38 MAPKs signal for downstream assistance. Biol. Chem. *383*, 1519–1536.

Sinclair, L. V, Rolf, J., Emslie, E., Shi, Y.-B., Taylor, P.M., and Cantrell, D.A. (2013). Control of amino-acid transport by antigen receptors coordinates the metabolic reprogramming essential for T cell differentiation. Nat. Immunol. *14*, 500–508.

Stone, J.D., Chervin, A.S., and Kranz, D.M. (2009). T-cell receptor binding affinities and kinetics: impact on T-cell activity and specificity. Immunology *126*, 165–176.

Su, B. (1994). JNK is involved in signal integration during costimulation of T lymphocytes. Cell *77*, 727–736.

Tamás, P., Hawley, S.A., Clarke, R.G., Mustard, K.J., Green, K., Hardie, D.G., and Cantrell, D.A. (2006). Regulation of the energy sensor AMP-activated protein kinase by antigen receptor and Ca2+ in T lymphocytes. J. Exp. Med. *203*, 1665–1670.

Tangeman, L., Wyatt, C.N., and Brown, T.L. (2012). Knockdown of AMP-activated protein kinase alpha 1 and alpha 2 catalytic subunits. J. RNAi Gene Silencing *8*, 470–478.

Tesmer, V.M., Ford, L.P., Holt, S.E., Frank, B.C., Yi, X., Aisner, D.L., Ouellette, M., Shay, J.W., and Wright, W.E. (1999). Two Inactive Fragments of the Integral RNA Cooperate To Assemble Active Telomerase with the Human Protein Catalytic Subunit (hTERT) In Vitro. Mol. Cell. Biol. *19*, 6207–6216.

Verdun, R.E., and Karlseder, J. (2007). Replication and protection of telomeres. Nature *447*, 924–931.

Vigna, E., and Naldini, L. Lentiviral vectors: excellent tools for experimental gene transfer and promising candidates for gene therapy. J. Gene Med. *2*, 308–316.

Wagner, E.F., and Nebreda, A.R. (2009). Signal integration by JNK and p38 MAPK pathways in cancer development. Nat. Rev. Cancer *9*, 537–549.

Wang, W., Yang, X., López de Silanes, I., Carling, D., and Gorospe, M. (2003). Increased AMP:ATP ratio and AMP-activated protein kinase activity during cellular senescence linked to reduced HuR function. J. Biol. Chem. *278*, 27016–27023.

Watson, J.D. (1971). The regulation of DNA synthesis in eukaryotes. Adv. Cell Biol. *2*, 1–46.

Wellen, K.E., and Thompson, C.B. (2012). A two-way street: reciprocal regulation of metabolism and signalling. Nat. Rev. Mol. Cell Biol. *13*, 270–276.

Weng, N.-P., Akbar, A.N., and Goronzy, J. (2009). CD28(-) T cells: their role in the age-associated decline of immune function. Trends Immunol. *30*, 306–312.

Wilson, R.C., and Doudna, J.A. (2013). Molecular mechanisms of RNA

interference. Annu. Rev. Biophys. *42*, 217–239.

Woods, A., Dickerson, K., Heath, R., Hong, S.-P., Momcilovic, M., Johnstone, S.R., Carlson, M., and Carling, D. (2005). Ca2+/calmodulin-dependent protein kinase kinase-beta acts upstream of AMP-activated protein kinase in mammalian cells. Cell Metab. *2*, 21–33.

Wurster, A.L., Tanaka, T., and Grusby, M.J. (2000). The biology of Stat4 and Stat6. Oncogene *19*, 2577–2584.

Xu, D., Erickson, S., Szeps, M., Gruber, A., Sangfelt, O., Einhorn, S., Pisa, P., and Grandér, D. (2000). Interferon alpha down-regulates telomerase reverse transcriptase and telomerase activity in human malignant and nonmalignant hematopoietic cells. Blood *96*, 4313–4318.

Zarubin, T., and Han, J. (2005). Activation and signaling of the p38 MAP kinase pathway. Cell Res. *15*, 11–18.

Zhang, J., Salojin, K. V, Gao, J.X., Cameron, M.J., Bergerot, I., and Delovitch, T.L. (1999). p38 mitogen-activated protein kinase mediates signal integration of TCR/CD28 costimulation in primary murine T cells. J. Immunol. *162*, 3819–3829.